



الجمهورية الجزائرية الديمقراطية الشعبية
People's Democratic Republic of Algeria
وزارة التعليم العالي والبحث العلمي
Ministry of Higher Education and Scientific Research
جامعة الشهيد حمزة لخضر الوادي
University of Echahid Hamma Lakhdar – El-OUED
كلية العلوم الطبيعية الحياة
Faculty of Natural Sciences and Life
قسم البيولوجيا الخلوية والجزيئية
Department of Cellular and Molecular Biology



THESIS

SUBMITTED TO OBTAIN 3rd CYCLE LMD DOCTORATE DEGREE IN BIOCHEMISTRY
Specialty: Applied Biochemistry

THEME

Effect of *Artemisia campestris* on the health of living beings

Presented by: Mrs. CHERFI Inasse

Graduated 19/03/2025

Jury Members:

Pr. DEROUCHE Samir	Professor	University of El-Oued	President
Dr. MAHBOUB Nasma	Assistant Professor A	University of El-Oued	Supervisor
Pr. TOUMI Ikram	Professor	University of El-Oued	Co-supervisor
Pr. CHEMSA A.Elkhalifa	Professor	University of El-Oued	Examiner
Pr. HADJADJ Soumia	Professor	University of Ouargla	Examiner
Pr. BENMOUSSA M.Taher	Professor	University of Batna	Examiner
Pr. LAOUINI Salah Eddine	Professor	University of El-Oued	Invited

2024/2025

Acknowledgments

Above all, I am grateful to God, the Almighty, for providing me with endurance and fortitude.

First, I want to sincerely thank **Dr. MAHBOUB Nasma** and **Pr. Toumi Ikram**, professors from Echahid Hamma Lakhdar University, thank you for your guidance and supervision of this effort. Their availability, counsel, and faith in me allowed me to complete this work. They have been aiding, encouraging, and providing permanent support during these years of work.

I would also like to sincerely thank the discussion committee members for accepting the invitation to discuss the thesis and for their patience and dedication in correcting and commenting to present it in the best academic form. Their names are as follows:

Pr. DEROUCHE Samir

Pr. CHAMSA A.Elkhalifa

Pr. HADJAJ Soumaia

Pr. BENMOUSSA M.Taher

I thank **Pr. LAOUINI Salah Eddine**, from whom I benefited from his precious help, encouragement, advice, and good humor.

I also want to thank all my teachers for teaching me the science fundamentals. I am grateful to my colleagues, **Dr. LAIB Ibtissam**, **Dr. GHERAISSA Noura**, **BENAISSA Abir**, **ALIA Khawla**, **Dr. BOUDABIA Wafa**, and **Dr. HASSAN Gamil**, for their unwavering support and encouragement. I send them my warmest kindness and best wishes.

Dedication

To my parents, who brought me into this world and instilled in me the strength to stand on my own two feet. Your prayers, encouragement, and unwavering support have been my foundation.

To my husband, who walks this path alongside me, providing significant support and continuous encouragement. Your presence has been invaluable in completing this work.

Inasse


ABSTRACT

ABSTRACT

ABSTRACT

Artemisia campestris L. is a medicinal plant known for its antioxidant and anti-inflammatory properties. However, its therapeutic potential in endocrine disorders, particularly polycystic ovarian syndrome (PCOS) and hypothyroidism, remains underexplored. This study investigates the biological activities of its aqueous extract and essential oil, evaluating their efficacy in managing these conditions. Fifteen mature Wistar rats were divided into three groups: control, PCOS-induced, and a PCOS group treated with 200 mg/kg *A. campestris L.* extract for 15 days. Treatment significantly reduced luteinizing hormone (LH) levels and improved ovarian histomorphometry. In a hypothyroidism model induced by Carbimazole, both the aqueous extract and essential oil (administered at 200 mg/kg BW) enhanced thyroid function, as indicated by increased FT4 and decreased TSH levels. The aqueous extract exhibited strong antioxidant activity, with IC_{50} values of 4.34 $\mu\text{g/mL}$ (DPPH $^{\circ}$), 6.19 $\mu\text{g/mL}$ (FRAP), and 3.27 $\mu\text{g/mL}$ (β -carotene). It also demonstrated notable α -amylase inhibitory activity ($IC_{50} = 2.418 \mu\text{g/mL}$). Histopathological analysis confirmed the protective effects on thyroid tissue morphology. Chemical characterization using ultra-performance liquid chromatography (UPLC) and gas chromatography-mass spectrometry (GC-MS) identified key bioactive compounds. The aqueous extract contained β -sitosterol (14.3 $\mu\text{g/mL}$), Arteannuin B (12.6 $\mu\text{g/mL}$), Scopoletin (8.22 $\mu\text{g/mL}$), Artemisinin (6.13 $\mu\text{g/g}$), and Rutin (5.8 $\mu\text{g/mL}$). GC-MS analysis of the essential oil revealed major constituents, including linalyl acetate (2.92%), geranyl acetate (2.45%), cyclononasiloxane (2.37%), cyclohexanol (1.76%), and eucalyptol (1.38%). The essential oil exhibited potent antioxidant activity ($IC_{50} = 11.09 \mu\text{g/mL}$ for DPPH $^{\circ}$, 15.81 $\mu\text{g/mL}$ for FRAP, and 22.70 $\mu\text{g/mL}$ for β -carotene) and inhibited peroxidase activity by 62% and 50%. *In silico* molecular docking studies supported these findings, revealing strong interactions between the identified compounds and thyroperoxidase, a key enzyme for thyroid function. Additionally, 3-cyclopentyl-N-(2-(3,4-dimethoxyphenyl)ethyl) was identified as a potential candidate for pancreatic cancer therapy due to its high binding affinity to cancer receptors. These findings highlight the therapeutic potential of *A. campestris L.* in managing PCOS and hypothyroidism, with its aqueous extract and essential oil demonstrating significant endocrine-modulating, antioxidant, and anti-inflammatory properties. The molecular docking results further suggest possible applications in cancer therapy, warranting further investigation into its pharmacological benefits.

Keywords: *Artemisia campestris L.*, Polycystic ovary syndrome, Hypothyroidism, Essential oil, Aqueous extract, Molecular docking, Antioxidant activity, Anti-inflammatory properties, GC-MS, UPLC, α -amylase inhibition, pancreatic cancer.

تأثير نبات *Artemisia campestris* على صحة الكائنات الحية

ملخص

تعتبر *Artemisia campestris* L نبتة طبية معروفة بخصائصها المضادة للأكسدة والمضادة للالتهابات. ومع ذلك، فإن إمكانياتها العلاجية في اضطرابات الغدد الصماء، وخاصة متلازمة تكيس المبايض (PCOS) وقصور الغدة الدرقية، لا تزال غير مستكشفة بشكل كافٍ. تهدف هذه الدراسة إلى تقييم الأنشطة البيولوجية لمستخلصها المائي وزيتها العطري، وقياس فعاليتها في إدارة هذه الحالات. تم تقسيم خمسة عشر جرماً ناضجاً من نوع ويستار إلى ثلاث مجموعات: مجموعة شاهدة، مجموعة مصابة بمتلازمة تكيس المبايض، ومجموعة مصابة تم علاجها بـ 200 ملغ/كغ من مستخلص *A. campestris* لمدة 15 يوماً. أدى العلاج إلى انخفاض ملحوظ في مستويات هرمون (LH) وتحسين الهيكل النسيجي للمبيض. وفي نموذج قصور الغدة الدرقية المستحث بواسطة الكاربامازول، تم تقييم التأثيرات الوقائية لكل من المستخلص المائي والزيت العطري عند جرعة 200 ملغ/كغ من وزن الجسم، مما أظهر تحسناً في وظائف الغدة الدرقية كما يتضح من ارتفاع مستويات FT4 وانخفاض TSH. أظهر المستخلص المائي نشاطاً مضاداً للأكسدة بدرجات IC_{50} بلغت 4.34 ميكروغرام/مل (DPPH°)، و 6.19 ميكروغرام/مل (FRAP)، و 3.27 ميكروغرام/مل (β -carotene). كما أظهر نشاطاً مثبطاً ملحوظاً لإنزيم α -amylase بقيمة $IC_{50} = 2.418$ ميكروغرام/مل. أكدت التحليلات النسيجية التأثيرات الوقائية على بنية الغدة الدرقية. تم تحديد المركبات النشطة بيولوجياً من خلال التحليل الكيميائي باستخدام كروماتوغرافيا السائل عالية الأداء (UPLC) وكروماتوغرافيا الغاز-مطياف الكتلة (GC-MS). احتوى المستخلص المائي على بيتا-ستيستيرون 14.3 ميكروغرام/مل وأرتينوين بـ 12.6 ميكروغرام/مل، سكوبوليتين 8.22 ميكروغرام/مل، أرتيميسينين 6.13 ميكروغرام/غ، وروتين 5.8 ميكروغرام/مل. أما تحليل GC-MS للزيت العطري فقد كشف عن مركبات رئيسية مثل أسيتات الليناليل (2.92%)، أسيتات الجيرانيل (2.45%)، سيكلونوناسيلوكسين (2.37%)، سيكلوهكسانول (1.76%)، والأوكالينول (1.38%). كما أظهر الزيت العطري نشاطاً مضاداً للأكسدة بقيم IC_{50} بلغت 11.09 ميكروغرام/مل (DPPH°)، و 15.81 ميكروغرام/مل (FRAP)، و 22.70 ميكروغرام/مل (β -carotene)، بالإضافة إلى تثبيط نشاط البيروكسيداز بنسبة 62% و 50%. أكدت دراسات الارتباط الجزيئي (*In Silico* Molecular Docking) هذه النتائج، حيث كشفت عن تفاعلات قوية بين المركبات النشطة المحددة وإنزيم ثايروبيروكسيداز، وهو إنزيم رئيسي في وظيفة الغدة الدرقية. بالإضافة إلى ذلك، تم تحديد المركب 3-cyclopentyl-N-(2-(3,4-dimethoxyphenyl)ethyl) كمرشح واعد لعلاج سرطان البنكرياس نظراً لارتباطه القوي بمستقبلات السرطان. تؤكد هذه النتائج الإمكانيات العلاجية الكبيرة لنبتة *A. campestris* L في إدارة متلازمة تكيس المبايض وقصور الغدة الدرقية، حيث أظهر مستخلصها المائي وزيتها العطري خصائص هامة مضادة للأكسدة ومضادة للالتهابات ومنظمة لوظائف الغدد الصماء. كما تشير نتائج الارتباط الجزيئي إلى إمكانية استخدامها في علاج السرطان، مما يستدعي مزيداً من البحث حول فوائدها الدوائية.

الكلمات المفتاحية: *Artemisia campestris*، متلازمة تكيس المبايض، قصور الغدة الدرقية، الزيت العطري، المستخلص المائي، الارتباط الجزيئي، النشاط المضاد للأكسدة، الخصائص المضادة للالتهابات، GC-MS، UPLC، تثبيط α -amylase، سرطان البنكرياس.

Effet d'*Artemisia campestris* sur la santé des êtres vivants

RESUME

Artemisia campestris L. est une plante médicinale reconnue pour ses propriétés antioxydantes et anti-inflammatoires. Toutefois, son potentiel thérapeutique dans les troubles endocriniens, en particulier le syndrome des ovaires polykystiques (PCOS) et l'hypothyroïdie, reste insuffisamment exploré. Cette étude vise à évaluer les activités biologiques de son extrait aqueux et de son huile essentielle, en analysant leur efficacité dans la gestion de ces pathologies. Quinze rats Wistar adultes ont été répartis en trois groupes : un groupe témoin, un groupe induit par le PCOS, et un groupe atteint du PCOS traité avec 200 mg/kg d'extrait de *A. campestris* L. pendant 15 jours. Le traitement a entraîné une réduction significative du taux de l'hormone lutéinisante (LH) ainsi qu'une amélioration de l'histomorphométrie ovarienne. Dans un modèle d'hypothyroïdie induite par le carbimazole, l'extrait aqueux et l'huile essentielle administrés à 200 mg/kg de poids corporel ont amélioré la fonction thyroïdienne, comme en témoignent l'élévation des niveaux de FT4 et la diminution des niveaux de TSH. L'extrait aqueux a démontré une activité antioxydante significative, avec des valeurs IC50 de 4,34 µg/mL (DPPH°), 6,19 µg/mL (FRAP) et 3,27 µg/mL (β-carotène). Il a également présenté une forte activité inhibitrice de l'α-amylase (IC50 = 2,418 µg/mL). L'analyse histopathologique a confirmé les effets protecteurs sur la morphologie du tissu thyroïdien. L'analyse chimique par chromatographie liquide ultra-haute performance (UPLC) et chromatographie en phase gazeuse couplée à la spectrométrie de masse (GC-MS) a permis d'identifier des composés bioactifs clés. L'extrait aqueux contenait notamment β-sitostérol (14,3 µg/mL), Artéannuin B (12,6 µg/mL), Scopolétine (8,22 µg/mL), Artémisinine (6,13 µg/g) et Rutine (5,8 µg/mL). L'analyse GC-MS de l'huile essentielle a révélé des constituants majoritaires tels que l'acétate de linalyle (2,92 %), l'acétate de géranyle (2,45 %), le cyclononasiloxane (2,37 %), le cyclohexanol (1,76 %) et l'eucalyptol (1,38 %). L'huile essentielle a montré une forte activité antioxydante, avec des valeurs IC50 de 11,09 µg/mL (DPPH°), 15,81 µg/mL (FRAP) et 22,70 µg/mL (β-carotène), ainsi qu'une inhibition de l'activité peroxydase de 62 % et 50 %. Les études de docking moléculaire in silico ont corroboré ces résultats en mettant en évidence des interactions positives entre les composés identifiés et la thyroperoxydase, une enzyme clé de la fonction thyroïdienne. De plus, le 3-cyclopentyl-N-(2-(3,4-diméthoxyphényl)éthyl) a été identifié comme un candidat prometteur pour le traitement du cancer du pancréas en raison de sa forte affinité de liaison avec les récepteurs cancéreux. Ces résultats soulignent le potentiel thérapeutique de *A. campestris* L. dans la gestion du PCOS et de l'hypothyroïdie, grâce aux propriétés endocrino-modulatrices, antioxydantes et anti-inflammatoires de son extrait aqueux et de son huile essentielle. En outre, les résultats du docking moléculaire suggèrent une application possible dans le traitement du cancer, nécessitant ainsi des recherches approfondies sur ses bénéfices pharmacologiques.

Mots-clés : *Artemisia campestris* L., PCOS, Hypothyroïdie, Huile essentielle, Extrait aqueux, Docking moléculaire, Activité antioxydante, Propriétés anti-inflammatoires, GC-MS, UPLC, Inhibition de l'α-amylase, Cancer du pancréas.

<i>Figure 1. Artemisia campestris L. (A) General plant, (B) and (C) Inflorescence (Dib et al., 2017).....</i>	<i>29</i>
<i>Figure 2. An overview of the PCOS study's experimental protocol.</i>	<i>36</i>
<i>Figure 3. Comparative antioxidant activities of A. campestris essential oil and BHA.</i>	<i>45</i>
<i>Figure 4. Structure of some polyphenolic compounds identified in extracts from A. campestris.</i>	<i>47</i>
<i>Figure 5. Effect of A. campestris extracts on protein denaturation (albumin).</i>	<i>53</i>
<i>Figure 6. Anti-inflammatory activity of A. campestris essential oil.</i>	<i>54</i>
<i>Figure 7. The inhibition of α-amylase by aqueous extracts of A. campestris.</i>	<i>55</i>
<i>Figure 8. The inhibition of Guaiacol peroxidase by aqueous extracts of A. campestris.</i>	<i>57</i>
<i>Figure 9. Peroxidase activity activity of Artemisia campestris essential oil.</i>	<i>58</i>
<i>Figure 10. (A) Histological analysis of normal rats. (B) rats with PCOS; (C) rats with PCOS treated A. campestris extract.</i>	<i>59</i>
<i>Figure 11. The mean expression levels of TSH and T4 in Lot I (control). Lot II (CBZ). Lot III (CBZ + A. campestris). and Lot IV (CBZ + LEV). Values with letters (a) are considered significantly different ($p < 0.05$). Many people sharing the same superscript letter exhibit no significant differences in LEV. Lyvotyroxin. CBZ. carbimazole. TSH. and thyroid-stimulating hormone.</i>	<i>61</i>
<i>Figure 12. The Mechanism of Beta-Sitosterol In The Treatment of Hypothyroidism.</i>	<i>63</i>
<i>Figure 13. Microscopic views of thyroid histological lots in rats at varied magnifications (A1. B1. C1. D1; 10x/ A2. B2. C2. D2; 40x/ A3. B3. C3. D3; 100x) across four distinct groups: (A) Control. (B) Group Treated with CBZ. (C) Group treated with investigated plant. and (D) Group Treated with Levothyrox[®].</i>	<i>64</i>
<i>Figure 14. Visualization of compound's interactions with thyroid peroxidase protein (PDB ID: 5FF1) in 2D (a) and 3D (b) views.</i>	<i>68</i>
<i>Figure 15. The crystallographic structure of targeted proteins of pancreatic cancer. Insulin-like growth factor 1 receptor (A). Mitogen-activated protein kinase kinase-1 (B). Phosphoinositide 3-kinase gamma (C). and Janus Kinase-1 (D).</i>	<i>69</i>
<i>Figure 16. Visualization of interactions in 2D (A) and 3D (B) of linalyl acetate bio-compound with active site residues of 3I81(1). 3SLS(2). 5JHB(3) and 6SM8(4) receptors.</i>	<i>73</i>

Table 1. Total phenolic and flavonoid in <i>A. campestris</i> extracts' aqueous extract.	41
Table 2. UPLC was used to identify secondary metabolites in the leaf. This revealed the presence of a total of 26 secondary metabolites belonging to different classes.....	42
Table 3. Antioxidant activity of <i>A. campestris</i> extracts. DPPH° activity. FRAP activity. and β -carotene activity.	44
Table 4. GCMS identification of secondary metabolites in the leaf.....	49
Table 5. UPLC was used to identify secondary metabolites in the leaf. خطأ! الإشارة المرجعية غير معروفة.	
Table 6. Polyphenols bind to androgen and estrogen receptors.....	56
Table 7. A comparison of the rats' mean levels of FSH and LH in the experimental. PCOS. and control groups.	58
Table 8. The conformability of compounds toward Lipinski's rules of five.....	64
Table 9. The acute toxicity prediction results of compounds.	64
Table 10. Absorption. Distribution. Metabolism. and Excretion (ADME) results.....	65
Table 11. Binding energy values of targeted compounds obtained by molecular docking approach.....	65
Table 12. RMSD (in Å) and binding affinity (in Kcal/mol) of potent compounds against their pancreatic cancer targeted protein.	69
Table 13. Binding energy (in Kcal/mol) of <i>A. campestris</i> bio-compounds against JAK1. PI3K. MEK1 and IGF1 proteins.....	70

LISTE OF ABBREVIATION

AlCl ₃	Aluminum chloride
ALP	Alkaline phosphatase
ATCC	American Type Culture Collection
Au ⁺	Gold cation
BSA	Bovine Serum Albumin
DMSO	Dimethyl sulfoxide
DNA	Deoxyribonucleic acid
DPPH°	2,2-diphenyl-1-picrylhydrazyl
DTNB	5,5'-Dithiobis-(2-nitrobenzoic acid)
EDTA	Ethylenediaminetetraacetic acid
FeCl ₃	Ferric chloride
FSH	Follicle-stimulating hormone
GSH	Glutathione
H ₂ O ₂	Hydrogen peroxide
LH	Luteinizing hormone
LPO	Lipid peroxidation
MDA	Malondialdehyde
MHB	Mueller Hinton Broth
PLT	Platelet
RBC	Red Blood Cell
ROS	Reactive oxygen species
SEM	Scanning electron microscopes
SPR	surface plasmon resonance
T ₃	Triiodothyronine
TBA	Thiobarbituric Acid
TBS	Tris buffer saline solution
TCA	Trichloroacetic Acid
TSH	Thyroid stimulating hormone
UV	Ultraviolet
UV-VIS	UV-VIS: Ultraviolet-visible spectroscopy
WBC	White Blood cell
Zn ⁺²	Zinc ion

Acknowledgments	1
ABSTRACT	5
خطأ! الإشارة المرجعية غير معرّفة. الملخص	
RESUME	7
INTRODUCTION	14
EXPERIMENTAL STUDY	27
CHAPTER I	28
Material & Methods	28
1. Materials	29
1.1. Plant	29
1.2. Extraction of essential oilsخطأ! الإشارة المرجعية غير معرّفة.	
1.3. Animals	30
1.4. Chemicals and reagents	30
2. Methods	30
2.1. Phytochemical analysis of <i>Artemisia campestris</i> L.	30
2.1.1. Extraction of <i>A. campestris</i> Aqueous extract.....	30
2.1.2. Phytochemical Screening.....	31
2.1.3. Quantification of phytochemicals compounds	31
2.1.3.1. Estimation of total phenolics	31
2.1.3.2. Estimation of total flavonoids.....	31
2.1.3.3. Estimation of condensed tannin.....	31
2.1.3.4. Qualitative analysis by HPLC.....	31
2.1.2. Extraction of <i>A. campestris</i> L'essential oil	32
2.1.2.1. GC-MS analysis technique	32
2.2. <i>In Vitro</i> Activity of the <i>A. campestris</i> aqueous extract and essential oil	32
2.2.1. Antioxidant activity	32
2.2.1.1. DPPH° free-radical scavenging activity	32
2.2.1.2. Ferric reducing antioxidant power assay (FRAP).....	33
2.2.1.3. β-carotene bleaching assay	33

2.2.2.	Anti-inflammatory activity (Albumin denaturation test)	34
2.2.3.	α -amylase inhibition assays	34
2.2.4.	Measurement of guaiacol peroxidase	35
2.3.	<i>In vivo</i> activity of aqueous extract	35
2.3.1.	PCOS Experiment	35
2.3.2.	Hypothyroidism Experiment	36
2.3.3.	Histopathological and blood sample	36
2.4.	Molecular Docking Study	37
2.4.1.	Drug likeness of ligands and pharmacological studies	37
2.4.2.	Ligands and receptors selection	38
2.4.3.	Ligands preparation	38
2.5.	Statistical analysis	39
CHAPTER II		40
Results and Discussion		40
1.	Determination of the total polyphenols and flavonoids	41
1.1.	UPLC composition analysis of leaf extract	41
2.	Anti-oxidant activity	43
2.1.	DPPH ^o scavenging test	43
2.2.	Reducing power test	44
2.3.	β -carotene bleaching assay	44
2.4.	Antioxidant activity of essential oil	44
2.5.	Gas Chromatography-Mass Spectrometry of Essential Oil	47
3.	Anti-inflammatory activity	52
3.1.	Anti-inflammatory activity of aqueous extract	52
3.2.	Anti-inflammatory activity of essential oil	53
4.	α -amylase inhibition	54
5.	Guaiacol peroxidase activity	56
6.	<i>In vivo</i> assays	58
6.1.	PCOS assay	58
6.1.1.	Hormonal analysis	58
6.2.	HPO assay	60

SUMMARY

.6.2.1	Hormonal analysis	60
6.2.2.	Histopathology and morphometry of thyroid tissue.....	62
7.	Molecular Docking:.....	64
7.1.	<i>In silico</i> study of pancreatic cancer proteins with essential oil.....	68
CONCLUSION		75
REFERENCES		78

INTRODUCTION

Introduction

Artemisia campestris L. is a chamaephyte plant systematically classified within the tribe of *Anthemideae* and the genus *Artemisia* (Brahmi *et al.* 2024). The main morphological feature distinguishing this species is the yellow capitula, which contains functionally male disk florets and pistillate ray florets with a glabrous receptacle (Dib and El Alaoui-Faris 2019). These morphological traits allowed the first taxonomic classification of *A. campestris* within the subgenera *Dracunculus* Besser (Marghich *et al.* 2023). *A. campestris* possesses many traditional uses (Dib *et al.* 2017), many of them have been pharmacologically evidenced, Like the antihypertensive (Rocha *et al.* 2021), anti-diabetic (Sriti *et al.* 2024), antihyperlipidemic (Zahnit *et al.* 2022), anti-venom (Trifan *et al.* 2022), anti-inflammatory (Mammeri *et al.* 2022), anti-leishmaniasis (Metoui *et al.* 2022), wound healing (Boudjelal *et al.* 2020), hepatoprotective (Saoudi *et al.* 2017), and kidney-protective (Sefi *et al.* 2012) effects, This plant also possesses culinary properties, especially as a food preservative (Obolskiy *et al.* 2011). *Artemisia campestris* L. is traditionally used in the El Oued region, located in the southeast of Algeria, for the treatment of various endocrine disorders, particularly hypothyroidism and polycystic ovarian syndrome (PCOS). In local traditional medicine, it is highly valued for its supposed benefits in hormonal regulation and metabolic balance. However, these uses remain primarily based on empirical knowledge and anecdotal observations, with limited scientific validation. Despite its widespread traditional application, few studies have explored its mechanisms of action or rigorously assessed its therapeutic potential through modern experimental and analytical approaches. This study aims to bridge this gap by investigating, through experimental models and biochemical analyses, the effects of *A. campestris* L. aqueous extract and essential oil on hypothyroidism and PCOS, providing scientific insight into its potential medicinal properties.

Artemisia campestris L., a widely distributed plant, is recognized for its chemical complexity, contributing significantly to its pharmacological efficacy. This species encompasses several subspecies, including *A. campestris* subsp. *glutinosa*, *campestris*, and *maritima* have been extensively studied, particularly for their flavonoid content. Research has shown that *A. campestris* is particularly rich in flavones such as chrysin, apigenin, luteolin, and their derivatives, including 6-methoxy apigenin (hispidulin), 7,4'-O-dimethyl apigenin, and cirsimaritin. These compounds, alongside other flavonoids like eupafolin and luteolin, have been found to exhibit potent antioxidant, anti-inflammatory, and antimicrobial activities, which are likely responsible for many of the plant's traditional therapeutic uses (Dib *et al.* 2017). Additionally, the flavonol subclass, represented by kaempferol, quercetin, and

INTRODUCTION

myricetin, includes a range of derivatives, such as 7-O-methyl kaempferol and 3,7-O-dimethyl kaempferol, which contribute to the plant's ability to mitigate oxidative stress and inflammation, essential factors in the prevention and treatment of chronic diseases such as cardiovascular disorders, diabetes, and neurodegenerative diseases (Alrumaihi *et al.* 2024).

Beyond flavonoids, *A. campestris* is also notable for its diverse phenolic acid content, Chlorogenic acid, trans-ferulic acid, vanillic acid, and isochlorogenic acids A, B, and C are among the key phenolic compounds in the plant, primarily responsible for its robust antioxidant properties. These compounds, particularly chlorogenic acid and caffeic acid, have been shown to possess anti-inflammatory, anti-hypertensive, and anticancer effects. Studies conducted on extracts of *A. campestris* from various regions, including Tunisia and Algeria, support its use as a natural source of bioactive compounds that may offer therapeutic benefits for a range of conditions, from metabolic diseases to inflammation-related disorders (Brahmi *et al.* 2024; Megdiche-Ksouri *et al.* 2015; Sebai *et al.* 2014). Moreover, these phenolic acids enhance the plant's potential as an agent for managing oxidative stress, which is a critical underlying cause of various chronic diseases.

While *A. campestris* does not traditionally contain coumarins, some studies have identified the presence of several coumarin derivatives in its extracts, such as esculetin, fraxidin, and scopoletin. These hydroxycoumarins are known for their diverse pharmacological actions, including anticoagulant, anti-inflammatory, and anticancer properties. These findings challenge earlier reports that suggested the absence of coumarins in the species (Chebbac *et al.* 2024; Naili *et al.* 2010), indicating that further investigation into the coumarin content of *A. campestris* may uncover additional bioactive compounds. Additionally, isocoumarins such as artemisinin, E-artemisinin, and epoxyartemidin, isolated from *A. campestris subsp. campestris*, further underscore the plant's value in traditional medicine, particularly in treating malaria and other parasitic infections (González-Minero, Bravo-Díaz, and Ayala-Gómez 2020; Sriti *et al.* 2024). Artemisinin and its derivatives have gained significant attention for their potent antimalarial activity, further establishing *A. campestris* as a plant of considerable pharmaceutical importance.

The rich phytochemical profile of *A. campestris* highlights its traditional uses and emphasizes its untapped potential as a source of therapeutic agents, with its diverse flavonoids, phenolic acids, and coumarin derivatives, *A. campestris* holds promise as a natural remedy for a wide range of diseases, including inflammatory, metabolic, and infectious conditions. The plant's antioxidant, anti-inflammatory, antimicrobial, and anticancer properties position it as a candidate for developing novel therapeutic agents. Further research into its chemical

INTRODUCTION

composition and biological activities is warranted to fully exploit the therapeutic potential of *A. campestris* in modern medicine (Llauradó Maury *et al.* 2020).

The pharmacological properties of *Artemisia campestris* L. have been extensively studied, revealing a broad spectrum of therapeutic effects that contribute to its potential applications in both traditional and modern medicine. These effects encompass antioxidant, hepatoprotective, nephroprotective, neuroprotective, anti-inflammatory, anti-hyperlipidemic, antidiabetic, antihypertensive, and antimicrobial activities, all of which are attributed to its rich chemical composition, including flavonoids, phenolic compounds, essential oils, and other bioactive molecules. The antioxidant capacity of *A. campestris* is one of its most well-documented features, with research showing that its aqueous extract effectively combats oxidative stress. Additionally, it enhanced the activity of critical antioxidant enzymes, including catalase (CAT), superoxide dismutase (SOD), and glutathione peroxidase (GSH-Px) in the kidney, liver, and brain. These findings suggest that *A. campestris* may play a significant role in protecting against diseases associated with oxidative damage, such as cardiovascular disorders and neurodegenerative conditions (Saoudi *et al.* 2010).

In terms of hepatoprotective activity, *A. campestris* has shown considerable promise. In one study, mice treated with carbon tetrachloride (CCl₄), a known hepatotoxin, displayed liver damage, but the administration of the aqueous extract at a dose of 5 mL/kg facilitated recovery, as evidenced by reduced serum levels of alanine aminotransferase (ALT) and aspartate aminotransferase (AST), which are biomarkers of liver damage. Additionally, there was an increase in the activity of aniline hydroxylase (anilineOH), a key enzyme involved in liver detoxification. A similar hepatoprotective effect was observed in rats subjected to oxidative stress induced by fenthion, a pesticide, where a diet supplemented with 5% *A. campestris* led to a reduction in key hepatic biomarkers such as lactate dehydrogenase (LDH), AST, and ALT, further supporting the plant's potential as a natural remedy for liver damage (Sagástegui-Guarniz William Antonio *et al.* 2020).

Artemisia campestris has also demonstrated nephroprotective effects. In rats treated with diclofenac, a drug known to induce nephrotoxicity, the aqueous extract normalized serum creatinine and urea levels, critical indicators of kidney function. In another study involving diabetic rats induced by alloxan, treatment with the aqueous extract of *A. campestris* leaves at a dose of 200 mg/kg for 21 days led to significant improvements in kidney function, with decreased serum levels of creatinine, urea, and uric acid, and an increase in creatinine clearance. These results indicate that *A. campestris* may be a promising therapeutic agent for

INTRODUCTION

kidney-related diseases, including those linked to diabetes and nephrotoxicity (Sefi *et al.* 2012).

The neuroprotective effects of *A. campestris* are also noteworthy, particularly in relation to neurodegenerative diseases and neurotoxicity. In experiments involving deltamethrin, a neurotoxic pesticide, rats co-treated with *A. campestris* essential oil experienced a significant decrease in brain lipid peroxidation, as evidenced by lower levels of malondialdehyde (MDA), a marker of oxidative damage. Additionally, pre-treatment with *A. campestris* essential oil helped to preserve brain histology, protecting against severe vacuolation and neuronal necrosis caused by deltamethrin exposure. These findings suggest that *A. campestris* may provide protective benefits to the central nervous system in the face of chemical or environmental stressors (Zahnit *et al.* 2022).

The plant also exhibits significant gastrointestinal protective effects. In rats with aspirin-induced gastric injury, the aqueous extract of *A. campestris* demonstrated superior protective effects when compared to the standard treatment, famotidine. The extract reduced the ulcer index by 13.66 mm² and provided 78% protection against gastric injury, indicating its potential as a treatment for conditions like gastric ulcers and gastritis, often exacerbated by oxidative stress and inflammation (Sebai *et al.* 2014).

Moreover, *A. campestris* has shown anti-hyperlipidemic properties, making it a valuable candidate for managing lipid imbalances and reducing the risk of cardiovascular diseases. In rats with alloxan-induced hyperlipidemia, the aqueous extract at 200 mg/kg for 21 days significantly reduced total cholesterol, triglycerides, and low-density lipoprotein cholesterol (LDL-C) levels. In pregnant rats with fenthion-induced hyperlipidemia, supplementation with a 5% *A. campestris* powder diet for 21 days restored normal lipid levels in the liver of both the mother rats and their offspring. These results suggest that *A. campestris* could be an effective natural treatment for hyperlipidemia, with potential benefits for both maternal and fetal health (Sefi *et al.* 2011).

In the context of diabetes, *A. campestris* has been shown to possess significant antidiabetic effects. In a study of alloxan-induced diabetic rats, treatment with the aqueous extract at 200 mg/kg for 21 days resulted in a 63% reduction in blood glucose levels, along with a 30% increase in serum insulin levels. Additionally, the plant extract improved glucose tolerance, as shown by a reduction in blood glucose levels during the glucose tolerance test. These findings highlight *A. campestris* as a promising candidate for managing diabetes, particularly in regulating blood sugar and improving insulin sensitivity (Rabehi *et al.* 2023).

The antihypertensive properties of *A. campestris* were confirmed in both hypertensive and normotensive rat models. In hypertensive rats treated with L-Nitro-Arginine Methyl Ester (L-

INTRODUCTION

NAME), a nitric oxide synthase inhibitor, the aqueous extract at a dose of 50 mg/kg prevented the onset of hypertension. In normotensive rats, intravenous administration of *A. campestris* extract caused a significant reduction in mean arterial pressure (MAP), systolic blood pressure (SBP), and diastolic blood pressure (DBP) without affecting heart rate. Both the essential oil and aqueous extract also exhibited vasorelaxant effects, inhibiting phenylephrine-induced contractions in isolated aortic rings, suggesting their potential for managing hypertension and improving vascular health (Sriti *et al.* 2024).

In wound healing studies, *A. campestris* has shown promising results. In rats with induced wounds, the aqueous extract led to a 50% reduction in wound size after just six days of treatment, with complete healing achieved by day 12. Histological examination revealed healthy tissue regeneration, including well-formed epidermal and dermal layers, complete re-epithelialization, and robust tissue granulation. These findings indicate that *A. campestris* may have applications in wound care and tissue regeneration, potentially benefiting those with chronic wounds or injuries (Ghlassi *et al.* 2016).

The anti-inflammatory effects of *A. campestris* are also significant. In one study, the essential oil of *A. campestris* neutralized the inflammatory effects of Cerastes venom in mice, reducing edema in the affected paw. Similarly, the aqueous extract administered at a dose of 200 mg/kg reduced the inflammation caused by carrageenan injection in rats, reducing edema volume and the number of inflammatory cells and restoring damaged tissues. This suggests that *A. campestris* could be a valuable natural anti-inflammatory agent (Younsi *et al.* 2017).

Furthermore, the plant has shown promise in anti-venom applications. In an experimental model of scorpion envenomation, the aqueous extract of *A. campestris* was administered prior to venom exposure, leading to a 30% reduction in mean arterial pressure in pregnant rats and a 10% reduction in non-pregnant rats. The co-administration of the extract with the venom prevented the hypertensive rise typically seen with envenomation, highlighting *A. campestris*'s potential as a natural antidote for venomous bites or stings (Hasegawa *et al.* 2021).

A. campestris has demonstrated antimicrobial activity, which could be useful in food safety and preservation. Due to their high phenolic content, its extracts' antimicrobial properties may help inhibit bacterial growth by disrupting bacterial cell membranes and producing hydroperoxides. This makes *A. campestris* a promising candidate for use in food control, helping to extend the shelf life of products by preventing spoilage and pathogenic bacterial contamination (Shaaban *et al.*, 2020).

INTRODUCTION

Polycystic ovary syndrome (PCOS) is a complex and multifactorial endocrine disorder that affects approximately 5–10% of women during their reproductive years, making it one of the leading causes of infertility in this population (Kicińska *et al.* 2023). This syndrome is characterized by hormonal, metabolic, and reproductive disruptions that impact a woman's health. PCOS is primarily marked by chronic anovulation, which leads to irregular menstrual cycles, an increased risk of infertility, and other systemic complications. However, it is important to note that some women with PCOS may still experience spontaneous ovulation and pregnancy, despite the common underlying reproductive dysfunction (Bilgory *et al.* 2023). The onset of menstrual irregularities often begins shortly after menarche and persists throughout the reproductive years, making the disorder a lifelong concern for many women (Karkera, Agard, and Sankova 2023).

The typical ovarian morphology observed in women with PCOS includes thickened ovarian cortices, numerous small cysts, and arrested follicular development. Histological examination reveals a range of abnormalities, including stromal hyperplasia, luteinization of the theca interna, and the development of immature follicles that fail to mature and ovulate. These morphological changes, which also include the presence of multiple cysts on the surface of the ovaries, disrupt normal ovulatory cycles and contribute to the infertility commonly associated with the disorder (Orsi, Baskind, and Cummings 2024). Ovarian size in women with PCOS can vary from average to significantly enlarged, with some cases exhibiting ovaries greater than 10 cm in diameter (Hoeger, Dokras, and Piltonen 2021). Ultrasonography remains a vital diagnostic tool for PCOS, revealing the characteristic "string of pearls" pattern, where multiple small antral follicles (typically between 6 and 10 mm in diameter) are arranged around the perimeter of the ovary (McGlacken-Byrne, Gunn, and Simpson 2024). This imaging characteristic is often seen in both humans and animal models of PCOS, further supporting its diagnostic utility.

In rodent models, particularly rats, PCOS is induced through various pharmacological or hormonal treatments, resulting in ovarian and metabolic changes that closely mimic those observed in humans. Histopathological examination of ovaries in these animal models typically shows an increase in atretic follicles, cystic follicles with thin granulosa cell layers, and thickened theca interna. Additionally, signs of stromal hyperplasia and luteinized unruptured follicles are often seen, reflecting similar pathophysiological processes to those found in human PCOS (Wang *et al.* 2023). These animal models provide valuable insights into the underlying mechanisms of PCOS and serve as a foundation for testing potential therapeutic interventions.

INTRODUCTION

The hormonal imbalances that define PCOS include elevated levels of androgens such as testosterone, androstenedione, dehydroepiandrosterone (DHEA), dehydroepiandrosterone sulfate (DHEAS), and 17-hydroxyprogesterone. These elevated androgen levels are responsible for many of the clinical manifestations of PCOS, including hirsutism, acne, scalp hair thinning, and an increased risk of metabolic disturbances. The excess androgen production is often due to the hyperactivity of the ovarian theca cells, which are stimulated by increased luteinizing hormone (LH) levels. This elevated LH-to-follicle-stimulating hormone (FSH) ratio further disrupts normal follicular development, preventing oocyte maturation and causing the ovaries' characteristic cystic appearance (Sabuncu *et al.* 2003). The combination of these hormonal changes leads to the characteristic symptoms of PCOS, which often include oligomenorrhea (infrequent menstruation), amenorrhea (absence of menstruation), and difficulty conceiving due to anovulation.

In addition to reproductive issues, women with PCOS often face several metabolic challenges, including insulin resistance, obesity, dyslipidemia, and an increased risk of cardiovascular disease. Insulin resistance is a key factor in the pathophysiology of PCOS, leading to compensatory hyperinsulinemia. This excess insulin not only promotes ovarian androgen production but also contributes to the accumulation of visceral fat, which exacerbates both metabolic and reproductive dysfunction. Many women with PCOS are overweight or obese, further complicating the metabolic issues associated with the disorder. Insulin resistance is also a significant risk factor for the development of type 2 diabetes, with women with PCOS being at a higher lifetime risk of developing this condition compared to the general population (Vyrides, El Mahdi, and Giannakou 2022). Additionally, PCOS is associated with a higher risk of developing metabolic syndrome, a cluster of conditions that include hypertension, hypertriglyceridemia, low HDL cholesterol, and central obesity. These metabolic disturbances increase the long-term cardiovascular risk in women with PCOS, highlighting the need for early and comprehensive management strategies.

The psychosocial impact of PCOS is also significant, as the condition can lead to emotional distress due to symptoms such as infertility, hirsutism, weight gain, and acne. The chronic nature of the disorder, combined with its visible and often stigmatizing symptoms, can lead to feelings of anxiety, depression, and low self-esteem. Women with PCOS may experience heightened psychological stress, which can further exacerbate metabolic and reproductive issues. As such, it is crucial for healthcare providers to address the mental health needs of women with PCOS as part of a holistic treatment plan. Psychological support, including counseling and support groups, can be an important aspect of managing the emotional burden of the condition (Vyrides, El Mahdi, and Giannakou 2022).

INTRODUCTION

The management of PCOS requires a multifaceted approach that addresses both the reproductive and metabolic aspects of the disorder. For women seeking to conceive, the primary treatment goal is to restore ovulation. This can be achieved through ovulation induction therapies, with clomiphene citrate being the most commonly prescribed medication. Clomiphene citrate works by stimulating the release of FSH, promoting follicular growth and ovulation. In cases where clomiphene is ineffective, gonadotropins or laparoscopic ovarian drilling may be used to enhance fertility. However, these treatments must be closely monitored to avoid complications such as ovarian hyperstimulation syndrome (OHSS) (Barzegar *et al.* 2017). For women who are not seeking pregnancy, hormonal therapies such as oral contraceptives are commonly used to regulate the menstrual cycle, reduce androgen levels, and improve symptoms such as hirsutism and acne. Anti-androgenic drugs, such as spironolactone, may be prescribed to reduce excessive hair growth, while metformin, a medication used to treat type 2 diabetes, can improve insulin sensitivity and promote ovulation (Vyrides, El Mahdi, and Giannakou 2022).

In addition to pharmacologic interventions, lifestyle modifications, particularly weight loss and regular physical activity, are critical for managing both the reproductive and metabolic symptoms of PCOS. Even modest weight loss (5-10% of body weight) can significantly improve insulin sensitivity, ovulatory function, and menstrual regularity. For overweight or obese women with PCOS, a combination of a balanced diet and regular exercise is essential not only for improving fertility but also for reducing the long-term risk of type 2 diabetes and cardiovascular disease (Barzegar *et al.* 2017).

In conclusion, PCOS is a complex, heterogeneous disorder that affects many aspects of a woman's health, including reproductive function, metabolic health, and psychological well-being. The pathophysiology of PCOS involves a combination of hormonal, metabolic, and ovarian changes that disrupt normal ovulation and increase the risk of long-term complications such as insulin resistance, type 2 diabetes, and cardiovascular disease. Early detection, comprehensive management, and multidisciplinary care are essential for optimizing health outcomes for women with PCOS. Ongoing research into the underlying mechanisms of PCOS and the development of new treatment modalities holds promise for improving the quality of life and long-term health of women affected by this prevalent and challenging condition (Karkera, Agard, and Sankova 2023).

Hypothyroidism is a clinical condition characterized by insufficient production of thyroid hormones, resulting in decreased circulating levels of thyroxine (T4) and triiodothyronine (T3). It primarily arises from dysfunction within the thyroid gland itself, a condition known as primary hypothyroidism. The causes of primary hypothyroidism include thyroidectomy,

INTRODUCTION

autoimmune thyroiditis (such as Hashimoto's thyroiditis), iodine deficiency, and the use of medications that interfere with thyroid hormone synthesis, such as thionamides, lithium, and iodine-based agents. Secondary hypothyroidism, or central hypothyroidism, occurs when the hypothalamus or pituitary gland fails to adequately stimulate the thyroid through thyroid-stimulating hormone (TSH) (Ibrahim *et al.* 2021). This dysfunction can also result in insufficient production of thyroid hormones, though less commonly. Both forms of hypothyroidism are further categorized into clinical and subclinical types. Clinical hypothyroidism presents with overt symptoms such as fatigue, weight gain, cold intolerance, and bradycardia, while an elevated TSH level characterizes subclinical hypothyroidism without the presence of significant clinical symptoms, though patients may still experience subtle manifestations of the disorder (Chaker *et al.* 2017).

The pathophysiology of hypothyroidism is complex and multifaceted. Thyroid hormones, particularly T3 and T4, play critical roles in regulating metabolism, thermogenesis, and energy homeostasis. They also influence lipid metabolism, and their deficiency often leads to lipid abnormalities. Hypothyroidism is commonly associated with elevated levels of low-density lipoprotein (LDL) cholesterol and total cholesterol, increasing the risk of atherosclerosis and cardiovascular diseases. A study by Ashwini *et al.* (2017) demonstrated that hypothyroid patients exhibited significant increases in LDL and total cholesterol levels, although other lipid fractions such as high-density lipoprotein (HDL) and triglycerides did not show marked deviations. Furthermore, hypothyroidism is known to contribute to reduced basal metabolic rate (BMR), which leads to common symptoms such as weight gain, cold intolerance, and generalized fatigue. Beyond metabolic disturbances, hypothyroidism can also affect the central nervous system, causing cognitive dysfunction, memory impairment, and depression, which can significantly impact patients' quality of life (Schlenker *et al.*, 2012).

To induce hypothyroidism in experimental animal models, researchers commonly use antithyroid drugs such as methimazole and propylthiouracil (CBZ), which inhibit thyroid hormone biosynthesis. These animal models help elucidate hypothyroidism's metabolic, cardiovascular, and neurocognitive effects (Ferreira *et al.* 2007). In clinical practice, the mainstay of hypothyroidism treatment is levothyroxine, a synthetic form of the inactive thyroid hormone T4. Levothyroxine is typically administered to normalize thyroid hormone levels, aiming to alleviate the symptoms of hypothyroidism and restore metabolic balance. Despite being widely used, levothyroxine therapy does not always fully resolve the clinical manifestations of hypothyroidism. Studies have shown that 10–15% of patients receiving levothyroxine monotherapy continue to experience symptoms, including fatigue, depression, and cognitive impairment. These persistent symptoms may be due to insufficient conversion

INTRODUCTION

of T4 to the more biologically active T3, or potentially due to peripheral resistance to thyroid hormones (McAninch and Bianco 2016). This highlights the need for a more individualized approach to treatment, as some patients may benefit from combination therapies involving both T4 and T3, although such treatments remain controversial and lack conclusive evidence in large-scale clinical trials (Chakera, Pearce, and Vaidya 2011).

Moreover, the management of hypothyroidism may be further complicated in patients with comorbid conditions, such as autoimmune diseases, that require special attention to therapy adjustments. While levothyroxine is considered the standard treatment, there has been growing interest in exploring alternative or adjunctive therapies for hypothyroidism, particularly through the use of herbal medicines and supplements. Various studies have investigated the efficacy of herbs such as ashwagandha, guggul, and selenium in managing hypothyroidism, with some suggesting that these may help enhance thyroid function and mitigate symptoms. However, further clinical studies are necessary to assess their safety, effectiveness, and potential integration into standard care (Pankhuri Wanjari and Jayadeepa 2012).

In conclusion, hypothyroidism is a complex metabolic and endocrine disorder that has far-reaching effects on various organ systems, particularly the cardiovascular and nervous systems. Despite the effectiveness of levothyroxine in managing the condition, a substantial proportion of patients continue to experience significant symptoms, underscoring the need for more personalized treatment strategies. Research into adjunctive therapies, including combination therapy with T3 and the potential role of herbal treatments, is essential for improving patient outcomes and enhancing quality of life. With appropriate treatment and management, individuals with hypothyroidism can achieve a substantial improvement in their health and well-being, though ongoing monitoring and adjustments to therapy are critical for optimal care.

This thesis aims to investigate the therapeutic potential of *Artemisia campestris* L. in modulating thyroid and ovarian functions, employing a multidisciplinary approach that integrates *in vitro*, *in vivo*, and *in silico* methodologies. The primary objective is to explore the effects of *Artemisia campestris* on thyroid and ovarian dysfunctions, with particular emphasis on its therapeutic efficacy *in vivo*, a pioneering aspect of this research. This study is structured into two principal sections, with the second part subdivided into three subcomponents, each addressing different experimental approaches. The first section of the thesis offers a comprehensive bibliographic overview of *Artemisia campestris* L., focusing on its chemical composition. It then provides a detailed analysis of its bioactive compounds, emphasizing their pharmacological properties and potential therapeutic implications.

INTRODUCTION

The second section of the thesis presents the experimental work, divided into three subparts: *in vitro*, *in vivo*, and *in silico* studies. The *in vitro* component begins with an aqueous extract of *Artemisia campestris*, followed by a thorough characterization of its bioactive compounds through qualitative and quantitative analyses. Biological assays assess the plant extract's antioxidant, anti-inflammatory, and enzymatic activities, identifying the bioactive compounds responsible for its therapeutic effects. The *in vitro* studies are designed to provide insight into the mechanisms by which *Artemisia campestris* exerts its effects at the cellular level, particularly about endocrine functions.

In vivo studies form the second subpart of the experimental work, where the therapeutic effects of *Artemisia campestris* are investigated in a rat model, specifically focusing on thyroid and ovarian dysfunctions. This aspect of the research is pioneering, as it represents the first *in vivo* investigation of the effects of *Artemisia campestris* on these endocrine systems. The *in vivo* studies aim to determine whether the plant extract has the potential to restore normal thyroid and ovarian function, assessing both hormonal and physiological markers of endocrine health.

The third subpart involves *in silico* studies, which utilize molecular docking to explore the interactions between the bioactive compounds of *Artemisia campestris* and key biological targets relevant to thyroid and ovarian function. Among the primary targets is thyroperoxidase, an enzyme essential for thyroid hormone synthesis. Additionally, proteins associated with ovarian function and other endocrine-related pathways are studied. This computational approach offers a molecular-level understanding of the interactions between the plant's bioactive compounds and their targets, complementing the findings from the *in vitro* and *in vivo* experiments.

The results and discussion section consolidates the findings from the experimental studies, providing strong evidence for the pharmacological potential of *Artemisia campestris* L. in modulating thyroid and ovarian dysfunctions. The data demonstrate that its bioactive compounds may exert significant therapeutic effects, restoring balance to these endocrine systems. These results are interpreted in the context of existing therapeutic approaches, highlighting the potential of *Artemisia campestris* as a novel, plant-based therapeutic option.

The significance of this research lies in the fact that current treatments for thyroid dysfunction, such as thyroidectomy or hormone replacement therapy, do not address the underlying pathophysiology of these disorders. Although these therapies are widely used, they often fail to restore normal thyroid function fully. By integrating *in vitro* assays, *in vivo* experiments, and *in silico* modeling, this study offers a novel perspective on the therapeutic mechanisms of *Artemisia campestris*, potentially leading to more effective plant-based

INTRODUCTION

therapeutic strategies for managing thyroid and ovarian disorders. The findings of this research may contribute to the development of alternative treatments that address the root causes of endocrine dysfunctions, offering a promising avenue for future therapeutic interventions.

EXPERIMENTAL STUDY

CHAPTER I

Material & Methods

1. Materials

1.1. Plant

Specimens of *Artemisia campestris* were collected in Sedrata, a city in the Souk-Ahras province of northeastern Algeria. This province is strategically located, bordered by El-Taref and Annaba to the north, Guelma to the west, Tbessa to the south, and Tunisia to the east, serving as a link between the northern region, the high plateaus, and the southern part of the country. The landscape is predominantly mountainous, comprising about 60% of the total area, with coordinates of approximately 36°17'36.98"N latitude and 7°53'14.23"E longitude, at an altitude of 755 meters. The collection occurred in May 2022 in a clean, unpolluted area and was conducted before sunrise to minimize the evaporation of bioactive compounds.

The leaves were then sent straight to the laboratory (LBEH). Dr. Chouikh Atef, a professor in the biological sciences department of the Faculty of Sciences of Natural and Life from Echahid Hamma Lakhedar University in El-Oued, Algeria, defined the leaves scientifically. The leaves were thoroughly cleaned and then air-dried. The premium dried leaves were kept in a dry plastic container until required for the extraction processes.



Figure 1. *Artemisia campestris* L. (CHERFI Inasse)

1.2. Animals

For this investigation, 30 adult albino Wistar rats were provided by the laboratory (LBEH). The Molecular and Cellular Biology Department. Faculty of Natural and Life Sciences, University of El-Oued, Algeria, animal house housed all the rats. Under identical laboratory circumstances of photoperiod (12 hours of light and 12 hours of darkness), relative humidity of $62\pm 3\%$, and room temperature of 25°C , the rats weighed $222.35\pm 2.91\text{g}$. During the trials, tap water and standard rat food were freely available. The local ethical committee's suggested methods were adhered to in the handling and care of the rats during all experimental procedures.

1.3. Chemicals and reagents

Alpha amylase, 3,5-Dinitrosalicylic acid (DNS) $((\text{O}_2\text{N})_2\text{C}_6\text{H}_2\text{-2-(OH)CO}_2\text{H})$, p-nitrophenyl α -D-glucopyranoside (PNPG) $(\text{C}_{12}\text{H}_{15}\text{NO}_8)$, Phosphate buffer $(\text{NaH}_2\text{PO}_4 \cdot 2\text{H}_2\text{O})$ 20 mM, pH 6.7, including 6.7 mM sodium chloride), and Starch (250 μl , 0.5% w/v). Phosphate buffer (2.5 mL, 50 mM, pH=7), H_2O_2 (1 mL, 1%), 1,1-Diphenyl-2-picrylhydrazyl (DPPH $^{\circ}$), ethylene diamine tetra-acetic acid (EDTA), trichloroacetic acid (TCA), thiobarbituric acid (TBA) and nitro blue tetrazolium (NBT), Butylated hydroxyanisole (BHA), were purchased from Biochem Chemophara. United Kingdom. However, commercial kits procured from Spinreact (Barcelona, Spain) were employed to test biochemical markers. Sigma-Aldrich provided the remaining chemicals, reagents, and organic solvents (USA).

Guaiacol peroxidase $(\text{C}_7\text{H}_8\text{O}_2)$ 1 mL, 1%) was obtained from the Department of Chemistry. Poznan, Poland, Estradiol valerate, Carbimazole (CBZ, 5 mg tablets), Levothyrox $^{\circledR}$ (LEV, 100 μg tablets), and estradiol valerate (EV 2mg tablets) were sourced from the El-Oued, Algeria pharmacy.

2. Methods

2.1. Phytochemical analysis of *Artemisia campestris* L.

2.1.1. Extraction of *A. campestris* Aqueous extract

The *A. campestris* leaves (20g) were dried, powdered, and added to 250 mL of distilled water. After 24 h at room temperature, the mixture was filtered with filter paper. Finally, the

filtrates were evaporated in an oven at 45°C to produce dried residues (active principles). The extract was stored at four °C in a refrigerator for subsequent experiments.

2.1.2. Phytochemical analysis

The standard methods include identifying phytochemical compounds in *A. campestris* aqueous crude extract (polyphenols, flavonoids, tannins) (Harborne and Harborne 1973; Evans 2009).

2.1.3. Quantification of phytochemicals compounds

2.1.3.1. Estimation of total phenolics

The folin-Ciocalteu method (Slinkard and Singleton 1977) was used to determine the total amount of phenolics, 1 mL of 10% Folin-Ciocalteu reagent, and 0.2 mL of the aqueous extract of *A. campestris* was added. After 4 minutes, 0.8 mL of sodium carbonate (75 g/L) was added. After two hours of incubation at room temperature, the absorbance was measured at 765 nm. Gallic acid was used as the standard for the linear calibration equation. The total phenolic content was expressed in ug equivalent of gallic acid per mg of extract.

2.1.3.2. Estimation of total flavonoids

To ascertain the total flavonoid content of the *A. campestris* extract, the aluminum chloride (AlCl₃) colorimetric method was employed (Wairata *et al.* 2022); 1 mL of the AlCl₃ solution was mixed with 1 mL of the sample. The same volume as the standard and the results are determined using a linear calibration equation with quercetin as the standard after 30 minutes. The absorbance at 430 nm was measured against the prepared reagent blank. The findings were shown as ug of quercetin for every milligram of extract.

2.1.3.3. Estimation of condensed tannin

The amount of tannin in the *A. campestris* leaf extract was measured (Kılıç *et al.*, 2024) 0.5 ml of the sample was well mixed with 3.0 mL of vanillin reagent (4% w/v vanillin in methanol) before adding 1.5 mL of 8% hydrochloric acid. After fifteen minutes, the reaction's absorbance was measured at 500 nm concerning water. The reference value of catechin was used to blot the sample amounts and the standard absorbance curve. The results were given as mg of extract divided by ug of catechin.

2.1.3.4. Qualitative analysis by UPLC

As described by Stuper-Szablewska and Perkowski (Stuper-Szablewska and Perkowski 2017). UPLC was used to determine the bioactive compounds. A customized Acquity H class UPLC system equipped with a Waters Acquity PDA detector (Waters, USA) was used to analyze the samples. A mixture of methanol, Acetonitrile, and water (85:10:5) was used for elution, with a flow rate of 0.4 milliliters per minute. An Acquity UPLC[®] BEH C18 column (100mm x 2.1 mm. particle size 1.7 μ m) (Waters, Ireland) was used for the chromatographic separation. Molecules were detected using a Waters Acquity PDA detector (Waters, USA) set at 282 nm.

2.1.2. Analysis of *A. campestris* L'essential oil

2.1.2.1. Extraction of essential oil

The extraction process was conducted at the Laboratory of Biology, Environment, and Health, Faculty of Natural Sciences and Life, El-Oued University. ACEO was extracted using hydro-distillation. Precisely, 100 g of the dried aerial parts were placed in a 500 mL flask filled with distilled water and boiled for 2-3 h. The resulting vapors were condensed and collected in a separating funnel; ACEO was stored in an opaque glass bottle at 4 ± 1 °C in a hermetically sealed vial to prevent air, light, and temperature degradation.

2.1.2.2. GC-MS analysis technique

The chemical composition of the ACEO was analyzed using gas chromatography-mass spectrometry (GC-MS) following the method of Stuper-Szablewska (Stuper-Szablewska and Perkowski 2017). The GC-MS analysis was performed on a Thermoquest-Finnigan Trace GC/MS instrument equipped with a DB-1 fused silica column (30 m, 0.25 mm i.d., film thickness 0.25 μ m). The oven temperature was programmed to increase from 60 °C to 250 °C at a rate of 5 °C/min, then held at 250 °C for 10 minutes. The transfer line temperature was set to 250 °C. Helium was used as the carrier gas at a flow rate of 1.1 mL/min with a split ratio of 1:50. Identifying essential oil constituents was achieved by comparing their mass spectra and retention times (Rt) with those reported in the literature and with authentic samples.

2.2. In Vitro Activity of the *A. campestris* aqueous extract and essential oil

2.2.1. Antioxidant activity

2.2.1.1. DPPH[°] free-radical scavenging activity

To evaluate the scavenging activity of 2,2-diphenyl-1-picrylhydrazyl (DPPH[°]). The procedure of Kumar *et al.* (Kumar *et al.* 2012) was used that the stable free radical DPPH[°] is frequently used to assess the antioxidant component's capacity to scavenge free radicals; It was modified slightly. A volume of *A. campestris* leaves extract at different concentrations (7

to 125 µg/mL) was mixed with 1 mL of methanolic solution of DPPH° (0.1 mM; 4 mg DPPH° was dissolved in 100 mL methanol). The mixture was forcefully agitated in the dark and at a room-temperature environment and left to settle for 30 minutes at 517 nm. The mixture's absorbance was measured using a spectrophotometer. The reaction mixture's lower absorbance showed a higher percentage of scavenging activity. The following equation yields the free radical scavenging activity:

$$\text{DPPH}^\circ \text{ scavenging effect (\%)} = ((A_0 - A_1)/A_0) \times 100$$

A₀. The absorbance of the control

A₁. Sample extract's absorbance after 30 minutes.

2.2.1.2. Ferric reducing antioxidant power assay (FRAP)

The ferric-reducing power of the extract of *A. campestris* leaves was measured using Oraiza (1986) methods with some modifications; 5–75 µg/mL concentrations of the samples were mixed with 1 mL of both potassium ferricyanide (1%), and phosphate buffer (0.2 M. pH = 6.6), After adding 0.5 mL of trichloroacetic acid (10% w/v), After 20 min at 50 °C incubation, the samples were centrifuged for 10 minutes. An identical amount of supernatant and deionized water, 0.125 mL of ferric chloride (0.1%), were combined. The exact process was used for ascorbic acid as a positive control. The absorbance was measured using a UV-vis spectrophotometer at 700 nm.

Total antioxidant activity (FRAP) was measured in milligrams of AAE per milligram of samples (Ahmouda *et al.*, 2022).

2.2.1.3. β-carotene bleaching assay

The *Artemisia campestris* aqueous extract's ability to inhibit β-carotene bleaching was evaluated following the methods outlined in the reference (Loucif *et al.*, 2020). A stock solution of β-carotene/linoleic acid was prepared by dissolving 0.5 mg of β-carotene, 25 mL of linoleic acid, and 200 mL of Tween 40 in 1 mL of chloroform. The chloroform was evaporated using a rotary evaporator at 40°C under vacuum. After this, 100 mL of bidistilled water was added and vigorously agitated to form an emulsion prepared fresh for each experiment. Aliquots (2.5 mL) of the β-carotene/linoleic acid emulsion were mixed with varying concentrations of ACAE in test tubes. After a two-hour incubation at 50°C, the

absorbance of each sample was measured at 470 nm, BHA was used as a positive control standard, and a control tube without any sample was included.

The antioxidant activity in the β -carotene bleaching model was calculated as a percentage using the following formula:

$$\text{Antioxidant activity\%} = \frac{1 - (A_0 - A_t)}{(A'_0 - A'_t)} * 100$$

A_0 and A'_0 represent the sample and blank absorbances, respectively, measured at time zero. A_t and A'_t represent the sample and blank absorbances, respectively, recorded two hours later. The tests were run three times; BHT was used as a positive control in the same process.

2.2.2. Anti-inflammatory activity (Albumin denaturation test)

The albumin denaturation model was chosen to evaluate the anti-inflammatory properties *in vitro* of crude extracts of *A. campestris*. According to the method described by Padmanabhan and Jangle (2012) with a few changes. 1 mL of the extract at various concentrations was combined with 1 mL of 5% human albumin. The tubes were incubated at 27 °C for 15 minutes and then for 10 minutes at 70 °C in a water bath; 660 nm was the wavelength for their absorbance after cooling to room temperature. As a baseline, diclofenac sodium is utilized. The findings are shown as mg of equivalent diclofenac sodium per mg of extract.

2.2.3. α -amylase inhibition assays

A 1% starch solution is prepared by dissolving 1 g of potato starch in 100 mL of a 20 mM sodium phosphate buffer, which consists of 0.1324 g $\text{NaH}_2\text{PO}_4 \cdot \text{H}_2\text{O}$ and 0.2788 g Na_2HPO_4 , supplemented with 6.7 mM sodium chloride (0.039 g), and adjusted to a pH of 6.9. Separately, an alpha-amylase solution is prepared by dissolving 0.0253 g of alpha-amylase in 100 mL of cold distilled water, yielding a concentration of 1 unit/mL. For the enzymatic assay, 100 μL of either the control, standard, or sample (comprising extracts or essential oils at a concentration of 100 $\mu\text{g}/\text{mL}$) is mixed with 900 μL of the alpha-amylase solution, followed by incubation at 37°C for 10 minutes. Subsequently, 500 μL of the starch solution is introduced, and the mixture undergoes a second incubation at 37°C for an additional 10 minutes. Following the incubation steps, 500 μL of dinitrosalicylic acid (DNS) reagent is added, and the reaction mixture is heated in a boiling water bath for 5 minutes. After cooling in an ice bath, 3 mL of distilled water is added, and the absorbance is recorded at 540 nm

against a blank. The assay measures maltose production, which is determined by the reduction of 3,5-dinitrosalicylic acid to 3-amino-5-nitrosalicylic acid, detectable at 540 nm. When beta-amylase inhibitors are present, maltose production decreases, leading to a corresponding reduction in absorbance (Nadji *et al.*, 2022).

Percentage inhibition is determined using the following equation:

$$inhibition (\%) = \frac{(Ac - (As1 - As0))}{Ac} * 100$$

In this context, Ac represents the absorbance of the control reaction, which includes all components except the standard or sample. As1 denotes the absorbance measured in the presence of the standard or sample (plant extract) combined with the enzyme and starch solution. In contrast, As0 corresponds to the absorbance observed when the standard or sample is present, but neither the enzyme nor the starch solution is included.

2.2.4. Measurement of guaiacol peroxidase

Guaiacol Peroxidase (GPX) activity was investigated using research methodology (Hadadi, Nematzadeh, and Ghahari 2020), Phosphate buffer (2.5 mL. 50 mM. pH=7), H₂O₂ (1 mL. 1%), guaiacol (1 mL. 1%). and enzyme extracts (20 µL) were the components of the reaction mixture. Using a spectrophotometer (Biochrom WPA Biowave II UV/Visible), the absorbance of the reaction solutions was measured at 470 nm. The increase in absorbance at 470 nm was monitored for one minute. The activity was expressed as mg⁻¹ protein mmole activity.

2.3. *In vivo* activity of aqueous extract

2.3.1. PCOS Experiment

The experimental design was modified from a recent study (Hosseini *et al.*, 2023). The rats were randomly divided into three groups:

Control Group: No injection; PCOS Group: Administered 2 mg/kg estradiol valerate for 60 days to induce polycystic ovary syndrome (PCOS); Experimental Group: Received 2 mg/kg estradiol valerate for 60 days, followed by 200 mg/kg body weight of *A. campestris* extract administered orally for an additional 15 days. The appearance of ovarian cysts was typically noted 60 days after the estradiol valerate injection.

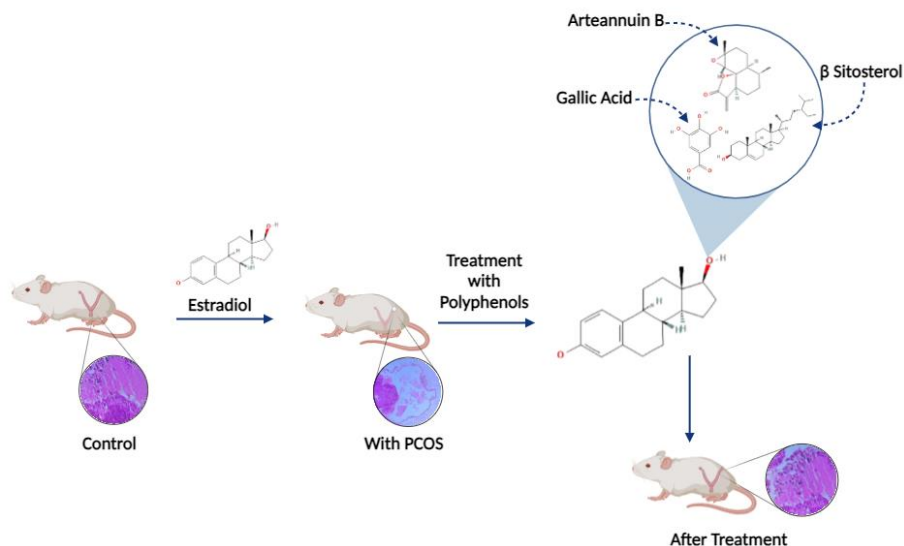


Figure 2. An overview of the PCOS study's experimental protocol.

2.3.2. Hypothyroidism Experiment

For a broader examination of thyroid function, another cohort of rats was created, consisting of four experimental lots with 20 albino rats ($n = 5$ per lot) based on the following treatments:

Lot I (Control): Untreated; Lot II: Induced hypothyroidism using carbimazole (CBZ) (Siddiqui *et al.*, 2015) at 20 mg/kg body weight; Lot III: Received CBZ alongside 200 mg/kg body weight of *A. campestris*; Lot IV: Administered levothyroxine (LEV) at 0.1 mg in conjunction with CBZ. At the beginning of the trial, all lots except Lot I had no HPO induced. The diet was standardized, comprising 10% mealworms, 30% wheat bran and 60% corn without iodine. Post-30 days of carbimazole therapy. Group III received an additional 30-day treatment of *A. campestris* alongside carbimazole. In contrast, Group IV was given levothyroxine concurrently with carbimazole. The study adhered strictly to ethical guidelines for medical animal research. Consistent with the Helsinki Declaration. It has also received approval from the Scientific Council of the Faculty of Natural Sciences and Life at El-Oued University. Algeria.

2.3.3. Histopathological and blood sample

After the rats were anesthetized and dissected, the sections of their thyroid and ovaries were taken, and they were preserved in 10% formaldehyde until the time came to cut the slices for examination. After being washed with xylene and submerged in paraffin, the samples were dehydrated in an increasingly graded ethanol series (60. 70%. 80%. and 100%).

Using a Thermo Scientific (Micron HM 325) Histoline Rotary Microtome, paraffin blocks were sectioned into 4-6 μm layers. The photograph was colored with hematoxylin and eosin, The histopathological inspection was done with a light microscope.

Blood samples were collected and centrifuged at 3000 rpm for 15 minutes at 4 °C to recover serum. The resulting plasma was stored at -20°C until analysis. Serum TSH levels were analyzed using radioimmunoassay (IRMA) employing commercial kits (IM3712 from Immunotech Inc, Beckman Coulter, France; A85726 from Cis Bio Bioassays. France). Serum concentrations of FT4 and T3 were determined using radioimmunoassay (RIA) kits (IM1363 and IM3321 for FT4 and A56719 for TPO-Ab assays, respectively, from Immunotech Inc, Beckman Coulter. France). Serum concentrations of FSH and LH were assessed using a Rat/mouse ELISA Kit (Cosmo Bio Co. Ltd.. Japan).

2.4. Molecular Docking Study

Five compounds were identified using UPLC and presented in Table 6 to study their potential behavior against thyroid peroxidase receptors; this might give an insight into the main compound that has the desired effect on the biological activity studied.

Using AutoDock tools 1.5.6 (Bullock *et al.*, 2010). the targeted receptor (PDB ID: 5FF1. resolution: 1.97 Å) is prepared by removing water molecules and heat atoms. Adding polar hydrogen only. and adding the Kollman charges. Further, the grid box center was set to 4.147 \times 4.077 \times 34.338 for x, y, and z, in order, with default grid size and spacing of 0.375 Å. LGA algorithm was chosen for calculations; the number of runs was 40, and the initial population was set to 150 individuals; all other parameters were set to default. The outcomes are compared regarding the binding affinity score for best-docked conformation to investigate the activity regarding binding affinity (Kcal/mol). The chosen compounds were based on the majority concentration in the plant extraction. 2,3-Butanediol, β -Sitosterol, β -Pinene. α -Curcumene, and Arteannuin B were downloaded from the PubChem database (<https://pubchem.ncbi.nlm.nih.gov/>) in sdf format with CIDs: 262, 222284, 14896, 442360, 6543478, respectively. Then, it was transformed to pdb format using Discovery Studio V 2021 (BIOVIA 2021). The docking interactions were analyzed and visualized in 2D and 3D according to the least binding affinity.

2.4.1. Drug likeness of ligands and pharmacological studies

Specific properties should be considered when it comes to drug discovery. The Lipinski rules of five are essential to predict active compounds, as shown in Table 2. According to

Lipinski's rules, several properties must be considered before conducting a molecular investigation. The studied compounds should have a molecular weight of <500 Da. Log-P value <5, donor hydrogen bond <5, Acceptor hydrogen bonds <10, and molar refractivity between 40-130. The significant features of novel drugs are ADME (Absorption, Distribution, Metabolism, and Excretion). The pharmacological properties of the drugs were evaluated using the SwissADME online web server (<http://www.swissadme.ch/>) as the physicochemical and pharmacokinetic ProTox-II server was employed to examine the toxicological traits.

2.4.2. Ligands and receptors selection

Seven bioactive compounds identified in the essential oil of *A. campestris* were selected for *in silico* studies based on their high concentration content, as determined by GC-MS analysis. The compounds were retrieved from PubChem (<https://pubchem.ncbi.nlm.nih.gov/>). The X-ray crystal structures of four target proteins—Insulin-like Growth Factor 1 Receptor (IGF1, PDB ID: 3I81), Mitogen-Activated Protein Kinase Kinase 1 (MEK1, PDB ID: 3SLS), Phosphoinositide 3-Kinase Gamma (PI3K, PDB ID: 5JHB), and Janus Kinase 1 (JAK1, PDB ID: 6SM8)—were obtained from the Protein Data Bank.

2.4.3. Ligands preparation

The selected compounds—Linalyl acetate (CID: 8294), 3-cyclopentyl-N-(2-(3,4-dimethoxyphenyl)ethyl)propanamide (CID: 918363), Cyclohexanol, 1-methyl-4-(1-methylethyl)-1-acetate (CID: 117304), Geranyl acetate (CID: 1549026), Isoeugenyl acetate (CID: 1715136), Lavandulyl acetate (CID: 14268092), and Eucalyptol (CID: 2758)—were downloaded from PubChem in SDF format. The SDF files were converted to PDB format using Discovery Studio V2021 (Trott and Olson 2010); for docking studies. The biomolecules were saved in pdbqt format using AutoDock Tools (V1.5.6) (BIOVIA 2021).

2.4.4. *In silico* study of pancreatic cancer

After water and hetatm were removed from the receptor's structure, the protein structures were saved in pdbqt format, Co-crystallized ligands of selected targets for pancreatic cancer. PDB IDs are BMS-754807, UCB1353770, PIKin3, and AZD4205 for IGF1 (Figure. 4. A), MEK1 (Figure. 4. B), PI3K (Figure. 4. C) and JAK1 (Figure. 4. D), respectively, were extracted from the receptor crystal structure and saved as pdbqt format using Auto Dock Tools for further process.

To evaluate the quality of the docking protocol, the extracted co-crystallized ligand, using Auto Dock Tools. from the crystallographic structure of the protein, were re-docked using AutoDock Vina packages (Trott and Olson 2010). and their Root Mean Square Deviation (RMSD) values were retrieved. An RMSD value cut-off is less than 2 Å compared to the crystallographic form of the ligand (Adeniji, Arthur, and Oluwaseye 2020). is considered a good prediction for computed ligand-protein confirmation. The docking output files were generated to analyze further the interactions between the biomolecules and the amino acids of protein in the active site. and 2D and 3D views were obtained using Discovery Studio Visualizer (Vianna and de Azevedo 2012).

2.5. Statistical analysis

The results are presented as mean \pm standard error of the mean (Mean \pm SE). The statistical package for social sciences (SPSS), version 22. was used to compare the means of the various groups. One-way ANOVA and Duncan's multiple range test (DMRT) at $p=0.05$ were used to calculate significant differences between means. At $p\leq 0.05$. differences were deemed significant.

- ✓ Significant (* or a $P \leq 0.05$).
- ✓ Highly significant compared with the control (** or b $P \leq 0.01$).
- ✓ Very highly significant compared with the control (***) or c $P \leq 0.001$).

CHAPTER II

Results and Discussion

1. Optimizing Extraction Yield

Paying attention to the methodological approach, optimizing the hydro-distillation extraction protocol of *Artemisia Campestris* L. leaves was conducted using Design Expert 12 software, employing Response Surface Methodology (RSM) along with the Box-Behnken Design (BBD). These approaches systematically evaluated the influence of three key parameters: extraction time, extractor power, and the plant-to-water ratio (g/mL). The use of RSM and BBD ensured a structured and scientific framework, helping to capture the interactions between the variables while minimizing the number of experimental runs. The objective was to identify optimal conditions that maximize extraction efficiency, demonstrating a rigorous and methodological approach to improving the extraction protocol.

The yield of the plant in essential oil can be determined by calculating the following ratio:

$$\text{Rdt (\%)} = \text{P1/ P2 x 100}$$

P1: weight of the essential oil obtained.

P2: weight of the initial plant material.

The yield is 22.22 percent.

2. Determination of the total polyphenols and flavonoids

Researchers have recently been interested in the pharmacological characteristics of therapeutic plants (antioxidants and anti-inflammatories); these plants are considered significant because they contain secondary metabolites. Table 1 shows the polyphenol, flavonoid, and tannin contents of the *Artemisia campestris* aqueous extract. Aqueous extracts have a significant polyphenol concentration. Djeridane *et al.*, (2006) discovered that the *A. campestris* extract had more total phenolic components than flavonoids and tannins. This investigation found that the aqueous extract had a significant flavonoid content.

Table 1. Total phenolic and flavonoid in *A. campestris* extracts' aqueous extract.

	Concentration
Polyphenols content	88.89±11 mg GAE/g Ext
Flavonoids content	19.72±05 mg QE/g Ext
Condensed tannins	5.19 ± 02 mg CTE/g Ex

GAE: Gallic acid equivalent

QE: Quercetin equivalent

CTE :Catechin equivalent

2.1.UPLC composition analysis of leaf extract

Table 2 showcases the secondary metabolites identified from the UPLC analysis of the *A. campestris* leaf extract. A total of 26 secondary metabolites were detected, highlighting the diversity of bioactive compounds present in the plant. These compounds belong to different classes, including phenolic acids, flavonoids, and terpenoids; Each playing a potential role in the biological activities of the extract. The compounds range from well-known substances such as artemisinin, scopoletin, and β sitosterol to various caffeoylquinic acid derivatives and flavonoids like quercetin and rutin. Among these. β -sitosterol was found in the highest concentration at 15.7 U/ μ g. followed by arteannuin B (3.1 U/ μ g) and scopoletin (1.2 U/ μ g). This suggests that sterols, sesquiterpenes, and phenolic acids are prominent extract components. Figure 1 presents the molecular structures of essential polyphenolic compounds identified, such as quercetin, chlorogenic acid, rutin, and various caffeoylquinic acid derivatives. These polyphenols are recognized for their antioxidant properties, contributing to the potential therapeutic uses of the leaf extract. The data from UPLC confirms the presence of a rich phytochemical profile in *A. campestris*, with various compounds exhibiting a wide range of biological activities that could be explored for pharmacological applications. UPLC was used to identify secondary metabolites in the leaf. This revealed the presence of a total of 26 secondary metabolites belonging to different classes.

Table 2. UPLC was used to identify secondary metabolites in the leaf. This revealed the presence of a total of 26 secondary metabolites belonging to different classes.

Compounds	Concentration U/ μ g	Retention time (min)
Artemisinin	0.60	2.20
Scopoletin	1.20	5.57
Arteannuin B	3.10	2.5
5-O-((E)-Caffeoyl)quinic acid	0.61	4.18
Quinic acid	0.40	0.81
1.3-Di-O-caffeoylquinic acid	0.90	8.93
3.5-Di-O-caffeoylquinic acid	0.04	6.87
3.4-Di-O-caffeoylquinic acid	0.01	6.69
Methyl-3.4-di-O-caffeoylquinic acid	0.77	12.57
Chlorogenic acid	0.03	3.85
3.6'-O-diferuloylsucrose	0.05	16.74
Gallic acid	0.33	0.63
5'- β -D-glucopyranosyloxyjasmonic acid	0.08	19.74
Jasmonic acid	0.01	2.50
Chrysosplenol D	0.04	3.07
Artemisinic acid	0.004	9.20
Deoxy-artemisinin	0.032	9.47
Artemetin	0.01	4.76
P-hydroxybenzoic acid	0.01	5.45

Nicotinic acid	0.04	2.98
Salicylic acid	0.06	13.31
β -sitosterol	15.7	2.90
Quercetagenin-6.7.3'.4'-tetramethyl ether	0.22	14.87
Rutin	0.36	13.11
Quercetin	0.15	20.7
t-cinnamic acid	0.21	14.50

3. Anti-oxidant activity

3.1.DPPH° scavenging test

The IC₅₀ value is inversely related to a compound's antioxidant activity, meaning that a lower IC₅₀ indicates a more remarkable ability to scavenge free radicals. According to our findings, the leaf extract demonstrates significant anti-free radical activity (IC₅₀ = 4.34 ± 0.02 µg/ml), notably superior to the reference antioxidant BHA (IC₅₀ = 5.73 ± 0.41 µg/ml). notably superior to the reference antioxidant BHA (IC₅₀ = 5.73 ± 0.41 µg/ml).

3.2.Reducing power test

In the FRAP test, ferric iron is reduced to ferrous iron. forming a chromogenic complex in the presence of reductive agents and the potassium ferrocyanide complex (Kalita *et al.*, 2013). Our findings revealed that aqueous extract possesses a significant capacity for iron reduction. Specifically, the aqueous extract demonstrated an average reducing power of 6.19 ± 0.43 $\mu\text{g/ml}$, which is lower than the 21.68 ± 0.51 $\mu\text{g/ml}$ reported in a recent study (Trifan *et al.*, 2022). it still shows a more robust iron-reducing capability than BHA, which exhibited an average reducing ability of 8.41 ± 0.67 $\mu\text{g/ml}$.

3.3. β -carotene bleaching assay

Several writers state that the test of inhibiting linoleic acid oxidation connected to β -carotene appears to be a beneficial mimetic model of lipid peroxidation in biological membranes (Tepe *et al.*, 2005). In the β -carotene/linoleic acid assay, the aqueous extract of *A. campestris* inhibited linoleic acid peroxidation strongly with 3.27 ($\mu\text{g/mL}$). These results were comparable to the standard, BHA 0.90 ± 0.02 ($\mu\text{g/mL}$) (Table 3).

Table 3. Antioxidant activity of *A. campestris* extracts. DPPH° activity. FRAP activity. and β -carotene activity.

Assay	IC ₅₀ ($\mu\text{g/mL}$)		
	DPPH°	Reducing Power (FRAP)	β -Carotene
Plant extract	4.34 ± 0.02	6.19 ± 0.43	3.27 ± 0.03
BHA	5.73 ± 0.41	8.41 ± 0.67	0.90 ± 0.02

3.4.Antioxidant activity of essential oil

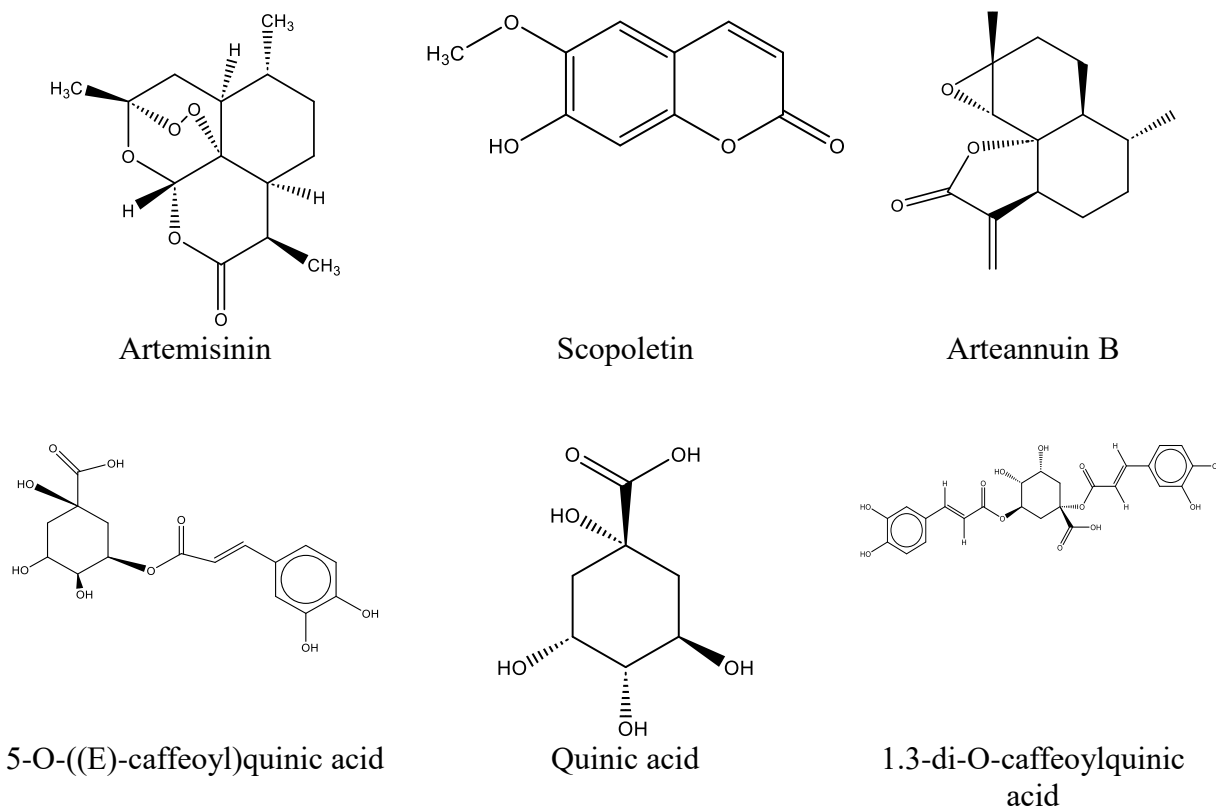
The antioxidant potential of ACEO was evaluated using three well-established methods: DPPH°, β -carotene bleaching, and FRAP assays. ACEO exhibited notable antioxidant activity, achieving values of 11.09 $\mu\text{g/mL}$ in the DPPH° assay and 22.70 $\mu\text{g/mL}$ in the β -carotene assay, which reflects its robust free radical scavenging properties, as illustrated in Figure. 3. Additionally, the FRAP assay demonstrated a ferric ion reduction potential of 15.81 $\mu\text{g/mL}$, further emphasizing the compound's capacity as a potent antioxidant. For comparison, the FRAP value reported by Djeridane *et al.*, (2006) was 871.28 ± 49.96 $\mu\text{g/mL}$, while the β -carotene assay value was 26.58 ± 3.34 $\mu\text{g/mL}$, underscoring the lower activity of ACEO relative to previously reported values. In the study by Bendifallah (Bendifallah and Merah 2023), the essential oil from *A. campestris* demonstrated an impressive EC₅₀ value of 2.55 $\mu\text{g/ml}$, This indicates a robust capacity to scavenge DPPH° radicals, suggesting a strong antioxidant potential. The authors attributed this high activity primarily to hydrocarbon

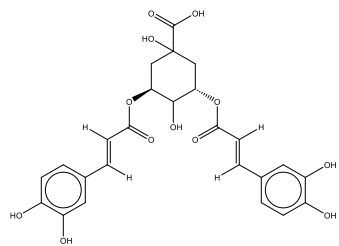
monoterpenes, which comprise about 40.76% of the oil. Among these, compounds like α -pinene and β -pinene are noted for their significant antiradical effects.

In contrast, the essential oil of our study reported a DPPH° value of 11.09 $\mu\text{g/mL}$, which is considerably higher than the IC_{50} value observed for the previous study (Bendifallah and Merah 2023). This difference suggests that our essential oil may have a lower radical scavenging capacity. Several factors may contribute to this discrepancy. First, the specific monoterpene profile and overall composition of essential oils can vary, influencing their radical-scavenging abilities. Additionally, differences in extraction techniques can affect both the yield and quality of essential oil components, which subsequently impacts their antioxidant potential. Finally, variations in plant source, environmental conditions, and harvesting times can lead to differences in phytochemical content. Together, these elements play a significant role in the observed differences in antioxidant activity.

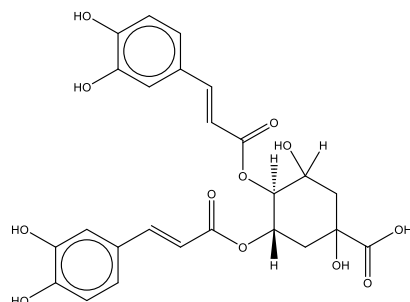
TABLE 4. COMPARATIVE ANTIOXIDANT ACTIVITIES OF *A. CAMPESTRIS* ESSENTIAL OIL AND BHA.

Assay	IC_{50} ($\mu\text{g/mL}$)		
	DPPH°	Reducing Power (FRAP)	β -Carotene
Plant EO	12 ± 0.02	17.5 ± 0.43	23 ± 0.03
BHA	5.73 ± 0.41	8.41 ± 0.67	0.90 ± 0.02

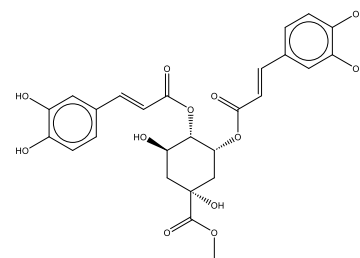




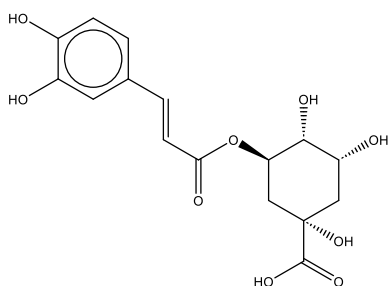
3,5-di-O-caffeoylquinic acid



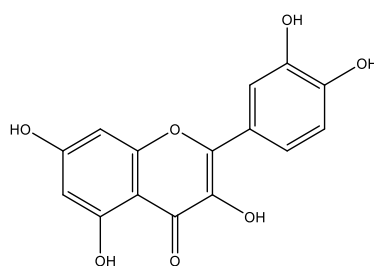
3,4-di-O-caffeoylquinic acid



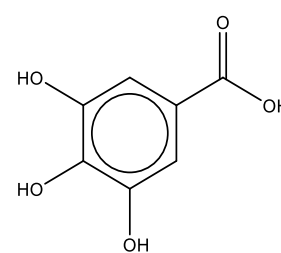
Methyl-3,4-di-O-caffeoylquinic acid



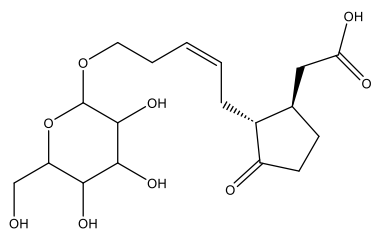
Chlorogenic acid



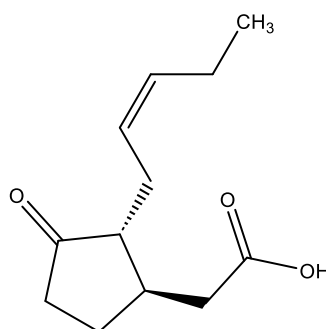
Quercetin



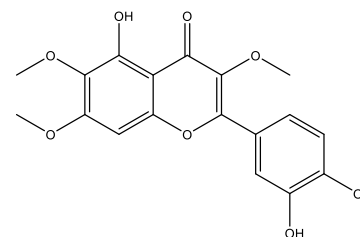
Gallic acid



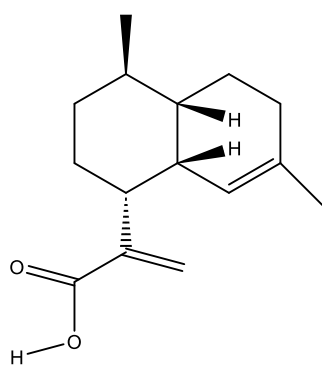
5'-β-d-Glucopyranosyloxyjasmonic acid



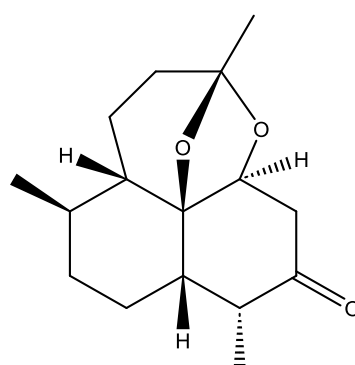
Jasmonic acid



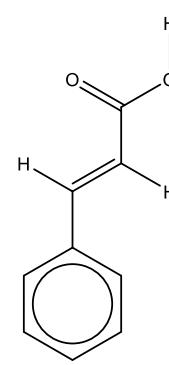
Chrysosplenol D



Artemisinic acid



Deoxy-artemisinin



T-cinnamic acid

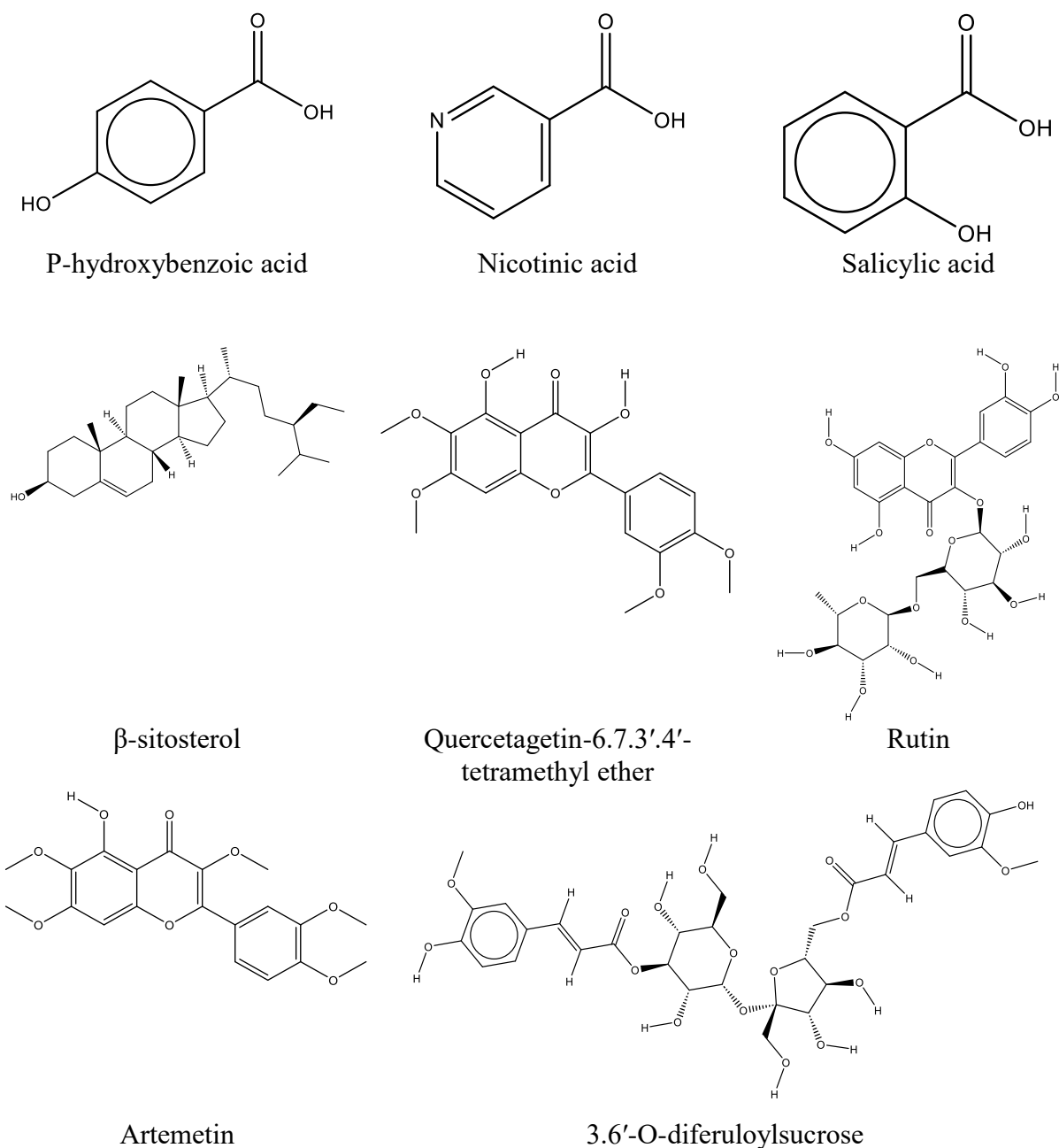


Figure 3. Structure of some polyphenolic compounds identified in extracts from *A. campestris*.

3.5. Gas Chromatography-Mass Spectrometry of Essential Oil

The chemical composition of *A. campestris* essential oil was analyzed using gas chromatography-mass spectrometry (GC-MS), with detailed results provided in Table 4 that revealed the presence of 62 compounds, Collectively constituting 10.02% of the overall chemical composition of *A. campestris* essential oil. Among these compounds, the major constituents included linalyl acetate (2.92%), geranyl acetate (2.45%), cyclononasiloxane (2.37%), cyclohexanol (1.76%), and eucalyptol (1.38%). Notably, levomenol (1.01%) was

also a significant component. These compounds were categorized into different classes, with monoterpenic hydrocarbons comprising the dominant class at 40.85%, followed by sesquiterpene hydrocarbons at 27.40%, monoterpene alcohols at 0.76%, and a minor presence of monoterpene aldehydes at 0.15%. Furthermore, as identified through ultra-performance liquid chromatography (UPLC), Table 5 elucidates the presence of various secondary metabolites in the ACEO. This analysis compares the differences in bioactive compounds detected by UPLC and GC-MS. Notable compounds identified in the essential oil include β -sitosterol (14.3 $\mu\text{g/ml}$), arteannuin B (12.6 $\mu\text{g/ml}$), scopoletin (8.22 $\mu\text{g/ml}$), artemisinin (6.13 $\mu\text{g/g}$), rutin (5.8 $\mu\text{g/ml}$), 1,3-di-O-caffeoylquinic acid (4.3 $\mu\text{g/g}$), gallic acid (4.2 $\mu\text{g/ml}$) and *t*-cinnamic acid (3.5 $\mu\text{g/g}$). These findings provide insights into the diverse secondary metabolites in *A. campestris*, shedding light on its potential pharmacological properties and therapeutic applications.

Table 5. GCMS identification of secondary metabolites in the leaf.

Compounds	Formula	R.T. (s)	Base Mass	Area %
Linalyl acetate	C₁₂H₂₀O₂	814.602	42.98	2.923
Cyclohexanol. 1-methyl-4-(1-methylethenyl)-. acetate	C₁₂H₂₀O₂	752.824	93.09	1.766
3-Cyclopentylpropionamide. N-(3,4-dimethoxyphenethyl)-	C ₁₈ H ₂₇ NO ₃	1035.62	164.14	1.705
Geranyl acetate	C₁₂H₂₀O₂	835.326	69.03	1.448
Butanoic acid. hexyl ester	C ₁₀ H ₂₀ O ₂	742.817	43.07	1.439
Phenol. 2-methoxy-4-(2-propenyl)-. acetate	C ₁₂ H ₁₄ O ₃	897.426	164.11	1.39
4-Hexen-1-ol. 5-methyl-2-(1-methylethenyl)-. (R)-	C ₁₀ H ₁₈ O	729.282	69.04	1.336
Hexyl tiglate	C ₁₁ H ₂₀ O ₂	867.324	101.07	1.325
Acetic acid. hexyl ester	C ₈ H ₁₆ O ₂	742.681	56.05	1.11
Geranyl acetate	C₁₂H₂₀O₂	834.398	69.05	1.004
Eucalyptol	C₁₀H₁₈O	577.6	42.99	0.955
cis-β-Farnesene	C ₁₅ H ₂₄	977.222	93.04	0.791
3-Allyl-6-methoxyphenol	C ₁₀ H ₁₂ O ₂	905.681	163.96	0.772
4-Hexen-1-ol. 5-methyl-2-(1-methylethenyl)-. acetate	C ₁₂ H ₂₀ O ₂	915.928	69	0.765
1,3,7-Nonatriene-1,1-dicarbonitrile. 4,8-dimethyl-. (E)-	C ₁₃ H ₁₆ N ₂	576.563	69.06	0.734
N.N.O-Triacetylhydroxylamine	C ₆ H ₉ NO ₄	885.154	43.03	0.715
Phenol. 2-methoxy-3-(2-propenyl)-	C ₁₀ H ₁₂ O ₂	906.384	164.22	0.646
Butanoic acid. 2-methyl-. hexyl ester	C ₁₁ H ₂₂ O ₂	782.351	103.05	0.623
1,3,7-Octatriene. 3,7-dimethyl-	C ₁₀ H ₁₆	589.413	93.05	0.575
Bicyclo[3.1.1]hept-2-ene. 3,6,6-trimethyl-	C ₁₀ H ₁₆	578.53	93.09	0.56
3,5-Heptadien-2-ol. 2,6-dimethyl-	C ₉ H ₁₆ O	767.216	91.03	0.539
14-Hydroxycaryophyllene	C ₁₅ H ₂₄ O	1092.73	41.03	0.507
2-Butanone. 3-chloro-	C ₄ H ₇ ClO	551.249	43.09	0.491
Bicyclo[3.1.1]hept-2-ene. 3,6,6-trimethyl-	C ₁₀ H ₁₆	578.692	93.07	0.491
Bi-2-cyclohexen-1-yl	C ₁₂ H ₁₈	927.63	81.04	0.475
Cyclooctasiloxane. hexadecamethyl-	C ₁₆ H ₄₈ O ₈ Si ₈	1139.79	73.02	0.466
Eucalyptol	C₁₀H₁₈O	577.885	55.02	0.43
Camphor	C ₁₀ H ₁₆ O	717.584	95.06	0.426
Humulene	C ₁₅ H ₂₄	985.881	93.04	0.413
3-Octanol. acetate	C ₁₀ H ₂₀ O ₂	686.729	43.02	0.406
Methyl Alcohol	CH ₄ O	892.593	31.98	0.397
Propyl pyruvate	C ₆ H ₁₀ O ₃	916.989	43.03	0.397
2,6-Octadien-1-ol. 3,7-dimethyl-. acetate. (Z)-	C ₁₂ H ₂₀ O ₂	904.371	69.03	0.326
(E)-β-Farnesene	C ₁₅ H ₂₄	980.42	69.05	0.295
Cyclononasiloxane. octadecamethyl-	C ₁₈ H ₅₄ O ₉ Si ₉	1356.82	73.02	0.279
trans-α-Bergamotene	C ₁₅ H ₂₄	964.645	93.04	0.273
Linalool	C ₁₀ H ₁₈ O	658.179	40.98	0.268
p-Cymen-7-ol	C ₁₀ H ₁₄ O	840.636	135.05	0.268
Fluorene. 9-benzenesulfonyl-	C ₁₉ H ₁₄ O ₂ S	1034.17	165.04	0.268
1,6-Octadien-3-ol. 3,7-dimethyl-. formate	C ₁₁ H ₁₈ O ₂	800.095	92.95	0.259
Lavandulyl butyrate	C ₁₄ H ₂₄ O ₂	946.754	69.05	0.245
Acetic acid. octyl ester	C ₁₀ H ₂₀ O ₂	758.145	43.01	0.244
Thymol	C ₁₀ H ₁₄ O	843.807	135.05	0.233

Camphor	C ₁₀ H ₁₆ O	716.599	95.13	0.196
3-Allyl-6-methoxyphenol	C ₁₀ H ₁₂ O ₂	903.175	149.07	0.191
Hexanoic acid, hexyl ester	C ₁₂ H ₂₄ O ₂	917.273	117.06	0.182
2,6-Octadien-1-ol, 3,7-dimethyl-3-Allyl-6-methoxyphenol	C ₁₀ H ₁₈ O	816.08	69	0.173
	C ₁₀ H ₁₂ O ₂	906.764	164.11	0.173
Naphthalene, 1,2,3,4-tetrahydro-1,6-dimethyl-4-(1-methylethyl)-, (1S-cis)-	C ₁₅ H ₂₂	1039.48	159.08	0.172
Trimethoquinol	C ₁₉ H ₂₃ NO ₅	906.878	164.07	0.154
α-Thujenal	C ₁₀ H ₁₄ O	757.304	79.03	0.138
2-Furanmethanol, tetrahydro-α,α,5-trimethyl-5-(4-methyl-3-cyclohexen-1-yl)-, [2S-[2α,5β(R*)]]-	C ₁₅ H ₂₆ O ₂	1142.13	43.01	0.129
1H-Inden-2-ol, 2,3-dihydro-1-methoxy-	C ₁₀ H ₁₂ O ₂	897.88	121.03	0.121
Naphthalene, 1,2,3,5,6,8a-hexahydro-4,7-dimethyl-1-(1-methylethyl)-, (1S-cis)-	C ₁₅ H ₂₄	1038.46	161.1	0.12
Hotrienol	C ₁₀ H ₁₆ O	684.085	71.02	0.115
Linalool	C ₁₀ H ₁₈ O	682.753	70.96	0.106
o-Cymene	C ₁₀ H ₁₄	566.926	119.06	0.101
Bornyl isovalerate	C ₁₅ H ₂₆ O ₂	1025.58	57.05	0.1
Linalool	C ₁₀ H ₁₈ O	683.528	55	0.095
Eucalyptol	C₁₀H₁₈O	568.335	43.02	0.032
p-Cymene	C ₁₀ H ₁₄	875.475	119.06	0.017

The essential oil composition of *A. campestris* varies significantly across different geographic regions, as demonstrated by studies from El Mergueb, Djebel Amour (BAKCHICHE *et al.*, 2022) and Beni-Khedache (Akrouit *et al.*, 2011). In these locations, β-pinene emerged as the main constituent, with proportions of 15.33%, 25.6%, and 45.8%, respectively. In contrast, the sample from Boussaâda exhibited a markedly lower β-pinene content of only 1.8%; Additionally, while all four samples contained notable amounts of limonene and γ-terpinene, these compounds were in lower concentrations in the Boussaâda sample (Belhattab *et al.*, 2011). Notably, the absence of spathulenol and β-Endemol in the Boussaâda sample contrasts with their appreciable levels in the El Mergueb and Djebel Amour samples. Interestingly, compounds such as germacrene D and ledeneoxide were identified in the Boussaâda sample at 6.15% and 2.42%, respectively, while these compounds were absent in the Djebel Amour sample. This variability in chemical composition across regions underscores the influence of local environmental factors. In Poland, Lis and Kowal (Lis and Kowal 2015) reported that *A. campestris* primarily contains germacrene D, β-caryophyllene, γ-humulene, and (Z)-falcarinol. This further emphasizes that the monoterpene fraction predominates in this species. The observed chemical variability of *A. campestris* essential oil across Europe, Africa, and Asia can be attributed to seasonal, climatic, and

geographical conditions (Benamar-Aissa *et al.*, 2024). Factors influencing this variability include exogenous elements such as sunlight, soil composition, temperature, altitude, and endogenous genetic factors (Barragan-Ferrer *et al.*, 2019). These parameters impact essential oils' quality and chemical composition (Mansinhos *et al.*, 2024). In contrast, our analysis of the essential oil from *A. campestris* reveals the presence of distinct compounds, including linalyl acetate, Cyclohexanol, 1-methyl-4-(1-methyl phenyl)-acetate, 3-cyclopentyl propionamide, and N-(3,4-dimethoxyphenethyl)-geranyl acetate. The presence of these constituents suggests a unique chemical profile that may differ significantly from those reported in other studies. This highlights the importance of considering regional influences on essential oil composition and the potential for distinct chemotypes within the species.

Table 6. UPLC was used to identify secondary metabolites in ACEO.

Compounds	Concentration U/ml
Artemisinin	6,13
Scopoletin	8,22
Arteannuin B	12,6
5- <i>O</i> -((<i>E</i>)-caffeoyl)quinic acid	3,1
Quinic acid	1,8
1,3-di- <i>O</i> -caffeoylquinic acid	4,3
3,5-di- <i>O</i> -caffeoylquinic acid	0,16
3,4-di- <i>O</i> -caffeoylquinic acid	0,21
Methyl-3,4-di- <i>O</i> -Caffeoylquinic acid	3,22
Chlorogenic acid	0,56
3,6'- <i>O</i> -diferuloylsucrose	1,1
Gallic acid	4,2
5'-β-d-Glucopyranosyloxyjasmonic acid	1,6
Jasmonic acid	0,22
Chrysosplenol D	0,78
Artemisinic acid	1,43
Deoxy-artemisinin	2,01
Artemetin	0,23
p-hydroxybenzoic acid	0,18
Nicotinic acid	2,7
Salicylic acid	1,3
β-sitosterol	14,3
Quercetagenin-6,7,3',4'-	2,6

Tetramethyl ether	
Rutin	5,8
Quercetin	1,7
t-cinnamic acid	3,5

4. Anti-inflammatory activity

4.1. Anti-inflammatory activity of aqueous extract

In the egg albumin denaturation assay, *A. campestris* demonstrates significant anti-inflammatory effects with an IC₅₀ value of 123.25 (figure 5). Protein denaturation involves a complex mechanism that includes alterations in electrostatic hydrogen bonds, hydrophobic interactions, and disulfide bonding (Amaya-Farfan *et al.*, 2021). This process produces autoantigens associated with inflammatory conditions such as rheumatic arthritis, cancer, and diabetes (Dharmadeva *et al.*, 2018). Inhibition of protein denaturation can attenuate inflammatory activity (Dharmadeva *et al.*, 2018). This study investigates the anti-inflammatory potential of *A. campestris*, supporting its traditional use in treating painful and inflammatory conditions. Phytochemical analysis of the plant revealed the presence of biologically active compounds such as flavonoids, tannins, phenolic compounds, and phytosterols, suggesting that one or a combination of these constituents may contribute to its analgesic and anti-inflammatory effects (Dharmadeva *et al.*, 2018). Denaturation of protein causes auto-antigens production in conditions such as rheumatic arthritis, cancer, and diabetes, which are inflammation conditions, as mentioned above. Hence, by inhibiting protein denaturation, inflammatory activity can also be inhibited (Mandal *et al.*, 2000). The egg albumin method provides a cheap alternative method of testing the anti-inflammatory activity of herbal medicine using the denaturation technique, and this method should be validated by conducting further studies.

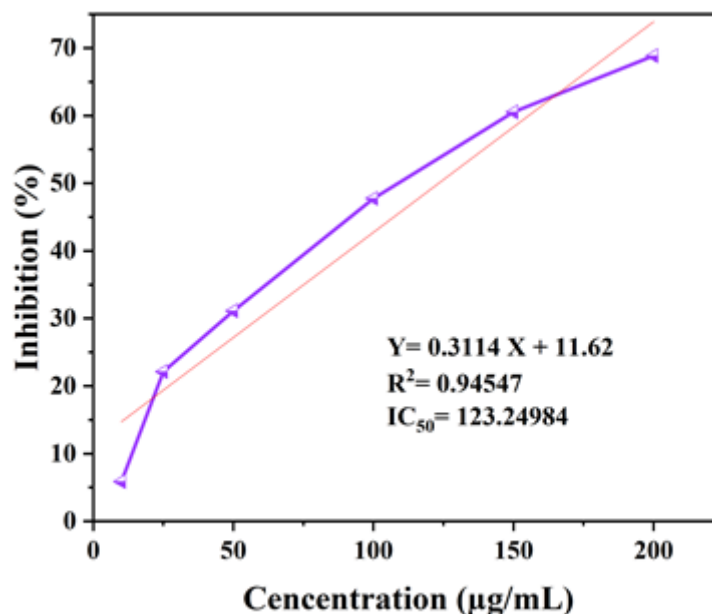


Figure 4. Effect of *A. campestris* extracts on protein denaturation (albumin).

4.2. Anti-inflammatory activity of essential oil

According to the results of protein denaturation (Figure 6) the ACEO shows promising anti-denaturation activity with $IC_{50} = 16.12 \mu\text{g/ml}$. Protein denaturation is when proteins lose their tertiary and secondary structures due to external stressors such as strong acids, bases, concentrated salts, organic solvents, or heat (Amaya-Farfan *et al.*, 2021). This loss of structure leads to a loss of function and is a well-documented cause of inflammation, contributing to various inflammatory diseases. The denaturation process involves disrupting electrostatic interactions, hydrogen bonds, hydrophobic interactions, and disulfide bridges that maintain the protein's three-dimensional structure (Akbarian and Chen 2022). This study suggests that the anti-denaturing activity of the ACEO may be due to interactions between extract components and specific sites on proteins, particularly those rich in amino acids like tyrosine, threonine, and lysine. These amino acids play crucial roles in maintaining protein structure through their involvement in hydrogen bonding, hydrophobic interactions, and electrostatic interactions. Stabilizing these bonds, the ACEO components prevents protein from unfolding under stress. This stabilization can reduce inflammation, as denatured proteins can trigger inflammatory responses. Therefore, the anti-denaturing properties of these ACEO have significant implications for treating inflammatory diseases. highlighting their potential as therapeutic agents (Fathima *et al.*, 2024). The anti-denaturing activity of our extracts may be due to the interaction of specific components with two sites (present in certain proteins

such as albumin) of bonds rich in tyrosine, threonine, and lysine (Yahia, Benhouda, and Takellalet 2023).

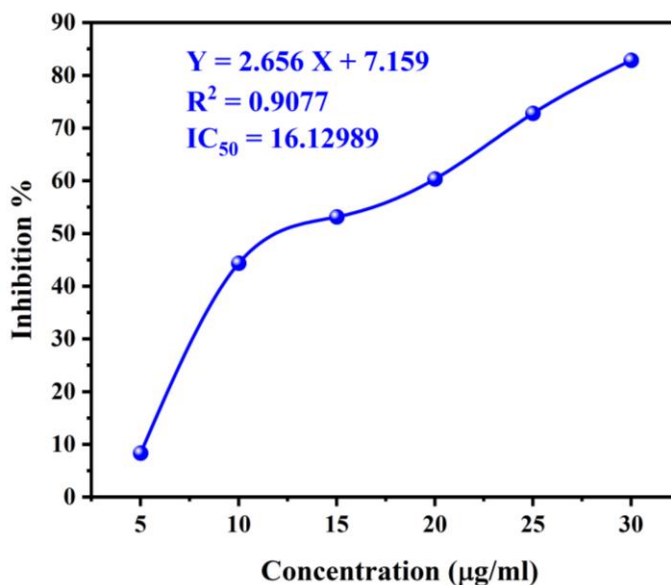


Figure 5. Anti-inflammatory activity of *A. campestris* essential oil.

5. α -amylase inhibition

Figure 7 summarizes the leaf extract's *in vitro* antidiabetic evaluation (α -amylase) from *A. campestris*. The antidiabetic review resulted in the inhibition of α -amylase activity. *In vitro*, antidiabetic data of the leaf extract of *A. campestris* have indicated α -amylase inhibitory activity, with an IC_{50} value of $2.42 \pm 0.71 \mu\text{g/mL}$, exhibited moderate inhibition, as determined by the sample's classification based on IC_{50} . An aqueous extract of *A. campestris* is an inhibitor of α -amylase and can treat type II diabetes mellitus, as indicated by the higher than 50% inhibition of α -amylase. Because α -amylase activity in the small intestine correlates with higher postprandial glucose levels (Zinjarde, Bhargava, and Kumar 2011), inhibiting it is crucial in treating type II diabetes mellitus, α -amylase inhibitors work by preventing carbohydrates' breakdown, making them valuable tools for reducing postprandial hyperglycemia (Wu and Xu 2014). Therefore, non-insulin-dependent diabetes mellitus reduces glucose metabolism without encouraging insulin secretion (Vazquez-Armenta, Cruz-Valenzuela, and Ayala-Zavala 2016). Suppose a diabetic patient has to maintain a healthy blood glucose level while using an oral antidiabetic medication. This plant may also be helpful (Dib and El Alaoui-Faris 2019); The extract from *A. campestris* may include flavonoids, which might explain this (Table 1). According to reports, flavonoids can block α -amylase and their mode of action is comparable to that of acarbose (Lo Piparo *et al.*, 2008). According to reports, flavonoids are now regarded as the preferred medications due to their

ability to treat PCOS-related hyperlipidemia, hyperglycemia, oxidative stress, and hyperandrogenism (Jahan *et al.*, 2016).

Compared with the findings from the study on *A. absinthium* and our results on the leaf extract of *A. campestris*, both plant extracts demonstrate significant inhibitory effects on pancreatic α -amylase activity. The study on *A. absinthium* reported an IC₅₀ value of 0.68 ± 0.01 mg/mL, indicating a notable level of efficacy in inhibiting the enzyme. In contrast, the leaf extract of *A. campestris* exhibited a higher IC₅₀ value of 2.42 ± 0.71 μ g/mL, suggesting weaker inhibitory activity compared to *A. absinthium*.

The more potent activity of *A. absinthium* may be linked to its specific phytochemical profile, potentially containing higher concentrations of active compounds that effectively inhibit α -amylase. This finding aligns with the growing interest in discovering new pancreatic α -amylase and intestinal α -glucosidase inhibitors from natural sources, particularly due to many current hyperglycemic medications' side effects and toxicity (Daoudi *et al.*, 2020).

Research has increasingly focused on plants that exhibit hypoglycemic effects with minimal or no side effects. Numerous plant species have been evaluated for their enzyme-inhibitory properties as part of diabetes management strategies (Hbika *et al.*, 2022); while *A. campestris* showed a higher IC₅₀ value, its traditional uses, and potential bioactive compounds warrant further investigation.

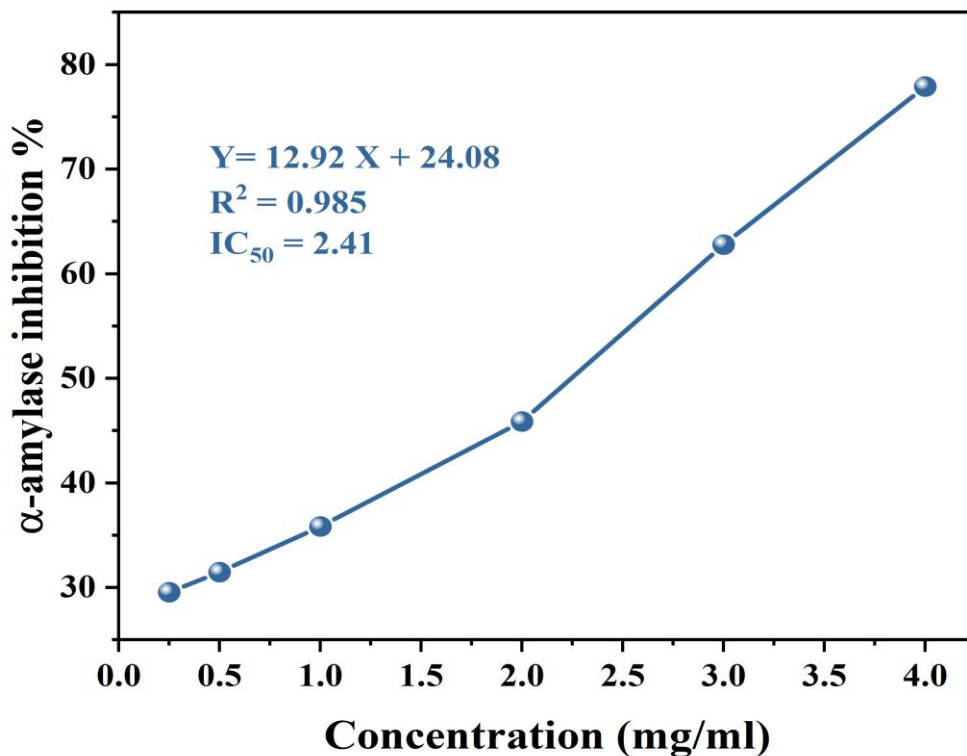


Figure 6. The inhibition of α -amylase by aqueous extracts of *A. campestris*.

TABLE 7. POLYPHENOLS BIND TO ANDROGEN AND ESTROGEN RECEPTORS.

Compound	Detail	Cell lines/model	Dose	Application	Ref
Quercetin	decreased 3 β -HSD and/or 17 β -HSD. the steroidogenic enzyme. activity	Letrozole-induced PCOS rats' model	25 mg/kg	<i>In vivo</i>	(Hong et al. 2018)
Quercetin	Suppressed the PI3K pathway to reduce the CYP17; Cyp17a1 gene expression.	Testosterone propionate-induced PCOS rats' mode	150 mg/kg	<i>In vivo</i>	(Shah and Patel 2016)
Quercetin	increased the SOD. CAT. GPX. GST. GSH. and GR levels.	Menopausal female Sprague-Dawley (SD) rats	12.5, 25, 50 mg/kg	<i>In vivo</i>	(Wang et al. 2018)
Rutin	increased GLUT4 expression and improved insulin-dependent receptor kinase activity	Letrozole-induced PCOS rats' model	100. 150 mg/kg	<i>In vivo</i>	(Jahan et al. 2016)
Rutin	BAT activation increases UCP1 expression and upregulates adiponectin expression.	DHEA-induced PCOS rats' model	100 mg/kg	<i>In vivo</i>	(Hu et al. 2017)
Rutin	decreased LH and testosterone output. as well as GnRH expression	5 α -DHT-induced PCOS rats' model	150. 300 mg/kg (intraperitoneal injection)	<i>In vivo</i>	(Gao et al. 2020)

6. Guaiacol peroxidase activity

Plants have evolved sophisticated antioxidant mechanisms that mitigate oxidative damage during periods of mild stress and typical development. These mechanisms are crucial for maintaining cellular integrity and overall plant health, mediated through enzymatic and non-enzymatic pathways. Enzymatic antioxidants, such as Superoxide Dismutase (SOD), Catalase (CAT), and Guaiacol Peroxidase (GPX), play significant roles (Gao *et al.*, 2020). SOD catalyzes the dismutation of superoxide radicals into oxygen and hydrogen peroxide, preventing cellular damage. CAT converts hydrogen peroxide into water and oxygen, avoiding its harmful accumulation (Sipka *et al.*, 2024). GPX uses guaiacol as a substrate to reduce hydrogen peroxide and organic hydroperoxides to their corresponding alcohols, detoxifying peroxides and protecting cellular components from oxidative damage; in addition to these enzymes, plants use non-enzymatic antioxidants like vitamins, flavonoids, and phenolic compounds, which directly scavenge reactive oxygen species (ROS), chelate metal ions, and regenerate oxidized enzymatic antioxidants. Plants often face environmental stressors such as air pollution, dehydration, and temperature fluctuations, which enhance ROS

production and necessitate a robust antioxidant response (Hadadi, Nematzadeh, and Ghahari 2020). The presence and activity levels of antioxidant enzymes like GPX indicate how well a plant manages oxidative stress. This study assessed GPX activity and found significant activity in ACEO, as shown in Figure. 8. indicating that this species effectively detoxifies peroxides and protects itself from oxidative stress. This significant GPX activity underscores its importance in the plant's antioxidant strategy, highlighting the adaptive mechanisms that enable plants to survive and thrive under varying stress conditions. Thus, the enzymatic antioxidant defense system., including enzymes such as SOD, CAT and GPX, is essential for plants to cope with oxidative stress induced by environmental factors (FEKETE *et al.*, 2024). The activity of GPX was assessed In this study, The outcomes are shown in Figure. 8 And Figure. 9 As demonstrated. The guaiacol peroxidase activity assay revealed significant activity in *Artemisia campestris* presence.

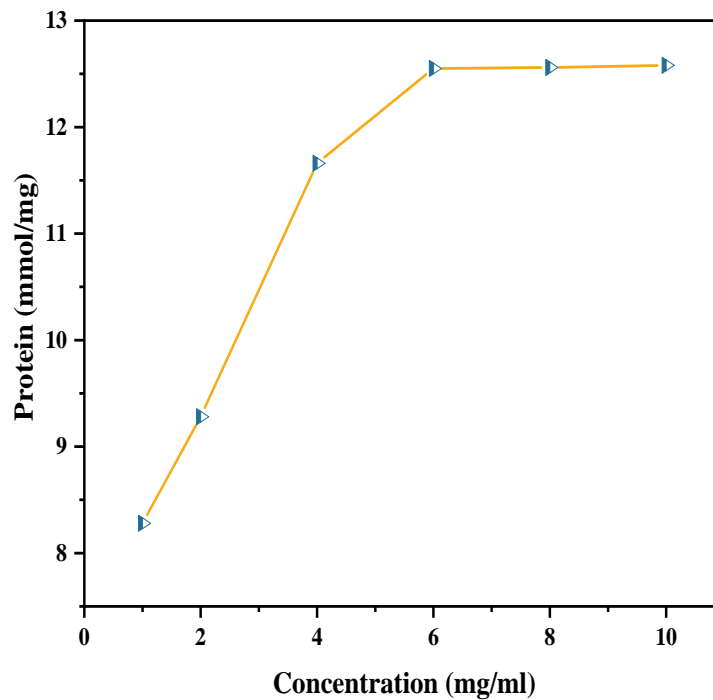


Figure 7. The inhibition of Guaiacol peroxidase by aqueous extracts of *A. campestris*

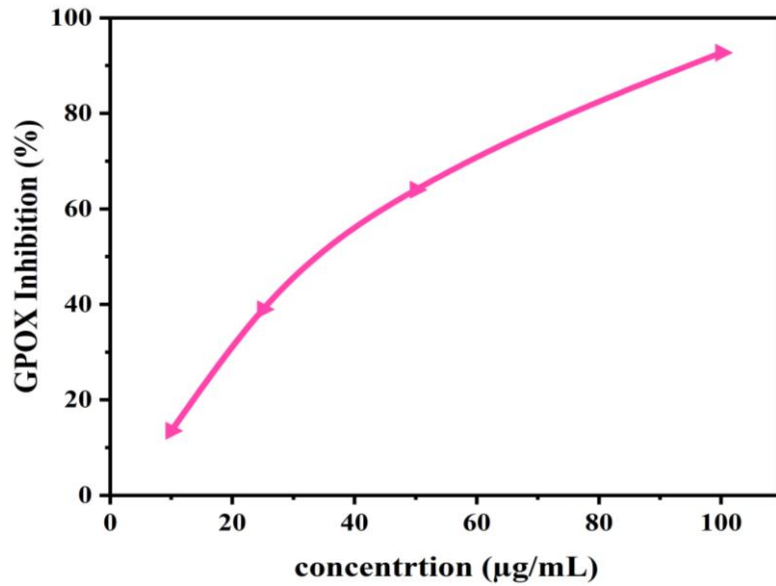


Figure 8. Peroxidase activity activity of *Artemisia campestris* essential oil.

7. In vivo assays

7.1. PCOS assay

7.1.1. Hormonal analysis

Hormonal observations revealed that LH levels were elevated in the PCOS group, whereas FSH levels were diminished compared to the control group Upon administering varying doses of *A. campestris* over a period of 15 days, compared to the PCOS control group, the injection of *A. campestris* extract significantly raised FSH levels and significantly decreased LH levels in all three experimental groups (Table 7).

Table 8. A comparison of the rats' mean levels of FSH and LH in the experimental. PCOS. and control groups.

	Control group	PCOS group	Experimental group
LH	0.23±0.03	0.34±0.03***	0.21±0.02***
FSH	0.18±0.04	0.13±0.03**	0.14±0.05*

***P<0.001; **P<0.01; *P<0.05.

7.1.2. Histomorphometric findings

The PCOS control group displayed a higher incidence of cystic follicles characterized by a thin granular layer and a thick theca. Additionally, a reduced number of corpus luteum was evident. indicating that the administration of estradiol valerate induced polycystic ovaries, resulting in diminished ovulation and fewer active follicles (Figure. 10). Morphological assessments of the treatment cohorts demonstrated that the administration of aqueous *A. campestris* extract over 15 days resulted in an augmentation of follicle numbers across various

stages. Moreover, it increased corpus luteum count while reducing the occurrence of cystic follicles (Figure. 10). Injection of *A. campestris* extract displayed significant alterations in ovarian tissues compared to the control group, with a notable reduction in cystic follicles. Conversely, in the experimental groups receiving the extract, there was a significant increase in the quantity of these follicles, while cystic follicles became far less common. It is noteworthy that escalating doses of *A. campestris* extract would likely amplify these observed changes (Table 7). PCOS induction was expected to result in elevated LH levels and reduced FSH levels. Histomorphometric analysis revealed a decrease in cystic follicles and an increase in primordial, primary, pre-antral, and antral follicles, as well as corpus luteum.

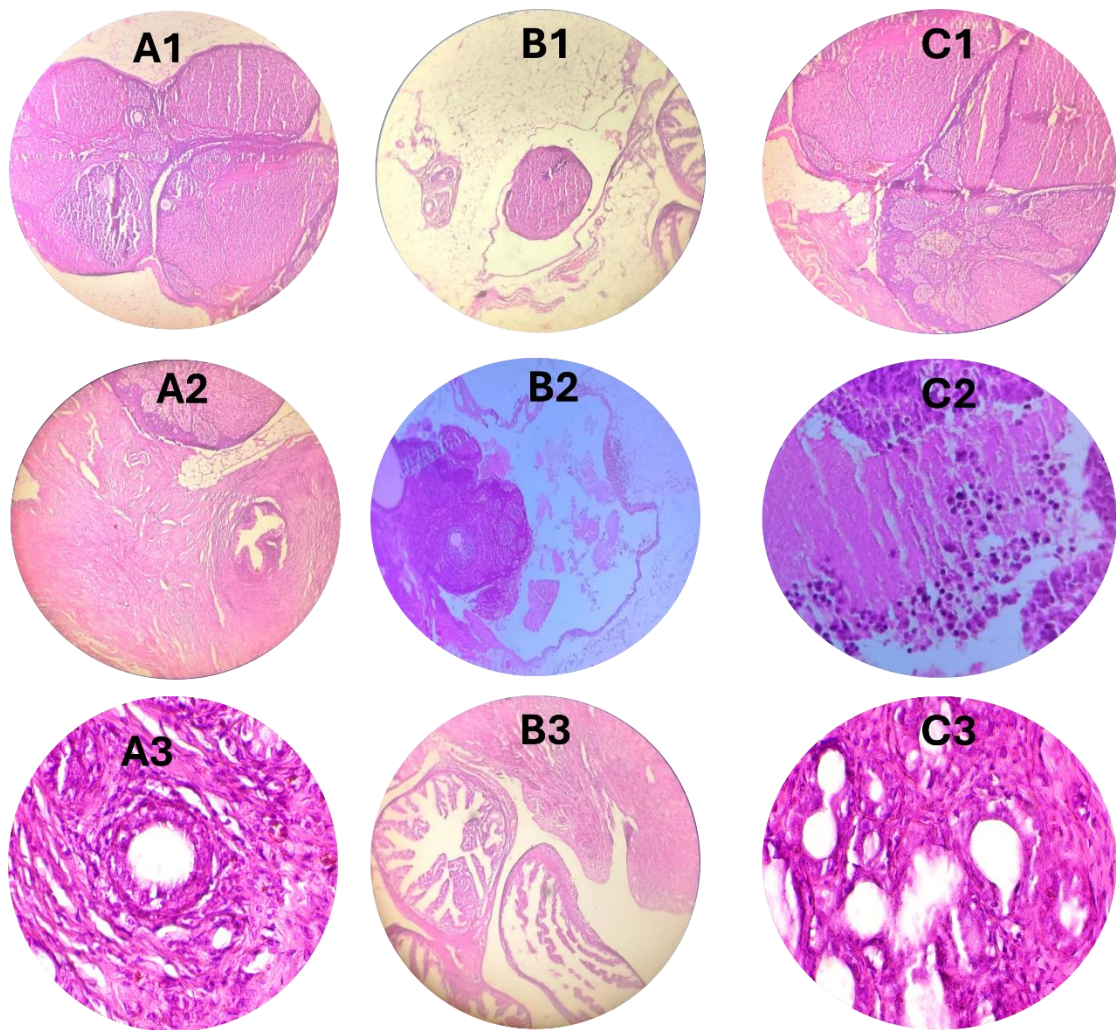


FIGURE 9. (A) HISTOLOGICAL ANALYSIS OF NORMAL RATS. (B) RATS WITH PCOS; (C) RATS WITH PCOS TREATED *A. CAMPESTRIS* EXTRACT.

A recent study revealed that following PCOS induction, the experimental group's follicle growth and development declined compared to the control group (Ghafurniyan *et al.* 2015). These outcomes agree with the current study's conclusions. Additionally, Calabró, Willerson,

and Yeh (2003) have reported that rats develop PCOS, causing the ovaries to develop many cysts. These cysts were shown to have originated from atretic follicles, which were distinguished by the thickening of the theca cells' outer layer and granulosa cell degeneration. Notably, our work shows that *A. campestris* extract reduces the first measurement of the follicular theca layer thickness in PCOS rats. Our reduction may be mediated by increased lipolysis and decreased layer hypertrophy; this layer's production of androgens and steroids may decline due to its decreased thickness. Furthermore, the study's results indicated an increase in ovarian cysts and a reduction in the corpus luteum and follicle count. It has been shown that *A. campestris* extract increases corpus luteum and follicle counts while lowering the incidence of cystic follicles in the ovary. Changes in sex hormones, especially steroids, are known to be associated with PCOS. However, because of the increased estrogen levels in the polycystic group. Alterations in the sensitivity of the pituitary and hypothalamus were seen (Vigorito *et al.*, 2007); The results of the 15-day infusion of *A. campestris* extract on hormone levels demonstrated a considerable reduction in luteinizing hormone levels. Consequently, there were persistently high levels of LH and low amounts of FSH. Hormone secretion can be regulated by consuming *A. campestris*. Additionally, it modifies the receptors for hormones and lessens the negative effects of hormone imbalance. In addition to causing phasic LH release, which induced ovulation and corpus luteum formation, high FSH levels in the normal control samples also led to follicular expansion and development.

7.2. HPO assay

7.2.1. Hormonal analysis

The serum TSH level increased considerably ($p < 0.05$) in Lot II. Conversely, the levels in rats given LEV or *A. campestris* were almost normal (Figure. 11). Serum FT4 levels dramatically decreased. Relative to those found in Lot I (control), III (CBZ + *A. campestris*), and IV (CBZ + LEV), with a significance level of ($p < 0.05$) in Lot II (CBZ). On the other hand. Lot IV (CBZ + LEV) did not exhibit a statistically significant increase in serum FT4 levels in contrast to Lot I (control) and III (CBZ + *A. campestris*; Figure. 10). In this study, CBZ was used to induce hypothyroidism. It inhibited thyroid functions, decreased the serum level of T4 and T3 and increased TSH hormone. Our result confirmed that CBZ could induce hypothyroidism and this is compatible with what has been reported in other studies (Alkalby and Alzerjawi 2013; Chaalal *et al.*, 2014). CBZ inhibited thyro-peroxidase enzyme reversibility; this enzyme is required for tyrosyl peroxidation during thyroid hormone synthesis. Furthermore, carbimazole inhibited deiodinase, which converts T4 to T3 in the peripheral tissues (Vagenakis and Braverman 1976). This study is the first to assess the

efficacy of *Artemisia campestris* “Tuguft” (the common name in Algeria) aqueous extract in treating animal hypothyroidism. The animals' thyroid hormone levels improved when *A. campestris* extract (200 mg/kg) was administered to hypothyroid rats; most of the time, the modifications resembled the standard controls. Serum levels of T4 considerably rose in the groups treated with Tuguft extract, while they declined in the negative control group. The hypothyroid group saw a considerable rise in TSH, a compensatory response to boost thyroid hormone production and secretion. Compared to the negative control group, the group that received Tuguft aqueous extract showed a substantial drop in TSH levels. Propylthiouracil reduced follicular diameters and colloids and had a deleterious effect on thyroid tissue, as demonstrated by Hwang *et al.* (Hwang *et al.*, 2018). In CBZ-treated rats, administering a polyherbal medication raised thyroid hormones in the blood and enhanced the histopathological characteristics in the thyroid tissue (Hwang *et al.*, 2018). It is possible, then, that the tuguft extract shields the thyroid gland from CBZ's harmful effects. Sitosterol, a principal compound in *A. campestris*, can potentially enhance the expression of the sodium/iodide symporter (NIS) and promote iodide absorption in the thyroid gland (Figure 11). Additionally, it may influence the activity of the thyroperoxidase enzyme, a hypothesis that will be further validated through docking studies.

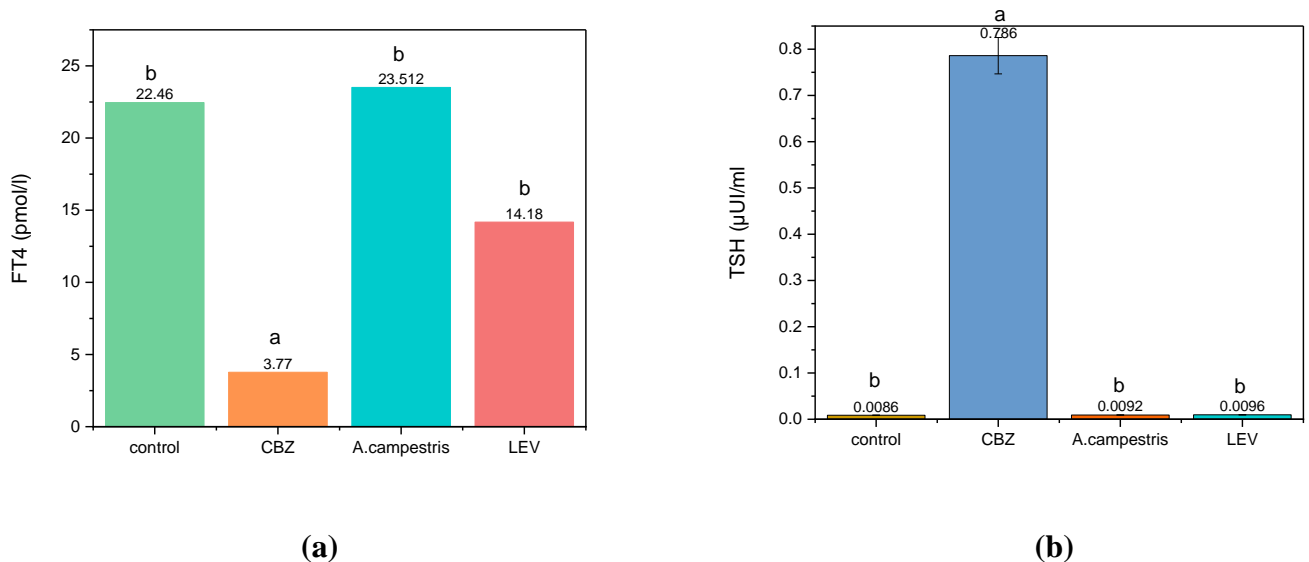


Figure 10. The mean expression levels of TSH and T4 in Lot I (control). Lot II (CBZ). Lot III (CBZ + *A. campestris*). and Lot IV (CBZ + LEV). Values with letters (a) are considered significantly different ($p < 0.05$). Many people sharing the same superscript letter exhibit no significant differences in LEV. Lyvotyroxin. CBZ. carbimazole. TSH. and thyroid-stimulating hormone.

7.2.2. Histopathology and morphometry of thyroid tissue

The control rats' thyroid glands showed many follicles of different sizes closely packed with a uniform acidophilic colloid; cuboidal follicular cells with rounded nuclei surrounded the follicles (Figure 13. A). On the other hand, Lot II's thyroid tissues showed a lack of standard follicular architecture and either little or no colloids. Numerous follicular cells exhibited enlargement and vacuolation, with some lacking nuclei. A dilated and desquamated cell cluster in the lumen and clogged blood vessels were observed (Figure 13. B). Other follicles in this lot showed destroyed architecture, several layers of follicular cells, and clogged capillaries (Figure 13. B). Lot III's thyroid tissues showed a typical architecture, and most of the follicles with acidophilic colloids were restored; the follicular cells had round to oval nuclei (Figure 13. C). Most follicles in Group IV showed a minor improvement. A small amount of congestion was seen in some follicles, which had inflated and vacuolated cells partly filled with acidophilic colloids (Figure 13. D). Carbimazole is absorbed and then changes into methimazole, the active form. Tyrosine residues on thyroglobulin are not iodinated by the thyroid peroxidase enzyme when methimazole is present, reducing the production of thyroid hormones T3 and T4 (Nayak and Burman, 2006), followed by an increase in TSH; this hormone was recognized for its ability to stimulate hyperplasia and hypertrophy of follicular cells in the thyroid gland, leading to the development of nodular goiter (Fountoulakis, Philippou, and Tsatsoulis 2007; Zbucki *et al.*, 2007). Furthermore, it corroborated the findings of Haiying *et al.*, (2006), who found that hypothyroid individuals were recognized when their T3 and T4 biochemical parameters fell below normal ranges. Their TSH levels rose above normal limits. Compared to control rats, *A.campestris* extract reduces TSH while increasing T4 and T3 levels in hypothyroid rat models (Figure. 13).

The current work used histological analyses to identify CBZ-induced follicular epithelial hyperplasia and hypertrophy, Due to hypertrophy induced by an elevation in TSH and the formation of numerous layers of follicular cells, follicle height increases (Amra *et al.*, 2022). The increased TSH level in Lot II may be attributed to dilated and blocked blood capillary infiltration into the interfollicular tissues. This conclusion aligned with another research study by Krohn *et al.*, (2005), which showed that methimazole medication causes the gland to vascularize. According to a recent study by Ibrahim *et al.*, (2021), CBZ raises TSH levels while lowering thyroid hormone levels; thyroid hormone levels in Lot II of the current research sharply decreased (Figure. 11). CBZ prevents Thyroglobulin's tyrosine clumps from being iodinated and coupled by the thyroid peroxidase enzyme. Levothyroxine and CBZ were

utilized in combination treatment to lower TH levels (Siddiqui *et al.*, 2015), This result aligns with our findings. Lot II had a much higher TSH level than Groups I, III, and IV (Figure. 11). Increased lysosomal activity in Lot II follicular cells is a phagocytosis marker since specific cells may have undergone degenerative changes (Scanlan *et al.*, 2004), Lot III was believed to have considerably better histology for this inquiry (Figure 11).

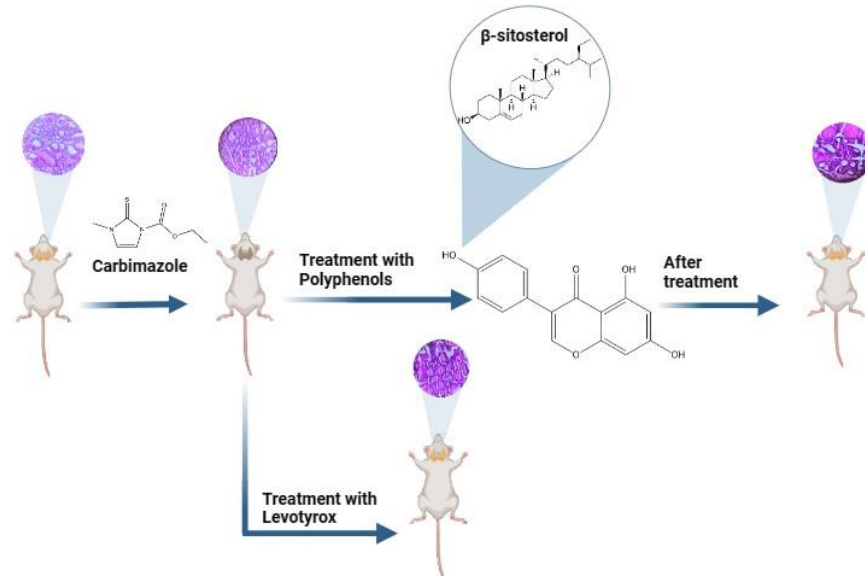


Figure 11. The Mechanism of Beta-Sitosterol In The Treatment of Hypothyroidism.

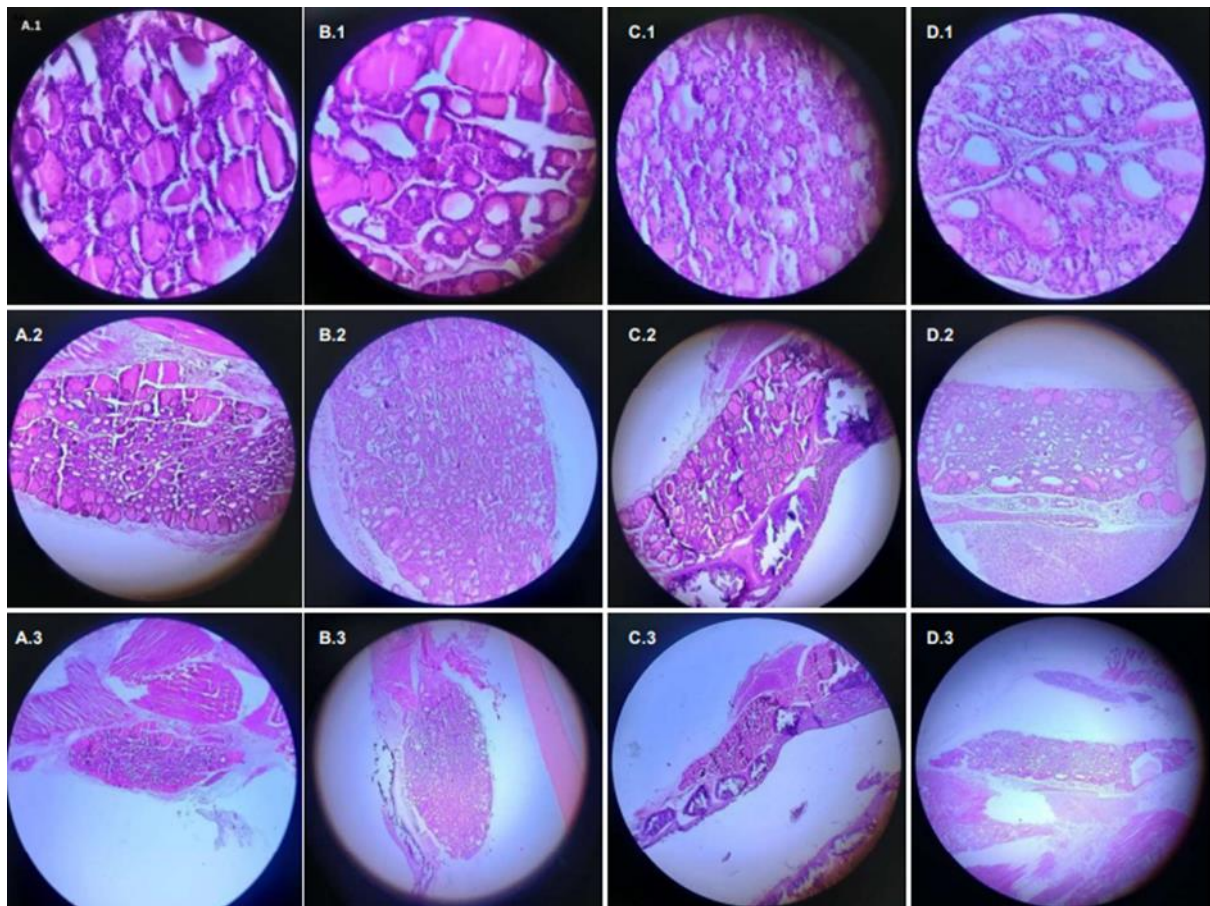


Figure 12. Microscopic views of thyroid histological lots in rats at varied magnifications (A1. B1. C1. D1; 10x/ A2. B2. C2. D2; 40x/ A3. B3. C3. D3; 100x) across four distinct groups: (A) Control. (B) Group Treated with CBZ. (C) Group treated with investigated plant. and (D) Group Treated with Levothyrox[®].

8. Molecular Docking:

Tested compound molecular weight <500 g/mol, the hydrogen bond donor (HBD) is not more than five, and the hydrogen bond acceptor (HBA) is less than ten so that the drug can penetrate the cell membrane to reach its target receptors. A molecular weight of less than 500 Da will diffuse to the cell membrane more easily than high ones (Lipinski *et al.*, 1997).

Table 9. The conformability of compounds toward Lipinski's rules of five.

	MW	HBD	HBA	Log-P	MR
2,3-Butanediol	90.12	2	2	1.26	23.67
β-Sitosterol	414.71	1	1	4.79	133.23
β-Pinene	136.23	0	0	2.59	45.22
α-Curcumene	202.34	0	0	3.50	69.55
Arteannuin B	248.32	0	3	2.86	67.73

MW: molecular weight (g/mol).. HBD: hydrogen bond donor. HBA: hydrogen bond acceptor. Log-P: partition coefficient.. MR: molar refractivity.

All targeted compounds agreed with Lipinski criteria. while alpha curcumin. beta-pinene. and beta-sitosterol were evaluated by the MLOGP rule (>4.15). Otherwise, they show more than two Lipinski criteria, considered high permeability (Choy and Prausnitz 2011).

Table 10. The acute toxicity prediction results of compounds.

	Hepatotoxicity	Neurotoxicity	Nephrotoxicity	Respiratory toxicity	Cardiotoxicity	LD ₅₀ (mg/kg)	Class
2,3-Butanediol	Inactive	Inactive	Inactive	Inactive	Inactive	3380	5
β-Sitosterol	Inactive	Active	Inactive	Active	Inactive	890	4
β-Pinene	Inactive	Active	Inactive	Inactive	Inactive	4700	5
α-Curcumene	Inactive	Inactive	Inactive	Inactive	Inactive	2000	5
Arteannuin B	Inactive	Inactive	Inactive	Active	Inactive	502	4

The first step in assessing molecules' toxicity is to predict their acute toxicity. Indeed, as shown in Table 8, the hepatotoxicity test of all compounds was predicted to be nontoxic to the liver; they also don't affect renal function or heart damage. Meanwhile, β-Sitosterol. β-Pinene, and arteannuin B are toxic to the nervous and respiratory systems. High toxicity class of compound is considered as a low toxicity effect. which is revealed as the experimental amount of compound that causes 50% of animal death (LD₅₀) when swallowed. 2,3-

Butanediol, β -Pinene and α -Curcumene are in the fifth category with a low toxicity effect. presented in Table 9, while β -Sitosterol and Arteannuin B are in the 4th class with 890 and 502 mg/kg, respectively.

Table 11. Absorption. Distribution. Metabolism. and Excretion (ADME) results.

	2.3-Butanediol	β -Sitosterol	β -Pinene	α -Curcumene	Arteannuin B
GI	High	Low	Low	Low	High
BBB	No	No	Yes	No	Yes
CYP2D6	No	No	No	Yes	No
CYP2C9	No	No	Yes	No	No
CYP3A4	No	No	No	No	No
Log-Kp	-7.50	-2.20	-4.18	-3.71	-5.98

GI: gastrointestinal absorption. **BBB:** the blood-brain barrier. **Log-Kp:** skin permeability (cm/s).

In drug discovery, it is essential to test the contraindicate of compounds toward detoxification enzymes. Cytochrome P450 has a crucial role in the body, mainly in the liver, oxidizing organic matter and excretion of drugs. Moreover, inhibition of these detoxification isoforms may also lead to drug toxicity due to decreased metabolic clearance of substrate. It is clear that from Table 9, 2.3-Butanediol, β -Sitosterol, and Arteannuin B compounds have no inhibition tendency toward cytochrome enzymes so that the P450 enzyme can metabolize them, except for α -Curcumene. The docked ligands with 5FFI receptors result in diverse binding energy; the stable conformation, which corresponds to the lowest one, was chosen as the best pose and used in the docking analysis. The binding energy of the docked compounds and their interactions with a protein are presented in Table 10.

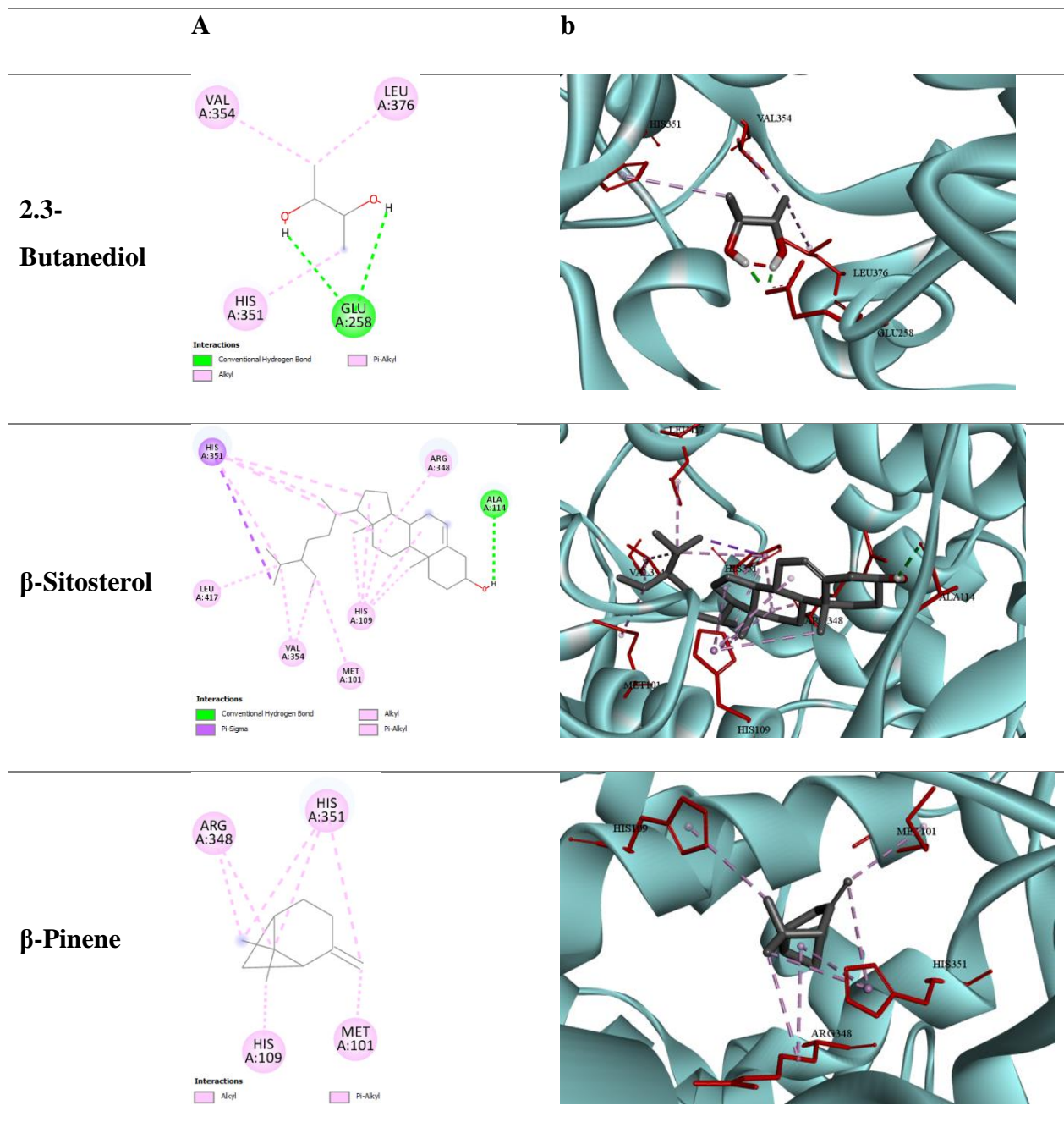
Table 12. Binding energy values of targeted compounds obtained by molecular docking approach.

Complex	Category	Type	Name	Distance (Å°)	$-\Delta G$ (Kcal.mol ⁻¹)
2.3-Butanediol	H-Bond	Conventional	GLU258	1.80 & 1.94	-3.09
	Hydrophobic	Alkyl	VAL354. LEU376	3.71. 4.92 & 4.64	
		Pi-Alkyl	& HIS351		
β-Sitosterol	H-Bond	Conventional	ALA114	2.42	-11.48
	Hydrophobic	Pi-Sigma	HIS351	3.86	
		Alkyl	ARG348. VAL354. LEU417. MET101 & VAL354	4.75. 4.79. 5.13. 4.44 & 4.31	

		Pi-Alkyl	HIS109	5.39. 5.47. 5.44. 3.95 & 5.23	
			HIS351	4.56. 4.28. 4.13 & 5.05	
β-Pinene	Hydrophobic	Alkyl	ARG348	4.76 & 4.41	-6.16
			MET101	5.11	
		Pi-Alkyl	HIS109	4.47	
			HIS351	4.33. 4.35 & 5.30	
α-Curcumene	Electrostatic	Pi-Anion	ASP108	3.41	-7.33
	Hydrophobic	Alkyl	VAL354	5.49. 4.57 & 4.15	
			MET101	5.20 & 4.24	
			LEU417	5.05	
			ARG348	4.65	
		Pi-Alkyl	PHE347	4.20	
			HIS351	4.86. 5.09 & 5.30	
			ARG348	4.76	
Arteannuin B	H-Bond	Conventional	ALA114	3.37	-7.22
		C-H Bond	PHE113	3.11	
	Hydrophobic	Alkyl	ARG348	4.06	
			LEU433	4.77	
		Pi-Alkyl	HIS351	5.23. 4.65 & 4.17	

Calculated binding energy indicates a high binding affinity between receptor and chosen compounds. The hydrophobic bonds are the most common interactions between ligands and HIS351 and ARG348 protein residues, as pi-alkyl and alkyl types, with a distance range of 3.71-5.30 Å. Conventional hydrogen bonds are considered the most vital Van der Waals forces between high electronegative atoms. such as F, Cl, O, N, and S, and low electronegative, mostly hydrogen atoms, Two shortest hydrogen bond lengths are formed. Besides all h-bonds formed with compounds, 2,3-butanediol exhibits two hydrogen bonds as shorter bond lengths, 1.80 and 1.94, interacted with GLU258 amino acid, and had the highest

binding energy -3.09 Kcal/mol. At the same time, pi-anion and carbon-hydrogen bonds are the only interactions formed with α -Curcumene and arteannuin B., respectively (Figure 14). Meanwhile, β -sitosterol is the only compound that has a pi-sigma bond and shows a pi-alkyl bond, and β -pinene with HIS109 residue.



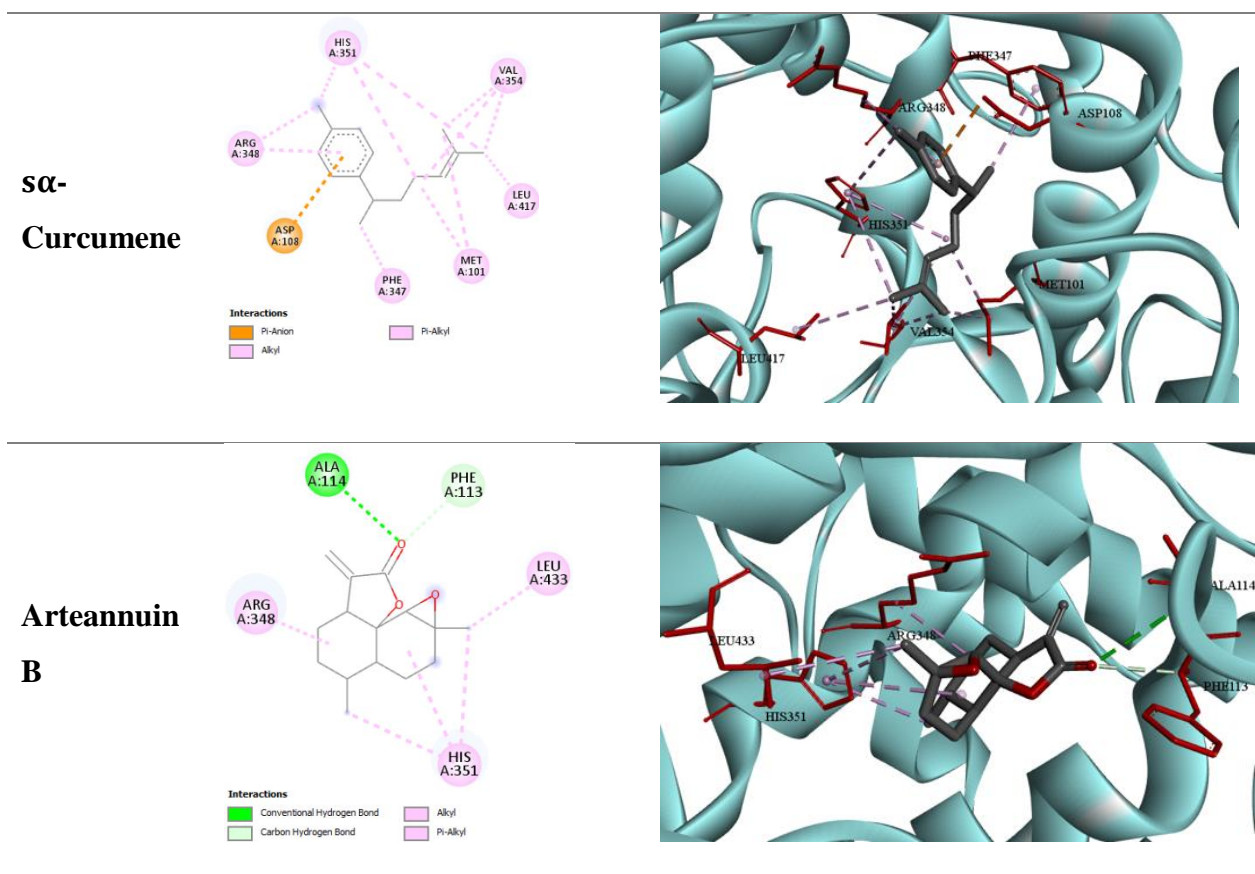


Figure 13. Visualization of compound's interactions with thyroid peroxidase protein (PDB ID: 5FF1) in 2D (a) and 3D (b) views.

β -sitosterol is an ancient compound found in diverse plants with effective biological activity. Hence, the molecule has a poor bioactivity effect, and its analogs exhibit very convenient activity toward various diseases. Although UPLC analysis reveals that the β -sitosterol compound is the second compound content, the 2,3-butanediol compound is the primary content. The docking results showed that the β -sitosterol compound had the lowest binding energy value of -11.48 Kcal/mol, even though the synergic effect of the plant extract component may improve its inhibition affinity to thyroid peroxidase receptor by enhancing its stimulation behavior and increase the production of antioxidant enzymes, which lead to hypothyroidism prevention (Saeidnia *et al.*, 2014).

8.1. *In silico* study of pancreatic cancer proteins with essential oil

In this study, the high concentration of compounds in *Artemisia campestris* L. essential oil was subjected to their bioactivity tendency, which presented as a binding affinity toward common pancreatic cancer proteins, shown in Figure 15.

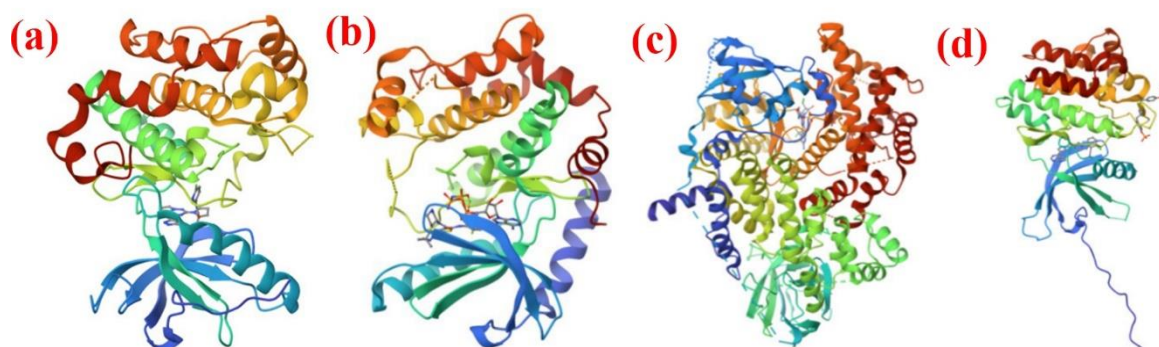
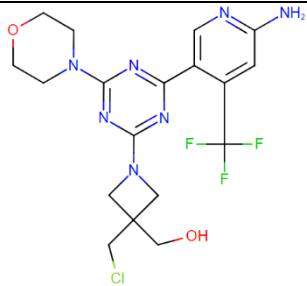
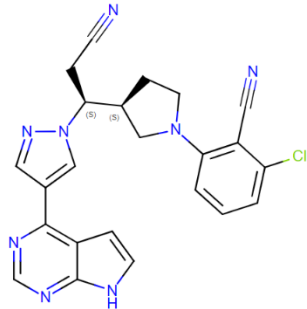


Figure 14. The crystallographic structure of targeted proteins of pancreatic cancer. Insulin-like growth factor 1 receptor (A). Mitogen-activated protein kinase kinase-1 (B). Phosphoinositide 3-kinase gamma (C). and Janus Kinase-1 (D).

Co-crystallized ligands of EBI, 77D, 6K5, and LKT., which are active against pancreatic cancer proteins with respective PDB_IDs 3I81, 3SLS, 5JHB, and 6SM8 were their reduced binding affinity scores -10.4, -10.9, -8.9, and -10.8 Kcal/mol. Those co-crystallized ligands presented RMSD values of 1.0018, 0.7973, 1.5305, and 2.3271 Å, respectively, as shown in Table 12.

Table 13. RMSD (in Å) and binding affinity (in Kcal/mol) of potent compounds against their pancreatic cancer targeted protein.

Cocrystal ID	Structure	Target Receptor	Binding Affinity (Kcal/mol)	RMSD (Å)
EBI		IGF1	-10.4	1.0018
77D		MEK1	-10.9	0.7973

6K5		PI3K	-8.9	1.5305
LKT		JAK-1	-10.8	2.3271

Among all screened molecules, compound C2. The second highest concentration content is in plant essential oil, shows more interactions with all receptors, with the lowest binding affinity -8.3, -8, -7.6, and -6.5 Kcal/mol towards PI3K, Janus kinase-1, MEK1 and Insulin-like growth factor 1, in order, Table 12, four hydrogen bonds with 3I81 protein, ASP1056, LEU975, ASP1123, GLY1055 residues while exhibiting three hydrogen bonds with PHE209, VAL211, SER212 amino acids of 3SLS binding site, Figure 13. Table 13. in order. Moreover, electrostatic interactions have been made through LYS833 and ASP1021 with 5JHB and 6SM8 receptors. At the same time, only Pi-Sulfur was observed by MET804 amino acid of 5JHB binding site with bio-molecule 3, demonstrated in Figure 6, in order, Meanwhile, C3, C5, C1, C4, C6, and C8 molecules reveal a binding affinity of -7.1, -6.6, -6, -6, -6, and -5.7 Kcal/mol towards JAK-1. Their inhibition tendency toward PI3K is -6.6 Kcal/mol for molecule C3, -6.5 Kcal/mol for compounds C4 and C6, while -6.3, -6.2 and 5.5 Kcal/mol for C1, C5 and C7, in order. as the lowest binding energy, presented in Table 13 and their interactions with amino acid residues are summarized in Table 14, visualized in 2D (A) and 3D (B) in Figure 13 and Figure 14.

Table 14. Binding energy (in Kcal/mol) of *A. campestris* bio-compounds against JAK1, PI3K, MEK1 and IGF1 proteins.

Bio-compounds	Structure	Binding affinity (Kcal/mol)			
		6SM8	5JHB	3SLS	3I81

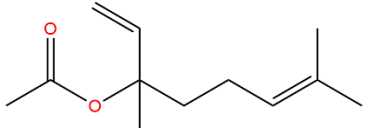
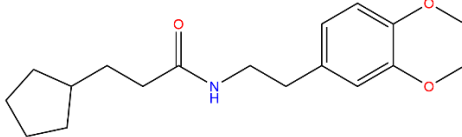
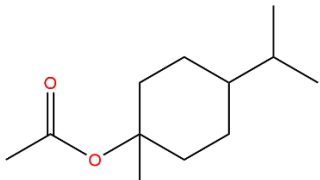
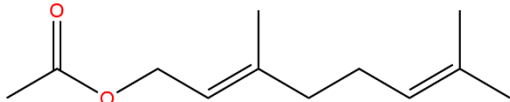
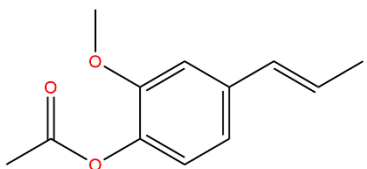
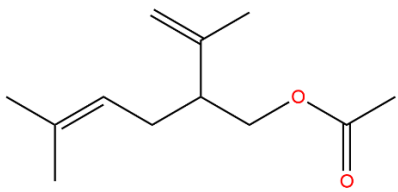
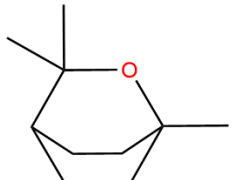
C1		-6	-6.3	-4.9	-5.4
C2		-8	-8.3	-7.6	-6.5
C3		-7.1	-6.6	-5.8	-6.1
C4		-6	-6.5	-6.1	-5.6
C5		-6.6	-6.2	-6	-5.8
C6		-6	-6.5	-5.3	-5.5
C7		-5.7	-5.5	-5	-5.8

Table 14. Hydrophobic and polar hydrogen binding of biomolecules with active site amino acids of chosen receptors.

Molecules	Protein PDB IDs	Bond Type	Amino acids interacted with
C1	3I81	H-Bond	ASP1123
		Hydrophobic	LEU975. VAL983. ALA1001. MET1126
	3SLS	H-Bond	VAL211. SER212
		Hydrophobic	LEU115. ILE99. LEU101. ILE139. ILE111. LEU215
	5JHB	H-Bond	ASP964
		Hydrophobic	TYR867. VAL882. ILE963. PHE961
6SM8	Hydrophobic	LEU1010. LEU881. ALA906. VAL889. PHE958	
C2	3I81	H-Bond	ASP1056. LEU975. ASP1123. GLY1055
		Hydrophobic	LEU975. MET1112. MET1126. VAL983. ALA1001
	3SLS	H-Bond	PHE209. VAL211. SER212
		Hydrophobic	PHE129. PHE209. LEU118. MET143. ILE111. LEU215

	5JHB	H-Bond	ASP964. SER806. ASP841	
		Hydrophobic	MET804. PRO810. ILE831. LYS833. TYR867. ILE963	
	6SM8	H-Bond	ARG1007. ASP1003	
		Hydrophobic	GLY882;GLU883;GLY884. LEU881. ALA906. LEU1010	
C3	3I81	H-Bond	ASP1123	
		Hydrophobic	LEU975. MET1126. VAL983. ALA1001	
	3SLS	Hydrophobic	LEU118. ILE141. PHE209	
	5JHB	H-Bond	LYS833	
		Hydrophobic	ILE831. TYR867. ILE963. ILE879	
	6SM8	Hydrophobic	LEU881. VAL889. ALA906. LEU1010	
C4	3I81	H-Bond	ASP1123	
		Hydrophobic	LEU975. LEU1051. MET1112. VAL983. ALA1001	
	3SLS	H-Bond	VAL211. SER212	
		Hydrophobic	LEU118. ILE141. PHE209	
	5JHB	Hydrophobic	ILE831. ILE879. ILE963. MET953. VAL882. ALA885. TYR867. PHE961	
	6SM8	H-Bond	SER963	
		Hydrophobic	LEU881. VAL889. ALA906. LEU1010	
	C5	3I81	H-Bond	ASP1123. MET1052
			Hydrophobic	LEU975. MET1126. VAL983. ALA1001
		3SLS	H-Bond	VAL211. SER212. GLY210
Hydrophobic			LEU118. ILE141. PHE209	
5JHB		Hydrophobic	LYS833. ILE879. ILE963. TYR867. ILE831	
6SM8		H-Bond	ARG1007	
	Hydrophobic	LEU881. ALA906. LEU1010. VAL889		
C6	3I81	H-Bond	ASP1123	
		Hydrophobic	LEU975. MET1126. VAL1033. MET1049	
	3SLS	H-Bond	VAL211. SER212	
		Hydrophobic	LEU118. ILE141. PHE209	
	5JHB	H-Bond	ASP964	
		Hydrophobic	LYS833. LEU838. ILE879. PRO810. ILE831. ILE963. TYR867	
	6SM8	H-Bond	ASP1021	
		Hydrophobic	LEU881. ALA906. LEU1010. VAL889. PHE958	
C7	3I81	Hydrophobic	VAL983. MET1126. ALA1001	
	3SLS	Hydrophobic	ILE111. ILE139. LEU115	
	5JHB	Hydrophobic	LYS833. ILE879. ILE831	
	6SM8	Hydrophobic	LEU1010. VAL889	

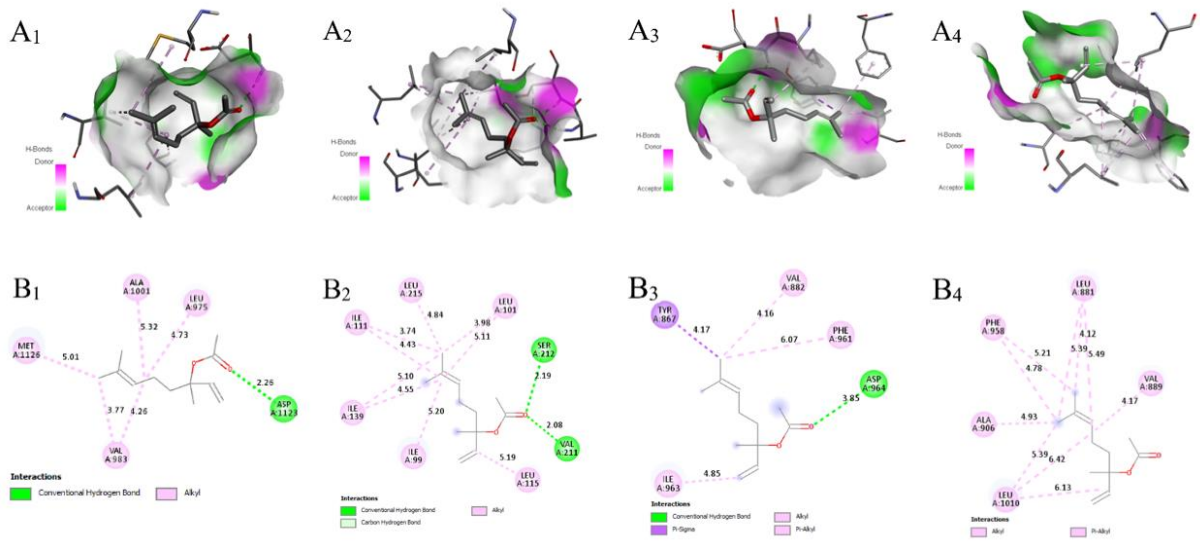


Figure 15. Visualization of interactions in 2D (A) and 3D (B) of linalyl acetate bio-compound with active site residues of 3I81(1), 3SLS(2), 5JHB(3) and 6SM8(4) receptors.

CONCLUSION

CONCLUSION

The findings of this study provide compelling evidence for the therapeutic potential of *Artemisia campestris* L. in managing the complex symptoms associated with Polycystic Ovary Syndrome (PCOS) and hypothyroidism, as well as its promising role in diabetes management and cancer therapy. In the context of PCOS, the study corroborates previous research that highlights the detrimental effects of induced PCOS on follicle growth and the development of ovarian cysts. Treatment with *A. campestris* extract demonstrated significant therapeutic benefits, notably through a reduction in the thickness of the follicular theca layer. This effect may be mediated by increased lipolysis and reduced hypertrophy, potentially leading to decreased androgen and steroid production, thereby alleviating some symptoms of PCOS. The extract's ability to reduce luteinizing hormone (LH) levels and modulate hormone receptor activity suggests it may help restore hormonal balance in affected individuals.

Furthermore, the inhibition of α -amylase by *A. campestris* extract indicates its potential utility in managing type II diabetes mellitus by lowering postprandial glucose levels. The presence of flavonoids within the extract likely contributes to this inhibitory effect, positioning it as a valuable adjunctive therapy for diabetic patients. The study also revealed the robust antioxidant activity of *A. campestris*, characterized by significant guaiacol peroxidase activity. This antioxidant capacity may provide protective benefits against oxidative stress, often implicated in various health conditions, including PCOS. Regarding hypothyroidism, the aqueous extract demonstrated a dose-dependent potential to restore thyroid hormone levels in hypothyroid rats, along with *in vitro* antioxidant and anti-inflammatory activities. Molecular docking studies showed promising bioactive interactions of certain compounds with thyroid peroxidase, indicating the extract's potential as an enzyme inhibitor. The binding energy of these compounds ranged from -3.09 to -11.48 kcal/mol, with favorable drug-like properties as assessed through ADME analysis. This suggests that the phenolic and flavonoid extracts of *A. campestris* warrant further investigation to identify specific compounds responsible for their protective roles against thyroid dysfunction.

Additionally, the essential oil of *A. campestris* was chemically profiled, revealing significant antioxidant and anti-inflammatory activities that support traditional uses of this species, particularly in treating inflammatory diseases.

The *in silico* analysis of bioactive compounds derived from *A. campestris* and their interactions with pancreatic cancer proteins using AutoDock Vina identified 3-cyclopentyl-N-

CONCLUSION

(2-(3,4-dimethoxyphenyl)ethyl) as a compound with the highest binding affinity to pancreatic cancer receptors, particularly phosphoinositide 3-kinase gamma. This highlights its potential for development as an effective anti-cancer drug.

In summary, the results of this study not only underscore the multifaceted therapeutic potential of *A. campestris* in addressing the symptoms of PCOS, hypothyroidism, diabetes, and cancer but also pave the way for future investigations involving molecular dynamics simulations and *in vitro* and *in vivo* studies to further elucidate its benefits and mechanisms of action. Given its promising therapeutic properties, the industrial interest in *A. campestris*, particularly within the pharmaceutical and food sectors, is thus warranted.

REFERENCES

REFERENCES

- Adeniji, Shola Elijah, David Ebuka Arthur, and Adedirin Oluwaseye. 2020. 'Computational modeling of 4-Phenoxy nicotinamide and 4-Phenoxy pyrimidine-5-carboxamide derivatives as potent anti-diabetic agent against TGR5 receptor', *Journal of King Saud University-Science*, 32: 102-15.
- Ahmouda, Kaouthar, Boubaker Benhaoua, Salah Eddine Laouini, and Asma Labbi. 2022. 'Plant extract FRAP effect on cation vacancies formation in greenly synthesized wüstite (FexO) nanoparticles: A new contribution', *Sustainable Chemistry and Pharmacy*, 25: 100563.
- Akbarian, Mohsen, and Shu-Hui Chen. 2022. 'Instability challenges and stabilization strategies of pharmaceutical proteins', *Pharmaceutics*, 14: 2533.
- Akrout, Ahmed, Lidia Alarcon Gonzalez, Hajer El Jani, and Pablo Campra Madrid. 2011. 'Antioxidant and antitumor activities of *Artemisia campestris* and *Thymelaea hirsuta* from southern Tunisia', *Food and Chemical Toxicology*, 49: 342-47.
- Alkalby, JM, and SJ Alzerjawi. 2013. 'Effect of propylthiouracil-induced hypothyroidism on reproductive efficiency of adult male rats', *Bas. j. vet. Res*, 12: 113-21.
- Alrumaihi, Faris, Saleh A Almatroodi, Hajed Obaid A Alharbi, Wanian M Alwanian, Fadiyah A Alharbi, Ahmad Almatroudi, and Arshad Husain Rahmani. 2024. 'Pharmacological Potential of Kaempferol, a Flavonoid in the Management of Pathogenesis via Modulation of Inflammation and Other Biological Activities', *Molecules*, 29: 2007.
- Amaya-Farfan, Jaime. 2021. 'Denaturation of proteins, generation of bioactive peptides, and alterations of amino acids.' in, *Chemical Changes During Processing and Storage of Foods* (Elsevier).
- Amel, Benchohra Hadria, Dif Mustapha Mahmoud, Adli Fatima Zohra, Benchohra Fatima Zohra, Tounsi Mohamed, and Medjaher Halima Essaadia Souhila. 2022. 'Antioxidant and Anti-Inflammatory Activity of *Artemisia campestris* L', *Egyptian Academic Journal of Biological Sciences. C, Physiology and Molecular Biology*, 14: 489-97.
- Amra, Elsabry Abu, Sohir Ali abd El Rehim, Fakhr Mostafa Lashein, and Heba Seleem Shoaeb. 2022. 'Effect of a bradykinin potentiating factor separated from honey bee venom on thyroid gland and testis in hypothyroid white rats', *The Journal of Basic and Applied Zoology*, 83: 1.
- Ashwini, S, Zachariah Bobby, MG Sridhar, and CC Cleetus. 2017. 'Insulin plant (*Costus pictus*) extract restores thyroid hormone levels in experimental hypothyroidism', *Pharmacognosy research*, 9: 51.
- BAKCHICHE, Boulanouar, Ahmet C GÖREN, Zeynep AYDOĞMUŞ, Emel MATARACIKARA, and Mosad A GHAREEB. 2022. 'Artemisia campestris and artemisia herbaalba: Ic-hresi-ms profile alongside their antioxidant and antimicrobial evaluation', *ACTA Pharmaceutica Scientia*, 60.
- Barragan-Ferrer, Jesus-Manuel, Stéphane Negny, Jonas Damasius, Diana Barragan-Ferrer, and Dalia Cizeikiene. 2019. 'TRIZ evolution trends as an approach for predicting the future development of the technological systems in the food industry', *Managing Innovation in Highly Restrictive Environments: Lessons from Latin America and Emerging Markets*: 247-77.
- Barzegar, Mohammad Hossein, Homayoun Khazali, Seyyed Mehdi Kalantar, and Arezoo Khoradmehr. 2017. 'Effect of *Citrullus colocynthis* hydro-alcoholic extract on hormonal and folliculogenesis process in estradiol valerate-induced PCOs rats model: An experimental study', *International Journal of Reproductive BioMedicine*, 15: 661.
- Belhattab, R, M Boudjouref, JG Barroso, LP Pedro, and AC Figureueirido. 2011. 'Essential oil composition from *Artemisia campestris* grown in Algeria', *Advances in Environmental Biology*, 5: 429-32.

- Benamar-Aissa, Boualem, Nadhir Gourine, Mohamed Ouinten, and Mohamed Yousfi. 2024. 'Synergistic effects of essential oils and phenolic extracts on antimicrobial activities using blends of *Artemisia campestris*, *Artemisia herba alba*, and *Citrus aurantium*', *Biomolecular Concepts*, 15: 20220040.
- Bendifallah, Leila, and Othmane Merah. 2023. 'Phytochemical and biocidal properties of *Artemisia campestris* subsp. *campestris* L.(Asteraceae) essential oil at the southern region of Algeria', *Journal of Natural Pesticide Research*, 4: 100035.
- Bilgory, Asaf, Yuval Atzmon, Nardin Aslih, Yasmin Shibli Abu Raya, Moamina Sharqawi, Maya Shavit, Daniela Estrada, and Einat Shalom-Paz. 2023. 'Ovulatory-cycle frozen embryo transfer: spontaneous or triggered ovulation and the impact of LH elevation at hCG triggering', *Scientific reports*, 13: 7195.
- BIOVIA, Dassault Systèmes. 2021. 'Discovery Studio Visualizer 4.5', *San diego: Dassault systèmes*.
- Boudjelal, Amel, Antonella Smeriglio, Giovanna Ginestra, Marcella Denaro, and Domenico Trombetta. 2020. 'Phytochemical profile, safety assessment and wound healing activity of *Artemisia absinthium* L', *Plants*, 9: 1744.
- Brahmi, Fairouz, Rachda Berrached, Salima Kebbouche Gana, Leila Kadik, and Nesrine Lenchi. 2024. 'Chemical composition, antimicrobial and antioxidant activities of methanolic extracts of the Algerian *Artemisia campestris* L. at different stage of growth', *Vegetos*, 37: 1084-97.
- Bullock, Casey W, Reed B Jacob, Owen M McDougal, Greg Hampikian, and Tim Andersen. 2010. 'Dockomatic-automated ligand creation and docking', *BMC Research Notes*, 3: 1-8.
- Calabró, Paolo, James T Willerson, and Edward TH Yeh. 2003. 'Inflammatory cytokines stimulated C-reactive protein production by human coronary artery smooth muscle cells', *Circulation*, 108: 1930-32.
- Chaalal, Amina, Roseline Poirier, David Blum, Brigitte Gillet, Pascale Le Blanc, Marie Basquin, Luc Buée, Serge Laroche, and Valérie Enderlin. 2014. 'PTU-induced hypothyroidism in rats leads to several early neuropathological signs of Alzheimer's disease in the hippocampus and spatial memory impairments', *Hippocampus*, 24: 1381-93.
- Chaker, L, AC Bianco, J Jonklaas, and RP Peeters. 2017. "Hypothyroidism Lancet 390 (10101): 1550–1562." In.
- Chakera, Ali J, Simon HS Pearce, and Bijay Vaidya. 2011. 'Treatment for primary hypothyroidism: current approaches and future possibilities', *Drug design, development and therapy*: 1-11.
- Chebbac, Khalid, Oussama Abchir, Mohammed Chalkha, Abdelfattah El Moussaoui, Azeddin El Barnossi, Soufyane Lafraxo, Samir Chtita, Ahmad Mohammad Salamatullah, Mohammed Bourhia, and Musaab Daelbait. 2024. 'Phytochemical analysis, antimicrobial and antioxidant activities of essential oils of the species *Artemisia mesatlantica* maire: in vitro and in silico approaches', *CyTA-Journal of Food*, 22: 2388269.
- Choy, Young Bin, and Mark R Prausnitz. 2011. 'The rule of five for non-oral routes of drug delivery: ophthalmic, inhalation and transdermal', *Pharmaceutical research*, 28: 943-48.
- Daoudi, Nour Elhouda, Mohamed Bouhrim, Hayat Ouassou, Abdelkhaleq Legssyer, Hassane Mekhfi, Abderrahim Ziyat, Mohammed Aziz, and Mohamed Bnouham. 2020. 'Inhibitory effect of roasted/unroasted *Argania spinosa* seeds oil on α -glucosidase, α -amylase and intestinal glucose absorption activities', *South African journal of botany*, 135: 413-20.
- Dharmadeva, Sharmila, Lahiru Sandaruwan Galgamuwa, C Prasadinie, and Nishantha Kumarasinghe. 2018. 'In vitro anti-inflammatory activity of *Ficus racemosa* L. bark

- using albumin denaturation method', *AYU (An international quarterly journal of research in Ayurveda)*, 39: 239-42.
- Dib, Ikram, Luc Angenot, Atika Mihamou, Abderrahim Ziyat, and Monique Tits. 2017. 'Artemisia campestris L.: Ethnomedicinal, phytochemical and pharmacological review', *Journal of Herbal Medicine*, 7: 1-10.
- Dib, Ikram, and Fatima Ezzahra El Alaoui-Faris. 2019. 'Artemisia campestris L.: Review on taxonomical aspects, cytogeography, biological activities and bioactive compounds', *Biomedicine & Pharmacotherapy*, 109: 1884-906.
- Djeridane, A, M Yousfi, B Nadjemi, D Boutassouna, P Stocker, and N Vidal. 2006. 'Antioxidant activity of some Algerian medicinal plants extracts containing phenolic compounds', *Food chemistry*, 97: 654-60.
- Evans, William Charles. 2009. *Trease and Evans' pharmacognosy* (Elsevier Health Sciences).
- Fathima, Syeda Nishat, Sayed Mohammed Firdous, Sourav Pal, Hesham S Ghazzawy, and Mostafa M Gouda. 2024. 'Assessment of In Vitro Antioxidant and Anti-Inflammatory Activities of Pumpkin (Cucurbita pepo) Natural Plant', *Natural Product Communications*, 19: 1934578X241257127.
- FEKETE, K, A GEÖSEL, S KECSKEMÉTI, and Z PAP. 2024. 'The effect of mulching materials on the arbuscular mycorrhiza fungi root colonisation, peroxidase activity, and chlorophyll content in Lactuca sativa', *BIOLOGIA PLANTARUM*, 68: 31-38.
- Ferreira, E, AE Silva, R Serakides, AES Gomes, and Geovanni Dantas Cassali. 2007. 'Model of induction of thyroid dysfunctions in adult female mice', *Arquivo Brasileiro de Medicina Veterinária e Zootecnia*, 59: 1245-49.
- Fountoulakis, Stelios, George Philippou, and Agathocles Tsatsoulis. 2007. 'The role of iodine in the evolution of thyroid disease in Greece: from endemic goiter to thyroid autoimmunity', *Hormones (Athens)*, 6: 25.
- Gao, Zixuan, Xiaochen Ma, Jing Liu, Yuhang Ge, Lei Wang, Ping Fu, Zhian Liu, Ruiqin Yao, and Xiaonan Yan. 2020. 'Trolox protects against DHT-induced polycystic ovary syndrome in rats', *Journal of ovarian research*, 13: 1-11.
- Ghafurniyan, Habibeh, Mahnaz Azarnia, Mohammad Nabiuni, and Latifeh Karimzadeh. 2015. 'The effect of green tea extract on reproductive improvement in estradiol valerate-induced polycystic ovarian syndrome in rat', *Iranian journal of pharmaceutical research: IJPR*, 14: 1215.
- Ghliissi, Zohra, Nadhim Sayari, Rim Kallel, Ali Bougateg, and Zouheir Sahnoun. 2016. 'Antioxidant, antibacterial, anti-inflammatory and wound healing effects of Artemisia campestris aqueous extract in rat', *Biomedicine & Pharmacotherapy*, 84: 115-22.
- González-Minero, Francisco José, Luis Bravo-Díaz, and Antonio Ayala-Gómez. 2020. 'Rosmarinus officinalis L. (Rosemary): An ancient plant with uses in personal healthcare and cosmetics', *Cosmetics*, 7: 77.
- Hadadi, Zahra, Ghorban Ali Nematzadeh, and Somayeh Ghahari. 2020. 'A study on the antioxidant and antimicrobial activities in the chloroformic and methanolic extracts of 6 important medicinal plants collected from North of Iran', *BMC chemistry*, 14: 1-11.
- Haiying, Yu, Yang Yan, Zhang Muxun, Lu Huiling, Zhang Jianhua, Wang Hongwei, and Cianflone Katherine. 2006. 'Thyroid status influence on adiponectin, acylation stimulating protein (ASP) and complement C3 in hyperthyroid and hypothyroid subjects', *Nutrition & metabolism*, 3: 1-8.
- Harborne, Jeffrey B, and JB Harborne. 1973. 'Phenolic compounds', *Phytochemical methods: A guide to modern techniques of plant analysis*: 33-88.
- Hasegawa, Tokio, Mayo Osaka, Yusaku Miyamae, Katsutoshi Nishino, Hiroko Isoda, Kiyokazu Kawada, Mohamed Neffati, Kazuhiro Irie, and Masaya Nagao. 2021. 'Two Types of PPAR γ Ligands Identified in the Extract of Artemisia campestris', *Chemistry*, 3: 647-57.

- Hbika, Asmae, Nour Elhouda Daoudi, Abdelhamid Bouyanzer, Mohamed Bouhrim, Hicham Mohti, El Hassania Loukili, Hamza Mechchate, Rashad Al-Salahi, Fahd A Nasr, and Mohamed Bnouham. 2022. 'Artemisia absinthium L. Aqueous and ethyl acetate extracts: Antioxidant effect and potential activity in vitro and in vivo against pancreatic α -amylase and intestinal α -glucosidase', *Pharmaceutics*, 14: 481.
- Hoeger, Kathleen M, Anuja Dokras, and Terhi Piltonen. 2021. 'Update on PCOS: consequences, challenges, and guiding treatment', *The Journal of Clinical Endocrinology & Metabolism*, 106: e1071-e83.
- Hong, Yanli, Yanyun Yin, Yong Tan, Ke Hong, Fengrong Jiang, and Yao Wang. 2018. 'Effect of quercetin on biochemical parameters in letrozole-induced polycystic ovary syndrome in rats', *Tropical Journal of Pharmaceutical Research*, 17: 1783-88.
- Hosseini, Seyede Fatemeh, Forouzan Khodaei, Zeynab Hasansagha, Hamidreza Khosravizadeh, Mostafa Abdollahi, and Ehsaneh Azaryan. 2023. 'Ameliorative Effect of Chitosan-Propolis Nanoparticles on the Estradiol Valerate-Induced PCOS in Rat'.
- Hu, Tao, Xiaoxue Yuan, Rongcai Ye, Huiqiao Zhou, Jun Lin, Chuanhai Zhang, Hanlin Zhang, Gang Wei, Meng Dong, and Yuanyuan Huang. 2017. 'Brown adipose tissue activation by rutin ameliorates polycystic ovary syndrome in rat', *The Journal of Nutritional Biochemistry*, 47: 21-28.
- Hwang, Ji Hye, Hyo Won Jung, Seok Yong Kang, An Na Kang, Jun Nan Ma, Xiang Long Meng, Min Sub Hwang, and Yong-Ki Park. 2018. 'Therapeutic effects of acupuncture with MOK, a polyherbal medicine, on PTU-induced hypothyroidism in rats', *Experimental and therapeutic medicine*, 16: 310-20.
- Ibrahim, AA, NA Mohammed, KA Eid, MM Abomughaid, AM Abdelazim, and AM Aboregela. 2021. 'Hypothyroidism: Morphological and metabolic changes in the testis of adult albino rat and the amelioration by alpha-lipoic acid', *Folia Morphologica*, 80: 352-62.
- Jahan, Sarwat, Faryal Munir, Suhail Razak, Anam Mehboob, Qurat Ul Ain, Hizb Ullah, Tayyaba Afsar, Ghazala Shaheen, and Ali Almajwal. 2016. 'Ameliorative effects of rutin against metabolic, biochemical and hormonal disturbances in polycystic ovary syndrome in rats', *Journal of ovarian research*, 9: 1-9.
- Kalita, Pallab, Barman K Tapan, Tapas K Pal, and Ramen Kalita. 2013. 'Estimation of total flavonoids content (TFC) and anti oxidant activities of methanolic whole plant extract of *Biophytum sensitivum* Linn', *Journal of Drug delivery and Therapeutics*, 3: 33-37.
- Karkera, Shilpa, Earlina Agard, and Larysa Sankova. 2023. 'The clinical manifestations of polycystic ovary syndrome (PCOS) and the treatment options', *European Journal of Biology and Medical Science Research*, 11: 57-91.
- Kicińska, Aleksandra Maria, Radoslaw B Maksym, Magdalena A Zabielska-Kaczorowska, Aneta Stachowska, and Anna Babińska. 2023. 'Immunological and metabolic causes of infertility in polycystic ovary syndrome', *Biomedicines*, 11: 1567.
- Kılıç, Ceyhun, Ayşenur Gürgeç, Sibel Yıldız, Zehra Can, and Atiye Değirmenci. 2024. 'Total phenolics, tannin contents, antioxidant properties, protein and sensory analysis of *Pleurotus ostreatus*, *Pleurotus citrinopileatus* and *Pleurotus djamor* cultivated on different sawdusts', *Maderas. Ciencia y tecnología*, 26.
- Kumar, Manish, Madhu Chandel, Subodh Kumar, and Satwinderjeet Kaur. 2012. 'Studies on the antioxidant/genoprotective activity of extracts of *Koelreuteria paniculata* laxm', *Am. J. Biomed. Sci.*, 1: 177-89.
- Lipinski, Christopher A, Franco Lombardo, Beryl W Dominy, and Paul J Feeney. 1997. 'Experimental and computational approaches to estimate solubility and permeability in drug discovery and development settings', *Advanced drug delivery reviews*, 23: 3-25.
- Lis, A, and M Kowal. 2015. 'Constituents of the essential oils from different organs of *Artemisia campestris* L. subsp. *campestris*', *Journal of Essential Oil Research*, 27: 545-50.

- Llauradó Maury, Gabriel, Daniel Méndez Rodríguez, Sophie Hendrix, Julio César Escalona Arranz, Yilan Fung Boix, Ania Ochoa Pacheco, Jesús García Díaz, Humberto J Morris-Quevedo, Albys Ferrer Dubois, and Elizabeth Isaac Aleman. 2020. 'Antioxidants in plants: A valorization potential emphasizing the need for the conservation of plant biodiversity in Cuba', *Antioxidants*, 9: 1048.
- Lo Piparo, Elena, Holger Scheib, Nathalie Frei, Gary Williamson, Martin Grigorov, and Chieh Jason Chou. 2008. 'Flavonoids for controlling starch digestion: structural requirements for inhibiting human α -amylase', *Journal of medicinal chemistry*, 51: 3555-61.
- Loucif, Karima, Hassiba Benabdallah, Fatima Benchikh, Soulaf Mehlous, Chawki Ben Souici, and Smain Amira. 2020. 'Total phenolic contents, DPPH radical scavenging and β -carotene bleaching activities of aqueous extract from *Ammoides atlantica*', *Journal of Drug delivery and Therapeutics*, 10: 196-98.
- Mammeri, Bakhtia, Fouad Bahri, Mohamed Kouidri, Bouharaoua Boudani, and Fatiha Arioui. 2022. 'Evaluation of chemical composition, anti-inflammatory, antibacterial activity and synergistic effect between antibiotics and the essential oil of *Artemisia campestris* L.', *Journal of Applied Biological Sciences*, 16: 230-47.
- Mandal, Subhash C, Tapan K Maity, J Das, BP Saba, and M Pal. 2000. 'Anti-inflammatory evaluation of *Ficus racemosa* Linn. leaf extract', *Journal of ethnopharmacology*, 72: 87-92.
- Mansinhos, Inês, Sandra Gonçalves, Raquel Rodríguez-Solana, José Manuel Moreno-Rojas, and Anabela Romano. 2024. 'Environmental factors related to climate change alter the chemical composition and biological activity of *Lavandula viridis* L'Her essential oil', *Agriculture*, 14: 1067.
- Marghich, Mohamed, Ouafa Amrani, Ahmed Karim, Tarik Harit, Leila Beyi, Hassane Mekhfi, Mohamed Bnouham, and Mohammed Aziz. 2023. 'Myorelaxant and antispasmodic effects of the essential oil of *Artemisia campestris* L., and the molecular docking of its major constituents with the muscarinic receptor and the L-type voltage-gated Ca^{2+} channel', *Journal of ethnopharmacology*, 311: 116456.
- McAninch, Elizabeth A, and Antonio C Bianco. 2016. 'The history and future of treatment of hypothyroidism', *Annals of internal medicine*, 164: 50-56.
- McGlacken-Byrne, Sinéad M, Harriet M Gunn, and Helen Simpson. 2024. 'Disorders of the Ovary.' in *Paediatric Endocrinology: Management of Endocrine Disorders in Children and Adolescents* (Springer).
- Megdiche-Ksouri, Wided, Najla Trabelsi, Khaoula Mkadmini, Soumaya Bourgou, Amira Noumi, Mejdi Snoussi, Rahma Barbria, Olfa Tebourbi, and Riadh Ksouri. 2015. 'Artemisia campestris phenolic compounds have antioxidant and antimicrobial activity', *Industrial Crops and Products*, 63: 104-13.
- Metoui, Rafika, Hedi Mighri, Jalloul Bouajila, Mansour Znati, Hajer El-Jani, and Ahmed Akrouf. 2022. 'Artemisia campestris dried leaf extracts: Effects of different extraction methods and solvents on phenolic composition and biological activities', *South African journal of botany*, 151: 288-94.
- Nadji, Said, Soumaya Boudjemaa, Abdelhakim Bounab, and Youcef HadeF. 2022. 'EVALUATION OF BIOLOGICAL ACTIVITIES OF MATRICARIA PUBESCENS FROM ALGERIA', *Bulletin of Pharmaceutical Sciences Assiut University*, 45: 723-36.
- Naili, Mahboba B, Rabia O Alghazeer, Nabil A Saleh, and Asma Y Al-Najjar. 2010. 'Evaluation of antibacterial and antioxidant activities of *Artemisia campestris* (Astraceae) and *Ziziphus lotus* (Rhamnaceae)', *Arabian Journal of Chemistry*, 3: 79-84.
- Nayak, Bindu, and Kenneth Burman. 2006. 'Thyrotoxicosis and thyroid storm', *Endocrinology and Metabolism Clinics*, 35: 663-86.

- Obolskiy, Dmitry, Ivo Pischel, Bjoern Feistel, Nikolay Glotov, and Michael Heinrich. 2011. 'Artemisia dracuncululus L.(tarragon): a critical review of its traditional use, chemical composition, pharmacology, and safety', *Journal of Agricultural and Food Chemistry*, 59: 11367-84.
- Oraiza, M. 1986. 'Studies on product of browning reaction prepared from glucosamine', *Japanese J Nutr*, 44: 307-15.
- Orsi, Nicolas M, N Ellissa Baskind, and Michele Cummings. 2024. 'Anatomy, Development, Histology and Normal Function of the Ovary.' in, *Pathology of the Ovary, Fallopian Tube and Peritoneum* (Springer).
- Padmanabhan, P, and SN Jangle. 2012. 'Evaluation of in-vitro anti-inflammatory activity of herbal preparation, a combination of four medicinal plants', *International journal of basic and applied medical sciences*, 2: 109-16.
- Pankhuri Wanjari, Pankhuri Wanjari, and RM Jayadeepa. 2012. 'A novel in-silico drug designing approach for identification of natural compounds for treatment of hypothyroid'.
- Rabehi, Sami Ahmed, Mohamed A Rezzaz, Louardi Kherrou, and Khalil Souiher. 2023. 'TOWARDS THE DEVELOPMENT OF ECOTOURISM IN THE OULED-MAIL MOUNTAINS: A CASE STUDY OF THE DJELFA MUNICIPALITY IN ALGERIA', *Geo Journal of Tourism and Geosites*, 50: 1411-29.
- Rocha, Maria Inês, Maria José Gonçalves, Carlos Cavaleiro, Maria Teresa Cruz, Cláudia Pereira, Patrícia Moreira, Lígia Salgueiro, and Artur Figureueirinha. 2021. 'Chemical characterization and bioactive potential of Artemisia campestris L. subsp. maritima (DC) Arcang. essential oil and hydrodistillation residual water', *Journal of ethnopharmacology*, 276: 114146.
- Sabuncu, Tevfik, Muge Harma, Mehmet Harma, Yasar Nazligul, and Feryal Kilic. 2003. 'Sibutramine has a positive effect on clinical and metabolic parameters in obese patients with polycystic ovary syndrome', *Fertility and sterility*, 80: 1199-204.
- Saeidnia, Soodabeh, Azadeh Manayi, Ahmad R Gohari, and Mohammad Abdollahi. 2014. 'The story of beta-sitosterol-a review'.
- Sagástegui-Guarniz William Antonio, William Antonio, Carmen R Silva-Correa, Villarreal-La Torre, E Víctor, José L Cruzado-Razco, Abhel A Calderón-Peña, Cinthya L Aspajo-Villalaz, César D Gamarra-Sánchez, Segundo G Ruiz-Reyes, and Juana E Chávez-Flores. 2020. 'Hepatoprotective and Nephroprotective Activity of Artemisia absinthium L. on Diclofenac-induced Toxicity in Rats', *Pharmacognosy Journal*, 12.
- Saoudi, Mongi, Mohamed Salah Allagui, Abdelwaheb Abdelmouleh, Kamel Jamoussi, and Abdelfattah El Feki. 2010. 'Protective effects of aqueous extract of Artemisia campestris against puffer fish *Lagocephalus lagocephalus* extract-induced oxidative damage in rats', *Experimental and Toxicologic Pathology*, 62: 601-05.
- Saoudi, Mongi, Marwa Ncir, Manel Ben Ali, Malek Grati, Kamel Jamoussi, Nouredine Allouche, and Abdelfattah El Feki. 2017. 'Chemical components, antioxidant potential and hepatoprotective effects of Artemisia campestris essential oil against deltamethrin-induced genotoxicity and oxidative damage in rats', *General Physiology and Biophysics*, 36: 331-42.
- Scanlan, Thomas S, Katherine L Suchland, Matthew E Hart, Grazia Chiellini, Yong Huang, Paul J Kruzich, Sabina Frascarelli, Dane A Crossley, James R Bunzow, and Simonetta Ronca-Testoni. 2004. '3-Iodothyronamine is an endogenous and rapid-acting derivative of thyroid hormone', *Nature medicine*, 10: 638-42.
- Schlenker, Evelyn H. 2012. 'Effects of hypothyroidism on the respiratory system and control of breathing: Human studies and animal models', *Respiratory Physiology & Neurobiology*, 181: 123-31.
- Sebai, Hichem, Mohamed-Amine Jabri, Abdelaziz Souli, Karim Hosni, Slimen Selmi, Haifa Tounsi, Olfa Tebourbi, Samir Boubaker, Jamel El-Benna, and Mohsen Sakly. 2014.

- 'Protective effect of *Artemisia campestris* extract against aspirin-induced gastric lesions and oxidative stress in rat', *Rsc Advances*, 4: 49831-41.
- Sefi, Mediha, Hanen Bouaziz, Nejla Soudani, Tahia Boudawara, and Najiba Zeghal. 2011. 'Fenthion induced-oxidative stress in the liver of adult rats and their progeny: Alleviation by *Artemisia campestris*', *Pesticide Biochemistry and Physiology*, 101: 71-79.
- Sefi, Mediha, Hamadi Fetoui, Nejla Soudani, Yassine Chtourou, Mohamed Makni, and Najiba Zeghal. 2012. '*Artemisia campestris* leaf extract alleviates early diabetic nephropathy in rats by inhibiting protein oxidation and nitric oxide end products', *Pathology - Research and Practice*, 208: 157-62.
- Shaaban, Hamdy A. 2020. 'Essential oil as antimicrobial agents: Efficacy, stability, and safety issues for food application', *Essential oils-bioactive compounds, new perspectives and applications*: 1-33.
- Shah, Krushangi N, and Snehal S Patel. 2016. 'Phosphatidylinositide 3-kinase inhibition: A new potential target for the treatment of polycystic ovarian syndrome', *Pharmaceutical biology*, 54: 975-83.
- Siddiqui, Maria Fareed, Humaira Anwer, Zahra Batool, Sidra Hasnain, Muhammad Imtiaz, Affia Tasneem, Ismat Fatima, Sarfraz Ahmad, and Rabail Alam. 2015. 'Assessment of carbimazole, propylthiouracil & l-thyroxine for liver markers in thyroid patients from Punjab, Pakistan', *Journal of Applied Pharmacy*, 7: 105-13.
- Sipka, Sándor, Andrea Nagy, János Nagy, Erdenetsetseg Nokhoijav, Éva Csősz, and Sándor Baráth. 2024. 'Measurement of chemiluminescence induced by cytochrome c plus hydrogen peroxide to characterize the peroxidase activity of various wines and the *Botrytis cinerea* related quality of Aszú wines of Tokaj in Hungary', *European Food Research and Technology*, 250: 111-18.
- Slinkard, Karen, and Vernon L Singleton. 1977. 'Total phenol analysis: automation and comparison with manual methods', *American journal of enology and viticulture*, 28: 49-55.
- Sriti, Jazia, Majdi Hammami, Nadia Fares, Sawssen Selmi, and Ferid Limam. 2024. 'Chapter-2 Phytochemical Contents, Antioxidant and Antimicrobial Activities of *Artemisia campestris*', *Aromatic and Medicinal Plants in Health Care*: 25.
- Stuper-Szablewska, Kinga, and Juliusz Perkowski. 2017. 'Level of contamination with mycobiota and contents of mycotoxins from the group of trichothecenes in grain of wheat, oats, barley, rye and triticale harvested in Poland in 2006-2008', *Annals of Agricultural and Environmental Medicine*, 24.
- Tepe, Bektas, Munevver Sokmen, H Askin Akpulat, and Atalay Sokmen. 2005. 'In vitro antioxidant activities of the methanol extracts of five *Allium* species from Turkey', *Food chemistry*, 92: 89-92.
- Trifan, Adriana, Monika E Czerwińska, Constantin Mardari, Gokhan Zengin, Kouadio Ibrahime Sinan, Izabela Korona-Glowniak, Krystyna Skalicka-Woźniak, and Simon Vlad Luca. 2022. 'Exploring the *Artemisia* genus: An insight into the phytochemical and multi-biological potential of *A. campestris* subsp. *lednicensis* (Spreng.) Greuter & Raab-Straube', *Plants*, 11: 2874.
- Trott, Oleg, and Arthur J Olson. 2010. 'AutoDock Vina: improving the speed and accuracy of docking with a new scoring function, efficient optimization, and multithreading', *Journal of computational chemistry*, 31: 455-61.
- Vagenakis, Apostolos G, and Lewis E Braverman. 1976. 'Drug induced hypothyroidism', *Pharmacology & Therapeutics. Part C: Clinical Pharmacology and Therapeutics*, 1: 149-59.
- Vazquez-Armenta, FJ, MR Cruz-Valenzuela, and JF Ayala-Zavala. 2016. 'Onion (*Allium cepa*) essential oils.' in, *Essential oils in food preservation, flavor and safety* (Elsevier).

- Vianna, Carolina Pasa, and Walter F de Azevedo. 2012. 'Identification of new potential Mycobacterium tuberculosis shikimate kinase inhibitors through molecular docking simulations', *Journal of Molecular Modeling*, 18: 755-64.
- Vigorito, Carlo, Francesco Giallauria, Stefano Palomba, Teresa Cascella, Francesco Manguso, Rosa Lucci, Anna De Lorenzo, Domenico Tafuri, Gaetano Lombardi, and Annamaria Colao. 2007. 'Beneficial effects of a three-month structured exercise training program on cardiopulmonary functional capacity in young women with polycystic ovary syndrome', *The Journal of Clinical Endocrinology & Metabolism*, 92: 1379-84.
- Vyrides, Andreas A, Essam El Mahdi, and Konstantinos Giannakou. 2022. 'Ovulation induction techniques in women with polycystic ovary syndrome', *Frontiers in Medicine*, 9: 982230.
- Wairata, Johanis, Arif Fadlan, Adi Setyo Purnomo, Muhammad Taher, and Taslim Ersam. 2022. 'Total phenolic and flavonoid contents, antioxidant, antidiabetic and antiplasmodial activities of *Garcinia forbesii* King: A correlation study', *Arabian Journal of Chemistry*, 15: 103541.
- Wang, Haoyu, Zhi Wang, Zihui Zhang, Jingchun Liu, and Li Hong. 2023. ' β -Sitosterol as a promising anticancer agent for chemoprevention and chemotherapy: mechanisms of action and future prospects', *Advances in Nutrition*, 14: 1085-110.
- Wang, Jiao, Xin Qian, Qiang Gao, Chunmei Lv, Jie Xu, Hongbo Jin, and Hui Zhu. 2018. 'Quercetin increases the antioxidant capacity of the ovary in menopausal rats and in ovarian granulosa cell culture in vitro', *Journal of ovarian research*, 11: 1-11.
- Wu, Hairong, and Baojun Xu. 2014. 'Inhibitory effects of onion against α -glucosidase activity and its correlation with phenolic antioxidants', *International Journal of Food Properties*, 17: 599-609.
- Yahia, Massinissa, Afaf Benhouda, and Karima Takellalet. 2023. 'Anti-inflammatory and hemostatic Activities of Methanolic Extract from ATRIPLEX HALIMUS Leaves collected in east of Algeria', *Arabian Journal of Medicinal and Aromatic Plants*, 9: 148-64.
- Younsi, Faten, Sameh Mehdi, Oumayma Aissi, Najoua Rahali, Rym Jaouadi, Mohamed Boussaid, and Chokri Messaoud. 2017. 'Essential oil variability in natural populations of *Artemisia campestris* (L.) and *Artemisia herba-alba* (Asso) and incidence on antiacetylcholinesterase and antioxidant activities', *Chemistry & biodiversity*, 14: e1700017.
- Zahnit, Wafa, Ouanissa Smara, Lazhar Bechki, Chawki Bensouici, Mohammed Messaoudi, Naima Benchikha, Imane Larkem, Chinaza Godswill Awuchi, Barbara Sawicka, and Jesus Simal-Gandara. 2022. 'Phytochemical profiling, mineral elements, and biological activities of *Artemisia campestris* L. grown in Algeria', *Horticulturae*, 8: 914.
- Zbucki, Robert Lukasz, Maria Malgorzata Winnicka, Boguslaw Sawicki, Beata Szynaka, Anna Andrzejewska, and Zbigniew Puchalski. 2007. 'Alteration of parafollicular (C) cells activity in the experimental model of hypothyroidism in rats', *Folia Histochemica et Cytobiologica*, 45: 115-21.
- Zinjarde, Smita S, Shobha Y Bhargava, and Ameeta R Kumar. 2011. 'Potent α -amylase inhibitory activity of Indian Ayurvedic medicinal plants', *BMC complementary and alternative medicine*, 11: 1-10.

Annexes

Annexe 1. Publications

Chemistry & Biodiversity

10.1002/cbdv.202402184

Assessment of *Artemisia campestris* L. Leaf Extract Effects on Polycystic Ovarian Syndrome in Rats, Antioxidant and α -Amylase Inhibition Activities

Inasse Cherfi^{1,2}, Nasma Mahboub^{1,2}, Ikram Toumi^{1,2}, Salah Eddine Laouini^{3,4}, Gamil Gamal Hasan³, Abderrhmane Bouafia^{3,4,*}, Fahad Alharthi⁵ and Talha Bin Emran^{6,7,8}

¹Faculty of Natural Science and Life, Department of Molecular and Cellular Biology, El Oued University, Algeria; inassecherfi284@gmail.com (I.C.); bioch_nasma@yahoo.fr (N.M.); elamine73@yahoo.fr (I.T.).

²Laboratory Biology, Environment, and Health, Faculty of Natural Sciences and Life, El-Oued University, P.O. Box 789, El-Oued, Algeria.

³Department of process engineering, Faculty of Technology, University of El Oued, El-Oued 39000, Algeria; salah_laouini@yahoo.fr (S.E.L.); hasan_gamil@yahoo.com (G.G.H.); abdelrahmanebouafia@gmail.com (A.B.)

⁴Laboratory of Biotechnology Biomaterial and Condensed Matter, Faculty of Technology, University of El Oued, 39000 El Oued, Algeria.

⁵Department of Chemistry, College of Science, King Saud University, Riyadh-11451, Kingdom of Saudi Arabia; fharthi@ksu.edu.sa (F.A.).

⁶Department of Pathology and Laboratory Medicine, Warren Alpert Medical School, Brown University, Providence, RI 02912, USA; talha_bin_emran@brown.edu (T.B.E.).

⁷Legorreta Cancer Center, Brown University, Providence, RI 02912, USA

⁸Department of Pharmacy, Faculty of Allied Health Sciences, Daffodil International University, Dhaka 1207, Bangladesh

*Corresponding author: E-mail: abdelrahmanebouafia@gmail.com (A.B.).

Abstract

Polycystic Ovarian Syndrome (PCOS) is characterized by metabolic and reproductive dysfunction, often associated with elevated oxidative stress markers in the bloodstream. This study examines the potential antioxidant properties and α -amylase inhibitory activity of *Artemisia campestris* leaves extract (*Artemisia campestris* L) and its effects on rats with induced PCOS. Estradiol valerate was administered to ten mature Wistar rats to induce PCOS, while a control group consisted of five mature Wistar rats. Following a 16-day induction period,

1

Cherfi, I., Mahboub, N., Toumi, I., Laouini, S. E., Hasan, G. G., Bouafia, A., Alharthi, F., & Emran, T. B. Assessment of *Artemisia campestris* L. Leaf Extract Effects on Polycystic

Ovarian Syndrome in Rats, Antioxidant and α -Amylase Inhibition Activities. *Chemistry & Biodiversity*, n/a(n/a), e202402184. <https://doi.org/https://doi.org/10.1002/cbdv.202402184>